LATERAL-TORSIONAL BUCKLING OF STRUCTURES WITH MONOSYMMETRIC CROSS-SECTIONS

by

Matthew J. Vensko

B.S. Pennsylvania State University, 2003

Submitted to the Graduate Faculty of the

Swanson School of Engineering in partial fulfillment

of the requirements for the degree of

Master of Science

University of Pittsburgh

2008

UNIVERSITY OF PITTSBURGH

SWANSON SCHOOL OF ENGINEERING

This thesis was presented

by

Matthew J. Vensko

It was defended on

November 21, 2008

and approved by

Kent A. Harries, Assistant Professor,
Department of Civil and Environmental Engineering

Albert To, Assistant Professor,
Department of Civil and Environmental Engineering

Morteza A. M. Torkamani, Associate Professor,
Department of Civil and Environmental Engineering,
Thesis Advisor

LATERAL-TORSIONAL BUCKLING OF STRUCTURES WITH MONOSYMMETRIC CROSS-SECTIONS

Matthew J. Vensko, M.S.

University of Pittsburgh, 2008

Lateral-torsional buckling is a method of failure that occurs when the in-plane bending capacity of a member exceeds its resistance to out-of-plane lateral buckling and twisting. The lateral-torsional buckling of beam-columns with doubly-symmetric cross-sections is a topic that has been long discussed and well covered. The buckling of members with monosymmetric cross-sections is an underdeveloped topic, with its derivations complicated by the fact that the centroid and the shear center of the cross-section do not coincide. In this paper, the total potential energy equation of a beam-column element with a monosymmetric cross-section will be derived to predict the lateral-torsional buckling load.

The total potential energy equation is the sum of the strain energy and the potential energy of the external loads. The theorem of minimum total potential energy exerts that setting the second variation of this equation equal to zero will represent a transition from a stable to an unstable state. The buckling loads can then be identified when this transition takes place. This thesis will derive energy equations in both dimensional and non-dimensional forms assuming

that the beam-column is without prebuckling deformations. This dimensional buckling equation will then be expanded to include prebuckling deformations.

The ability of these equations to predict the lateral-torsional buckling loads of a structure is demonstrated for different loading and boundary conditions. The accuracy of these predictions is dependent on the ability to select a suitable shape function to mimic the buckled shape of the beam-column. The results provided by the buckling equations derived in this thesis, using a suitable shape function, are compared to examples in existing literature considering the same boundary and loading conditions.

The finite element method is then used, along with the energy equations, to derive element elastic and geometric stiffness matrices. These element stiffness matrices can be transformed into global stiffness matrices. Boundary conditions can then be enforced and a generalized eigenvalue problem can then be used to determine the buckling loads. The element elastic and geometric stiffness matrices are presented in this thesis so that future research can apply them to a computer software program to predict lateral-torsional buckling loads of complex systems containing members with monosymmetric cross-sections.

TABLE OF CONTENTS

LIST OF FIGURES

NOMENCLATURE

Symbol	Description
A	area of member
a	distributed load height
$\overline{a}$	non-dimensional distributed load height
$\{D\}$	global nodal displacement vector for the structure
$\{D_e\}$	global nodal displacement vector for an element
$\{d_e\}$	local nodal displacement vector for an element
E	modulus of elasticity
e	concentrated load height
$\overline{e}$	non-dimensional concentrated load height
F	axial load
$\overline{F}$	non-dimensional axial load
G	shear modulus

$[g_e]$	element local geometric stiffness matrix for initial load set
$[g_e]_P$	element local geometrix stiffness matrix for prebuckling
h	depth of the member
I_x	moment of inertial about the x axis
I_y	moment of inertial about the y axis
I_ω	warping moment of inertia
J	torsional constant
K	beam parameter
$[k_e]$	element local stiffness matrix
$[k_e]_P$	element local stiffness matrix for prebuckling
k_z	torsional curvature of the deformed element
L	member length
M_{cr}	classical lateral buckling uniform bending moment
M_x	bending moment
$[N]$	shape function matrix
P	concentrated load
P_{cr}	critical concentrated load

γ_P	non-dimensional concentrated load
q	distributed load
q_{cr}	critical uniformly distributed load
γ_q	non-dimensional distributed load
r_o	polar radius of gyration about the shear center
$\bar{r}_o$	non-dimensional polar radius of gyration
$[T_e]$	transformation matrix
$[T_r]$	rotation transformation matrix
t_p	perpendicular distance to P from the mid-thickness surface
U	strain energy
U_e	strain energy for each finite element
u	out-of-plane lateral displacement
u_p	out-of-plane lateral displacement of point P_o
u_1, u_3	out-of-plane lateral displacements at nodes 1 and 2
u_2, u_4	out-of-plane rotation at nodes 1 and 2
u'	out-of-plane rotation
$\bar{u}$	non-dimensional out-of-plane lateral displacement

v	in-plane bending displacement
v_M	displacement through which the applied moment acts
v_P	in-plane bending displacement of point P_o
v_q	displacement through which the distributed load acts
v_1, v_3	in-plane displacements at nodes 1 and 2
v_2, v_4	in-plane rotation at nodes 1 and 2
v'	in-plane rotation
w	axial displacement
w_F	longitudinal displacement through which the axial load acts
w_P	longitudinal displacement of point P_o
$\hat{y}_o$	shear center displacement
$\bar{y}_o$	non-dimensional shear center displacement
z_P	concentrated load location from left support
$\bar{z}$	non-dimensional member distance
$\bar{z}_p$	non-dimensional distance to concentrated load
β_x	monosymmetry parameter
$\bar{\beta}_x$	non-dimensional monosymmetry parameter

ε_P	longitudinal strain of point P_o
ϕ	out-of-plane twisting rotation
ϕ_1, ϕ_3	out-of-plane twisting rotation at nodes 1 and 2
ϕ_2, ϕ_4	out-of-plane torsional curvature at nodes 1 and 2
ϕ'	out-of-plane torsional curvature
γ_P	shear strain of point P_o
λ	buckling parameter
$\prod$	total potential energy
$\overline{\prod}$	non-dimensional total potential energy
ρ	degree of monosymmetry
σ_P	longitudinal stress of point P_o
τ_P	shear stress of point P_o
ω	warping function
Ω	potential energy of the loads
Ω_e	potential energy of the loads for each finite element
θ	rotation of the member cross-section

1.0 INTRODUCTION

The members of a steel structure, commonly known as beam-columns, are usually designed with a thin-walled cross-section. Thin-walled cross-sections are used as a compromise between structural stability and economic efficiency and include angles, channels, box-beams, I-beams, etc. These members are usually designed so that the loads are applied in the plane of the weak axis of the cross-section, so that the bending occurs about the strong axis. However, when a beam, usually slender in nature, has relatively small lateral and torsional stiffnesses compared to its stiffness in the plane of loading, the beam will deflect laterally and twist out of plane when the load reaches a critical limit. This limit is known as the *elastic lateral-torsional buckling load*.

The lateral buckling and twisting of the beam are interdependent in that when a member deflects laterally, the resulting induced moment exerts a component torque about the deflected longitudinal axis which causes the beam to twist (Wang, *et al*. 2005). The lateral-torsional buckling loads for a beam-column are influenced by a number of factors, including cross-sectional shape, the unbraced length and support conditions of the beam, the type and position of the applied loads along the member axis, and the location of the applied loads with respect to the centroidal axis of the cross section.

This paper will focus on the lateral-torsional buckling of steel I-beams with a monosymmetric cross-section. In a beam with a monosymmetric cross-section, the shear center

and the centroid of the cross-section do not coincide. The significance of this can be explained by the Wagner effect (Anderson and Trahair, 1972), in which the twisting of the member causes the axial compressive and tension stresses to exert an additional disturbing torque. This torque can reduce the torsional stiffness of a member in compression and increase the torsional stiffness of a member in tension. In I-beams with doubly-symmetric cross-sections, these compressive and tensile stresses balance each other exactly and the change in the torsional stiffness is zero. In I-beams with monosymmetric cross-sections where the smaller flange is further from the shear center, the Wagner effect results in a change in the torsional stiffness. The stresses in the smaller flange have a greater lever arm and predominate in the Wagner effect. The torsional stiffness of the beam will then increase when the smaller flange is in tension and decrease when the smaller flange is in compression.

When a structure is simple, such as a beam, an energy method approach may be used directly to calculate the lateral-torsional buckling load of the structure. Assuming a suitable shape function, the equations derived using the energy method can provide approximate buckling loads for the structure. However, when a structure is complex, this is not possible. In this case, the energy method in conjunction with the finite element method may be used to calculate the lateral-torsional buckling load of the structure.

The finite element method is a versatile numerical and mathematical approach which can encompass complicated loads, boundary conditions, and geometry of a structure. First, element elastic stiffness and geometric stiffness matrices are derived for an element using the energy equations for lateral-torsional buckling. The structure in question must be divided into several elements, and a global coordinate system can be selected for that structure. The element elastic stiffness and geometric stiffness matrices are transformed to the global coordinate system for

each element, resulting in global element elastic and geometric stiffness matrices for the structure. After this assembly process, boundary conditions are enforced to convert the structure from an unrestrained structure to a restrained structure. The derived equilibrium equations are in the form of a generalized eigenvalue problem, where the eigenvalues are the load factors that, when multiplied to a reference load, result in lateral-torsional buckling loads for the structure.

The main objective of this thesis is to formulate equations for lateral-torsional buckling of monosymmetric beams using the energy method. Suitable shape functions will be applied to these equations to provide approximate buckling solutions that can be compared to previous data. The finite element method will be used to derive element elastic and geometric stiffness matrices that can be used in future works in conjunction with computer software to determine lateral-torsional buckling loads of more complex structures.

2.0 LITERATURE REVIEW

This section reviews available literature that explores lateral-torsional buckling as the primary state of failure for beams used in structures. A beam that has relatively small lateral and torsional stiffnesses compared to its stiffness in the plane of loading tends to deflect laterally and twist out of plane. This failure mode is known as lateral-torsional buckling. Two methods are used to derive the critical load values that result in lateral-torsional buckling beam failure: the method utilizing differential equilibrium equations and the energy method. The differential equilibrium method of stability analysis assumes the internal and external forces acting on an object to be equal and opposite. The energy method refers to an approach where the total potential energy of a conservative system is calculated by summing the internal and external energies. The buckling loads for the system can then be approximated if a suitable shape function for the particular structure is used, thus reducing the system from one having infinite degrees of freedom to one having finite degrees of freedom. This approach is known as the Rayleigh-Ritz method. This method will provide acceptable results as long as the assumed shape function is accurate. Both the differential equilibrium method and energy methods are examined in this literature review.

2.1 EQUILIBRIUM METHOD

The closed form solutions for various loading conditions and cross-sections are demonstrated below using the equilibrium method. The beams are assumed to be stationary and therefore the sum of the internal forces of the structure and the external forces is assumed to be zero. The equations are rearranged in terms of displacements resulting in a second order differential equation from which the buckling loads can be solved. The beams are assumed in this section to be elastic, initially perfectly straight, and in-plane deformations are neglected. Rotation of the beam, ϕ, is assumed small, so for the small angle relationships $\sin\phi = \phi$ and $\cos\phi = 1$ can be used.

Consider a simply supported beam with a uniform rectangular cross section as shown in Figure 2.1a and Figure 2.1b. Note that *u, v* and *w* are the displacements in the *x-, y-,* and *z-* directions, respectively. The section rotates out of plane at an angle ϕ. The differential equilibrium equations of minor axis bending and torsion of a beam with no axial force ($F = 0$) are derived from statics as (Chen and Lui. 1987)

$$EI_y \frac{d^2 u}{dz^2} = -M_x \phi \tag{2.1}$$

$$GJ \frac{d\phi}{dz} = M_x \frac{du}{dz} + M_z \tag{2.2}$$

where $EI_y = \frac{Ehb^3}{12}$ and $GJ = \frac{Ghb^3}{3}$

EI_y represents the flexural rigidity of the beam with respect to the *y*-axis and *GJ* represents the torsional rigidity of the beam with respect to the *z*-axis. M_x and M_z are the internal moments of the beam acting about the *x*-axis and the *z*-axis, respectively. In Eq. (2.1), the component of M_x in the *y*-direction is represented by $-M_x \sin\phi$ which, by way of the small angle theorem, reduces to $-M_x\phi$. In Eq. (2.2), the torsional component of M_x acting in the *z*-direction is represented by $M_x \dfrac{du}{dz}$.

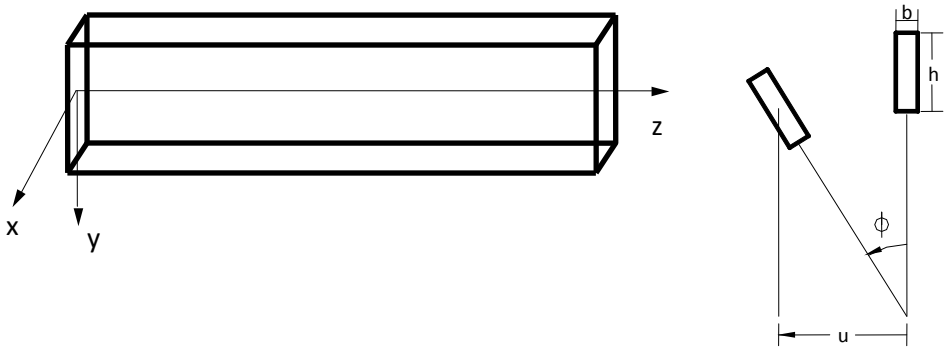

Figure 2.1a Beams of Rectangular Cross-Section

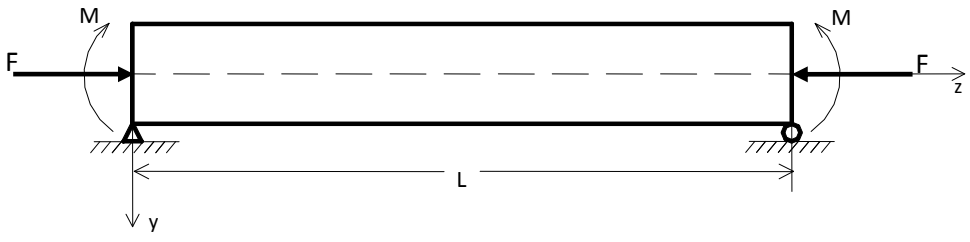

Figure 2.1b Beams of Rectangular Cross-Section with Axial Force and End Moments

2.1.1 Closed Form Solutions

Case 1: A beam that is subjected to only equal end moments M about x-axis

This loading case is shown in Figure 2.1b, with $F = 0$. Since there is no torsional component of the moment, let $M_x = M$ and $M_z = 0$. The equilibrium equations given in Eq. (2.1) and (2.2) reduce to

$$EI_y \frac{d^2 u}{dz^2} = -M \phi \tag{2.3}$$

$$GJ \frac{d\phi}{dz} = M \frac{du}{dz} \tag{2.4}$$

Solving for u from Eqs. (2.3) and (2.4) yields (respectively):

$$\frac{d^2 u}{dz^2} = \frac{-M\phi}{EI_y} \tag{2.5}$$

$$\frac{d^2 u}{dz^2} = \frac{GJ}{M} \frac{d^2 \phi}{dz^2} \tag{2.6}$$

Eliminating u yields a single differential equation of the form

$$\frac{d^2 \phi}{dz^2} + \frac{M^2}{GJEI_y} \phi = 0 \tag{2.7}$$

Solving the second order differential equation yields the general solution as

$$\phi(z) = A \sin\left(\frac{Mz}{\sqrt{EI_y GJ}} \right) + B \cos\left(\frac{Mz}{\sqrt{EI_y GJ}} \right) \tag{2.8}$$

By applying the boundary condition $\phi = 0$ at $z = 0$, B is equal to zero.

The constant A may then not be equal to zero because it provides a trivial solution. Therefore at $z = L$

$$\sin \frac{M_{cr} L}{\sqrt{EI_y GJ}} = 0 \tag{2.9}$$

Solving for M_{cr} to provide the smallest nonzero buckling load yields

$$M_{cr} = \frac{\pi \sqrt{EI_y GJ}}{L} \tag{2.10}$$

where M_{cr} is the critical value of M that will cause the beam to deflect laterally and twist out of plane.

Case 2: A linearly tapered beam with a rectangular cross section that is subjected to only equal end moments M about x-axis

For this case, consider a linearly tapered beam with initial depth h_o which increases at a rate $\frac{z}{L}\delta$ as shown in Figure 2.2 where

$$h(z) = (1 + \frac{z}{L}\delta)h_o \tag{2.11}$$

In Eq. (2.11), $h(z)$ is the linear tapered depth of the beam as a function of z, h_o is the depth of beam at $z = 0$, and $(1 + \delta)$ is the ratio of height of tapered beam at $z = L$ to $z = 0$.

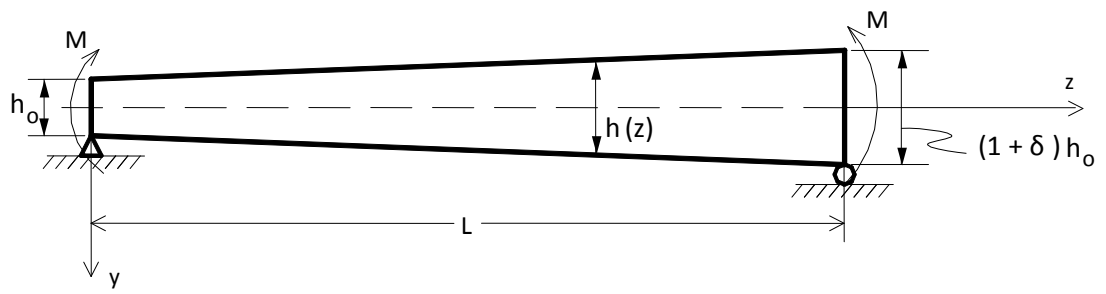

Figure 2.2 Linear Tapered Beam Subjected to Equal and Opposite End Moments

The beam properties of the tapered section can be written as

$$EI_y = EI_o\eta \tag{2.12}$$

$$GJ = GJ_o\eta \tag{2.13}$$

$$\text{where } I_o = \frac{h_o b^3}{12}\ ,\ J_o = \frac{h_o b^3}{3}\text{, and } \eta = 1 + \frac{z}{L}\delta . \tag{2.14}$$

As in *Case 1*, there is no torsional component of the moment so that $M_x = M$ and $M_z = 0$.

Substituting Eqs. (2.12) and (2.13) into the equilibrium equations yield

$$EI_o\eta\frac{d^2u}{dz^2} = -M\phi \tag{2.15}$$

$$GJ_o\eta\frac{d\phi}{dz} = M\frac{du}{dz} \tag{2.16}$$

The derivative of η with respect to z is

$$\frac{d\eta}{dz} = \frac{\delta}{L} \tag{2.17}$$

which enables the following relationships

$$\frac{d\phi}{dz} = \frac{d\phi}{d\eta}\frac{d\eta}{dz} = \frac{\delta}{L}\frac{d\phi}{d\eta} \tag{2.18}$$

and

$$\frac{d^2\phi}{dz^2} = \left(\frac{\delta}{L}\right)^2 \frac{d^2\phi}{d\eta^2} \tag{2.19}$$

Substituting Eqs. (2.17) – (2.19) into the equilibrium Eqs. (2.15) and (2.16) yield

$$EI_o\eta\left(\frac{\delta}{L}\right)^2 \frac{d^2u}{d\eta^2} = -M\phi \tag{2.20}$$

$$GJ_o\eta\left(\frac{\delta}{L}\right)\frac{d\phi}{d\eta} = M\left(\frac{\delta}{L}\right)\frac{du}{d\eta} \tag{2.21}$$

Differentiating Eq. (2.21) and combining it with Eq.(2.20) in order to eliminate u yields

$$\eta^2\frac{d^2\phi}{d\eta^2} + \eta\frac{d\phi}{d\eta} + k^2\phi = 0 \tag{2.22}$$

where

$$k^2 = \frac{M^2L^2}{EI_oGJ_o\delta^2} \tag{2.23}$$

The general solution of Eq. (2.22) is given by (Lee, 1959)

$$\phi = A\sin(k\ln\eta) + B\cos(k\ln\eta) \tag{2.24}$$

Applying the boundary condition $\phi = 0$ at $z = 0$, B is equal to zero. The constant A may then not be equal to zero because it provides a trivial solution. Therefore the boundary condition $\phi = 0$ at $\eta = (1+\delta)$ yields

$$\sin(k\ln(1+\delta)) = 0 \tag{2.25}$$

Solving for M_{cr} to provide the smallest nonzero buckling load yields

$$M_{cr} = \frac{\pi\delta}{\ln(1+\delta)}\frac{\sqrt{EI_o GJ_o}}{L} \tag{2.26}$$

where M_{cr} is the critical value of M that will cause the beam to deflect laterally and twist out of plane. It is important to recognize that if $\delta = 0$, meaning that the beam is not tapered, Eq. (2.26) reduces to

$$M_{cr} = \frac{\pi\sqrt{EI_o GJ_o}}{L} \tag{2.27}$$

which is the result obtained in *Case 1*.

Case 3: A simply supported beam with a concentrated load, P, at midspan (at z = L/2)

For this case, consider a non-tapered beam with a concentrated load, P, at midspan as shown in Figure 2.3.

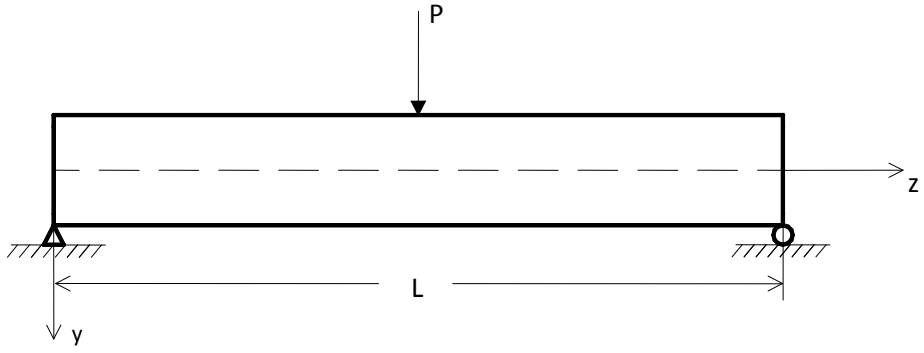

Figure 2.3 Simply Supported Beam with Concentrated Load, *P*, at Midspan

The moments M_x and M_z are derived using basic equilibrium concepts as

$$M_x = \frac{Pz}{2} \tag{2.28}$$

$$M_z = \frac{P}{2}(u^* - u) \tag{2.29}$$

Where u^* represents the lateral deflection at the centroid of the middle cross section and u represents the lateral deflection at any cross section.

By substituting the relationships for M_x and M_z into Eqs. (2.1) and (2.2), the differential equations for this case become

$$EI_y \frac{d^2 u}{dz^2} = -\frac{Pz}{2}\phi \tag{2.30}$$

$$GJ\frac{d\phi}{dz} = \frac{Pz}{2}\frac{du}{dz} + \frac{P}{2}(u^* - u) \tag{2.31}$$

Combining the above equations to eliminate the term u yields

$$\frac{d^2\phi}{dz^2} + \frac{P^2 z^2}{4EI_y GJ}\phi = 0 \tag{2.32}$$

For simplicity, the following non-dimensional relationships are used

$$\eta = \frac{z}{L} \tag{2.33}$$

$$\zeta = \sqrt{\frac{P^2 L^4}{4EI_y GJ}} \tag{2.34}$$

Eq. (2.32) can then be reduced to

$$\frac{d^2\phi}{d\eta^2} + \zeta^2\eta^2\phi = 0 \tag{2.35}$$

The general solution utilizes Bessel functions (Arfken, 2005) of the first kind of orders 1/4 and -1/4 shown below as

$$\phi = \sqrt{\eta}\left[AJ_{1/4}\left(\frac{\zeta\eta^2}{2}\right) + BJ_{-1/4}\left(\frac{\zeta\eta^2}{2}\right)\right] \tag{2.36}$$

Applying the boundary conditions $\phi = 0$ at $\eta = 0$ and $\frac{d\phi}{d\eta} = 0$ at $\eta = \frac{1}{2}$

gives $J_{-3/4}\left(\frac{\zeta}{8}\right) = 0$ then $\frac{\zeta}{8} = 1.0585$ yielding an expression for the buckling load, P_c, as

$$P_c = \frac{16.94}{L^2}\sqrt{EI_y GJ} \tag{2.37}$$

where P_c is the lateral-torsional buckling load (Wang, et al. 2005).

Case 4: A simply supported I –beam with a monosymmetric cross-section subjected to equal end moments, M, and an axial load, F, acting through the centroid:

In this case, consider a non-tapered monosymmetric I-beam subjected to end moments, *M*, and an axial force, *F*, as shown in Figure 2.4a with the cross-section of the beam shown in Figure 2.4b.

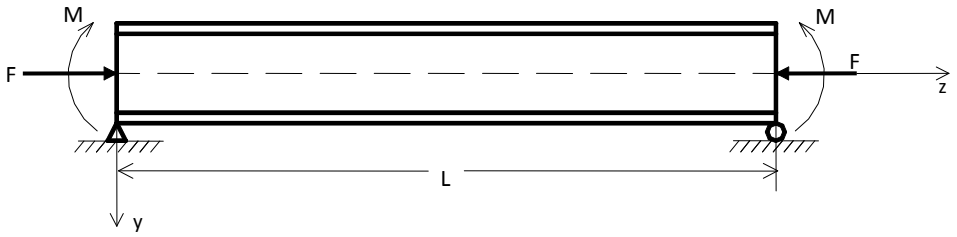

Figure 2.4a Monosymmetric Beam subjected to End Moments and Axial Force

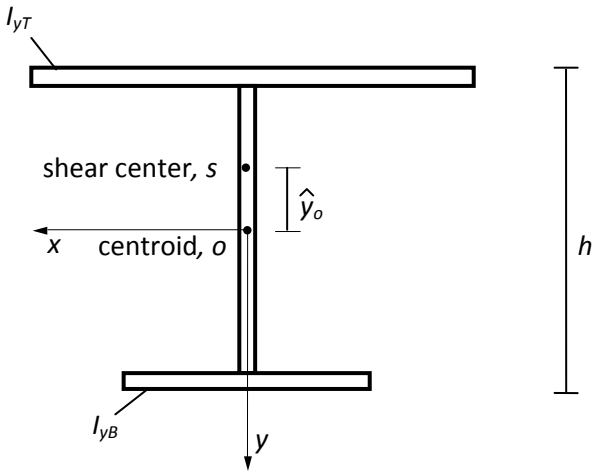

F**igure 2.4b Cross-Section of Monosymmetric Beam**

The minor axis distributed force equilibrium equation and the distributed torque equilibrium equation for the member can be expressed as (Kitipornchai and Wang. 1989)

$$EI_y \frac{d^4u}{dz^4} = -(M + Fy_o)\frac{d^2\phi}{dz^2} - F\frac{d^2u}{dz^2} \tag{2.38}$$

$$(GJ - F \cdot r_o^{\,2} + M\beta_x)\frac{d\phi}{dz} - EI_w \frac{d^3\phi}{dz^3} = M\frac{du}{dz} \tag{2.39}$$

Where the warping rigidity is

$$EI_w = EI_y \rho(1-\rho)h^2 \tag{2.40}$$

and the degree of monosymmetry can be expressed as

$$\rho = \frac{I_{yT}}{(I_{yT} + I_{yB})} = \frac{I_{yT}}{I_y} \tag{2.41}$$

where I_{yT} and I_{yB} are the second moments of inertia about the *y*-axis of the top and bottom flanges, respectively, as shown in Figure 2.4b. Because the beam has a monosymmetric cross-section, the centroid of the beam, *o*, and the shear center, *s*, do not coincide. This introduces a term, $\hat{y}_o$, which represents the vertical distance between the centroid and the shear center. The polar radius of gyration about the shear center, r_o, can be expressed as

$$r_o^{\,2} = \frac{I_x + I_y}{A} + y_o^{\,2} \tag{2.42}$$

The monosymmetric parameter of the beam (Trahair and Nethercot, 1984) is

$$\beta_x = \frac{1}{I_x}\left(\int_A x^2 y dA + \int_A y^3 dA\right) - 2y_o \tag{2.43}$$

where *x* and *y* are coordinates with respect to the centroid. β_x accounts for the Wagner effect, which is the change in effective torsional stiffness due to the components of bending compressive and tensile stresses that produce a torque in the beam as it twists during buckling.

Recognizing that, since the beam is simply supported, the boundary conditions become

$$\phi = 0 \text{ and } \frac{d^2\phi}{dz^2} = 0 \text{ at } z = 0, L.$$

With the elimination of *u* and the implementation of the above boundary conditions, Eqs. (2.36) and (2.39) yield a closed form solution for critical values *F* and *M* (Trahair and Nethercot, 1984) as

$$(M + Fy_0)^2 = r_o^2 F_z F_E \left(1 - \frac{F}{F_E}\right)\left(1 - \frac{F}{F_z} + \frac{M\beta_x}{r_o^2 F_z}\right) \tag{2.44}$$

where F_E is the Euler buckling load given by

$$F_E = \frac{\pi^2 EI_y}{L^2} \tag{2.45}$$

and F_z is given as (Wang, *et al*. 2005)

$$F_z = \frac{GJ}{r_o^2}\left(1 + \frac{\pi^2 EI_w}{GJL^2}\right) \tag{2.46}$$

In order to obtain a non-dimensional elastic buckling moment, use is made of the non-dimensional parameters (Kitipornchai and Wang. 1989)

$$\overline{K} = \sqrt{\frac{\pi^2 EI_y h^2}{4GJL^2}} \tag{2.47}$$

$$\eta = \frac{4}{h^2}\left(\frac{I_x + I_y}{A}\right) \tag{2.48}$$

$$\upsilon = \frac{2y_0}{h} \tag{2.49}$$

$$\Lambda = \frac{F}{F_E} \tag{2.50}$$

$$\lambda = \left[-\upsilon\Lambda + \frac{\beta_x}{h}(1 - \Lambda)\right]\overline{K} \tag{2.51}$$

$$\gamma = \frac{ML}{\sqrt{EI_y GJ}} \tag{2.52}$$

Where h is the distance between the centroids of the top and bottom flange and $\overline{K}$ is the beam parameter. The practical range for values of $\overline{K}$ is between 0.1 and 2.5, with low values

corresponding to long beams and/or beams with compact cross-sections, and higher values corresponding to short beams and/or beams with slender cross sections.

Using the above nondimensional parameters, Eq. (2.44) may be rewritten as (Wang, *et al*. 2005)

$$\gamma = \pi\left[\lambda \pm \sqrt{\lambda^2 - \upsilon\overline{K}^2\Lambda + (1-\Lambda)\left\{1 + \overline{K}^2\left[4\rho(1-\rho) - \eta\Lambda\right]\right\}}\right] \qquad (2.53)$$

The non-dimensional buckling equation shown above is the general solution of M for monosymmetric beams. Eq. (2.53) is a versatile equation because it also accurately predicts the lateral-torsional buckling loads for beams of doubly symmetric cross-sections by simplifying the terms in the equation so that the monosymmetric parameter, β, is equal to zero and the degree of monosymmetry, ρ, is reduced to $\frac{1}{2}$.

2.2 ENERGY METHOD

The second method used for determining lateral-torsional buckling loads in thin-walled structures is the energy method. The energy method serves as a basis for the modern finite element method of computer solution for lateral-torsional buckling problems of complex structures. The energy method is related to the differential equations of equilibrium method in that calculus of variation can be used to obtain the differential equations derived by the first method. The energy method is based on the principle that the strain energy stored in a member during lateral-torsional buckling is equal to the work done by the applied loads. The critical buckling loads can then be obtained by substituting approximate buckled shapes back into the energy equation if the shape function is known. This approach is known as the Rayleigh-Ritz method.

The strain energy stored in a buckled member can be broken down into two categories, the energy from St. Venant torsion and from warping torsion. Pure or uniform torsion exists when a member is free to warp and the applied torque is resisted solely by St. Venant shearing stresses. When a member is restrained from warping freely, both St. Venant shearing stresses and warping torsion resist the applied torque. This is known as non-uniform torsion.

2.2.1 Uniform Torsion

When a torque is applied to a member that is free to warp, the torque at any section is resisted by shear stresses whose magnitudes vary based on distance from the centroid of the section. These shear stresses are produced as adjacent cross-sections attempt to rotate relative to one another. The St. Venant torsional resistance must directly oppose the applied torque as

$$T_{sv} = GJ\frac{d\phi}{dz} \tag{2.57}$$

where ϕ is the angle of twist of the cross-section, G is the shearing modulus of elasticity, J is the torsional constant, and z is direction perpendicular to the cross section, as illustrated in Figure 2.5.

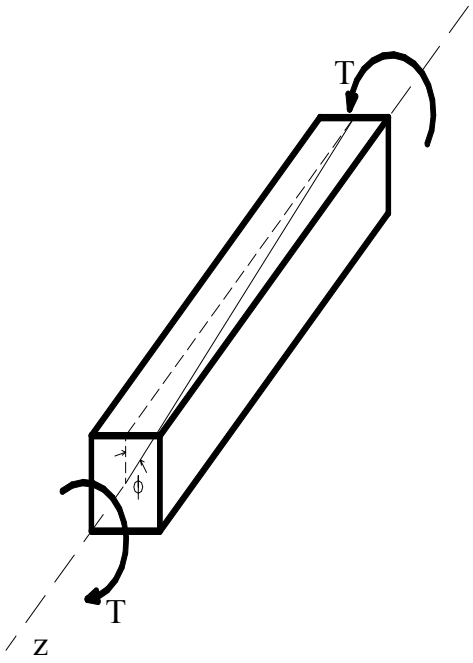

Figure 2.5 Twisting of a Rectangular Beam that is Free to Warp

2.2.2 Non-uniform Torsion

If the longitudinal displacements in the member are allowed to take place freely and the longitudinal fibers do not change length, no longitudinal stresses are present and warping is permitted to take place. However, certain loading and support conditions may be present that prevent a member from warping. This warping restraint creates stresses which produce a torsion in the member. Non-uniform torsion occurs when both St. Venant and warping torsion act on the same cross section. The expression for non-uniform torsion can be given as

$$T = T_{sv} + T_w \tag{2.58}$$

where T_w is the warping torsion, which, for an I section, is

$$T_w = V_f h \tag{2.59}$$

where V_f is the shear force in each flange and h is equal to the height of the section. Recognizing that the shear in the flange is the derivative of the moment present in the flange, Eq. (2.59) becomes

$$T_w = -\frac{dM_f}{dz} h \tag{2.60}$$

The bending moment in the upper flange, M_f, can be written in terms of the displacement in the x-directon, $\overline{u}$, as

$$M_f = EI_f \frac{d^2\overline{u}}{dz^2} \tag{2.61}$$

Recognizing that

$$\overline{u} = \frac{\phi h}{2} \tag{2.62}$$

and introducing the cross-sectional property known as the warping moment of inertia

$$I_w = \frac{I_f h^2}{2} \tag{2.63}$$

the warping torsion can now be expressed as

$$T_w = -EI_w \frac{d^3\phi}{dz^3} \tag{2.64}$$

The differential equation for non-uniform torsion is obtained by substituting Eq. (2.57) and Eq. (2.64) into Eq. (2.58) is

$$T = GJ\frac{d\phi}{dz} - EI_w \frac{d^3\phi}{dz^3} \tag{2.65}$$

The first term refers to the resistance of the member to twist and the second term represents the resistance of the member to warp. Together, the terms represent the resistance of the section to an applied torque.

2.2.3 Strain Energy

The strain energy stored in a twisted member can be broken into two categories, the energy due to St. Venant torsion and the energy due to warping torsion. The strain energy due to St. Venant torsion (Chajes, 1993) is

$$dU_{sv} = \frac{T_{sv}\, d\phi}{2} \tag{2.66}$$

where it can be seen that the change in strain energy stored in element *dz* due to St. Venant torsion is equal to one half the product of the torque and the change in the angle of twist. Solving for $d\phi$ from Eq. (2.57)

$$d\phi = \frac{T_{sv}}{GJ} dz \tag{2.67}$$

and substituting it into Eq. (2.66) yields

$$dU_{sv} = \frac{T_{sv}^{\ 2}}{2GJ} dz \tag{2.68}$$

Substituting Eq. (2.57) into Eq. (2.68) and integrating results in the expression for strain energy due to St. Venant torsion.

$$U_{sv} = \frac{1}{2}\int_0^L GJ\left(\frac{d\phi}{dz}\right)^2 dz \tag{2.69}$$

The strain energy due to the resistance to warping torsion of an I-beam, for example, is equal to the bending energy present in the flanges. The bending energy stored in an element *dz* of one of the flanges is equal to the product of one half the moment and the rotation as

$$dU_w = \frac{1}{2} EI_f \left(\frac{d^2\bar{u}}{dz^2}\right)^2 dz \tag{2.70}$$

Substituting Eqs. (2.62) and (2.63) into Eq. (2.70) yields

$$dU_w = \frac{1}{4} EI_w \left(\frac{d^2\phi}{dz^2}\right)^2 dz \tag{2.71}$$

Integrating Eq. (2.71) over the length of the member, *L*, and multiplying by two to account for the energy in both flanges results in the expression for the strain energy in a member caused by resistance to warping.

$$U_w = \frac{1}{2}\int_0^L EI_w \left(\frac{d^2\phi}{dz^2}\right)^2 dz \tag{2.72}$$

The total strain energy in a member is then represented by the addition of Eqs. (2.69) and (2.72).

$$U = \frac{1}{2}\int_o^L GJ\left(\frac{d\phi}{dz}\right)^2 dz + \frac{1}{2}\int_0^L EI_w \left(\frac{d^2\phi}{dz^2}\right)^2 dz \tag{2.73}$$

2.2.4 Solutions Using Buckling Shapes

Case 5: A simply supported, doubly symmetric I-beam that is subjected to only equal end moments M about x-axis

The loading in this case is identical to *Case 1*, but this case consists of a beam with an I cross-section instead of a rectangular cross-section. As in *Case 1*, $M_x = M$ and $M_z = 0$.

The boundary conditions for the case of uniform bending are given below.

$$u = v = \frac{d^2u}{dz^2} = \frac{d^2v}{dz^2} = 0 \qquad \text{at } z = 0, L \tag{2.74}$$

$$\phi = \frac{d^2\phi}{dz^2} = 0 \qquad \text{at } z = 0, L \tag{2.75}$$

In order to find the critical moment by use of the energy method, it is necessary to find the moment for which the total potential energy has a stationary value. The strain energy stored in the beam consists of two parts; the energy due to the bending of the member about the *y*-axis and the energy due to the member twisting about the *z*-axis. The total strain energy for the section is

$$U = \frac{1}{2}EI_y\int_0^L\left(\frac{d^2u}{dz^2}\right)^2 dz + \frac{1}{2}GJ\int_0^L\left(\frac{d\phi}{dz}\right)^2 dz + \frac{1}{2}EI_w\int_0^L\left(\frac{d^2\phi}{dz^2}\right)^2 dz \tag{2.76}$$

The strain energy, U, must now be added to the potential energy of the external loads, Ω, to determine a stationary value for $\Pi = U + \Omega$. For a member subjected to uniform bending, the external potential energy is equal to the negative product of the applied moments and the angles through which they act upon the beam.

$$\Omega = -2M\psi \tag{2.77}$$

where ψ is the angle of rotation about the x-axis of the beam and can be expressed as

$$\psi = \frac{1}{2}\int_0^L \frac{du}{dz}\frac{d\phi}{dz}dz \tag{2.78}$$

Combining Eqs. (2.77) and (2.78) yields an expression for the potential energy of the external loads as

$$\Omega = -M\int_0^L \frac{du}{dz}\frac{d\phi}{dz}dz \tag{2.79}$$

and yields the following expression for the total potential energy of the beam.

$$\Pi = \frac{1}{2}EI_y\int_0^L\left(\frac{d^2u}{dz^2}\right)^2 dz + \frac{1}{2}GJ\int_0^L\left(\frac{d\phi}{dz}\right)^2 dz + \frac{1}{2}EI_w\int_0^L\left(\frac{d^2\phi}{dz^2}\right)^2 dz - M\int_0^L \frac{du}{dz}\frac{d\phi}{dz}dz \tag{2.80}$$

As stated at the beginning of this section, the Rayleigh-Ritz method for determining critical loads requires the assumption of suitable expressions for buckling modes. The following buckling shapes satisfy our boundary conditions:

$$u = A\sin\frac{\pi z}{L} \tag{2.81}$$

$$\phi = B\sin\frac{\pi z}{L} \tag{2.82}$$

Substituting the buckled shapes into Eq. (2.80) and identifying that

$$\int_0^L \sin^2\frac{\pi z}{L}dz = \int_0^L \cos^2\frac{\pi z}{L}dz = \frac{L}{2} \tag{2.83}$$

the total potential energy of the beam, Π, becomes

$$\Pi = \frac{EI_yA^2L}{4}\left(\frac{\pi}{L}\right)^4 + \frac{GJB^2L}{4}\left(\frac{\pi}{L}\right)^2 + \frac{EI_wB^2L}{4}\left(\frac{\pi}{L}\right)^4 - \frac{MABL}{2}\left(\frac{\pi}{L}\right)^2 \tag{2.84}$$

Setting the derivative of Π with respect to A and B equal to zero, the critical moment can be obtained.

$$\frac{d\Pi}{dA} = \frac{EI_y\pi^2}{L}A - MLB = 0 \tag{2.85}$$

$$\frac{d\Pi}{dB} = MLA - \left(GJL + \frac{E\,I_w\pi^2}{L}\right)B = 0 \tag{2.86}$$

If the deformed configuration of the beam is to yield a nontrivial solution, the determinant of the coefficients A and B in Eqs. (2.85) and (2.86) must vanish leaving

$$\frac{EI_y\pi^2}{L}\left(GJL + \frac{E\,I_w\pi^2}{L}\right) - M^2L^2 = 0 \tag{2.88}$$

Solving for M in Eq. (2.88) yields the critical moment for a simply supported beam in uniform bending as

$$M_{cr} = \frac{\pi}{L}\sqrt{EI_y\left(GJ + EI_w\frac{\pi^2}{L^2}\right)} \tag{2.89}$$

Case 6: A doubly symmetric I-beam with fixed ends that is subjected to only equal end moments M about x-axis

For this case, as in *Case 1,* $M_x = M$ and $M_z = 0$.

Consider an I-beam whose ends are free to rotate about a horizontal axis but restrained against displacement in any other direction, as shown in Figure 2.6.

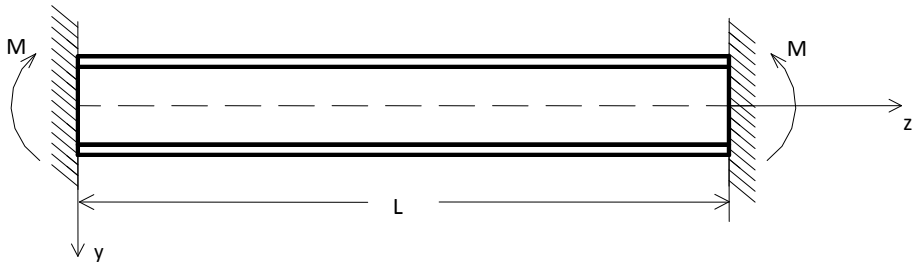

Figure 2.6 I-beam Fixed at Both Ends Subjected to End Moments

The boundary conditions are as follows

$$u = \frac{du}{dz} = 0 \qquad \text{at z = 0, } L \tag{2.90}$$

$$v = \frac{d^2v}{dz^2} = 0 \qquad \text{at z = 0, } L \tag{2.91}$$

$$\phi = \frac{d\phi}{dz} = 0 \qquad \text{at z = 0, } L \tag{2.92}$$

The following buckling shapes satisfy the geometric boundary conditions

$$u = A\left(1 - \cos\frac{2\pi z}{L}\right) \tag{2.93}$$

$$\phi = B\left(1 - \cos\frac{2\pi z}{L}\right) \tag{2.94}$$

Substituting the buckled shapes into Eq. (2.80) and using the simplification in Eq. (2.83), the total potential energy of the beam becomes

$$\Pi = \frac{\pi^2}{l}\left(4EI_y\frac{A^2\pi^2}{L^2} + GJB^2 + 4EI_wB\frac{\pi^2}{L^2} - 2MAB\right) \tag{2.95}$$

Setting the derivative of the Π equations with respect to A and B equal to zero, yield the following two equations.

$$\frac{d\Pi}{dA} = \frac{\pi^2}{L}\left(8EI_y A\frac{\pi^2}{L^2} - 2MB\right) = 0 \tag{2.96}$$

$$\frac{d\Pi}{dB} = \frac{\pi^2}{L}\left(2GJB + 8EI_w B\frac{\pi^2}{L^2} - 2MA\right) = 0 \tag{2.97}$$

Eqs. (2.95) and (2.96) expressed in matrix form is

$$\begin{bmatrix} 4EI_y\dfrac{\pi^2}{L^2} & -M \\ -M & GJ + 4EI_w\dfrac{\pi^2}{L^2} \end{bmatrix}\begin{Bmatrix} A \\ B \end{Bmatrix} = 0 \tag{2.98}$$

If the deformed configuration of the beam is to yield a nontrivial solution, the determinant of the coefficients A and B in Eq. (2.98) must vanish leaving

$$4EI_y\frac{\pi^2}{L^2}\left(GJ + 4EI_w\frac{\pi^2}{L^2}\right) - M^2 = 0 \tag{2.99}$$

Solving for M as the critical moment yields

$$M_{cr} = \frac{2\pi}{L}\sqrt{EI_y\left(GJ + 4EI_w\frac{\pi^2}{L^2}\right)} \tag{2.100}$$

It is interesting to note that the critical moment for the restrained beam is proportional to that of the simply supported beam. If the warping stiffness is negligible compared to that of the St. Venant stiffness, the critical moment for the fixed beam is twice that of the hinged beam. If the St. Venant stiffness is negligible compared to that of the warping stiffness, the critical moment of the fixed beam is four times that of the hinged beam. The reason for this is that lateral bending strength and warping strength depend of the length of the beam, where St. Venant stiffness does not. St. Venant stiffness is therefore unaffected by a change in boundary conditions.

3.0 LATERAL-TORSIONAL BUCKLING OF BEAM-COLUMNS

The energy method detailed in Chapter 2, in conjunction with the Raleigh-Ritz method, is useful in determining closed form or approximate solutions, with a high degree of accuracy, when a suitable buckling mode can be identified. In more complex structural systems, identification of the buckling mode is not possible. In this case, a finite element approach is an ideal method that may be used to calculate the buckling load. In order to formulate element elastic and geometric stiffness matrices that represent different load cases, one approach is to derive total potential energy of a beam-column element with a concentrated force, distributed force, end moments, and an axial force. Therefore, the objective of this chapter is to derive energy equations for a beam-column element with the above mentioned loads.

Lateral-torsional buckling of a beam-column occurs when the loads on an element become large enough to render its in-plane state unstable. When the loads on the member reach these critical values, the section will deflect laterally and twist out of the plane of loading. At critical loading, the compression flange of the member becomes unstable and bends laterally while the rest of the member remains stable restraining the lateral flexure of the compression flange, causing the section to rotate. This is common in slender beam-columns with insufficient lateral bracing that have a much greater in-plane bending stiffness than their lateral and torsional stiffnesses. It is important to know the critical load for lateral-torsional buckling because this

method of failure is often the primary failure mode for thin-walled structures. The focus of this chapter is to formulate energy equations that can be used to derive element elastic and geometric stiffness matrices of a beam-column with a monosymmetric I cross-section.

The basic assumptions used in the following derivations are:

1. The member has a monosymmetric cross-section.
2. The beam-column remains elastic. This implies that the member must be long and slender.
3. The cross-section of the member does not distort in its own plane after buckling and its material properties remain the same.
4. The member is initially perfectly straight, with no lateral or torsional displacements present before buckling.
5. The member is a compact section.

The orientation of the member used to derive the energy equations is depicted in Figure 3.1 using the *xyz* coordinate system with the origin being at *o*. The *x*-axis is the major principle axis and the *y*-axis is the minor principle axis with the *z*-axis being oriented along the length of the member, coinciding with the centroidal axis of the undeformed beam-column.

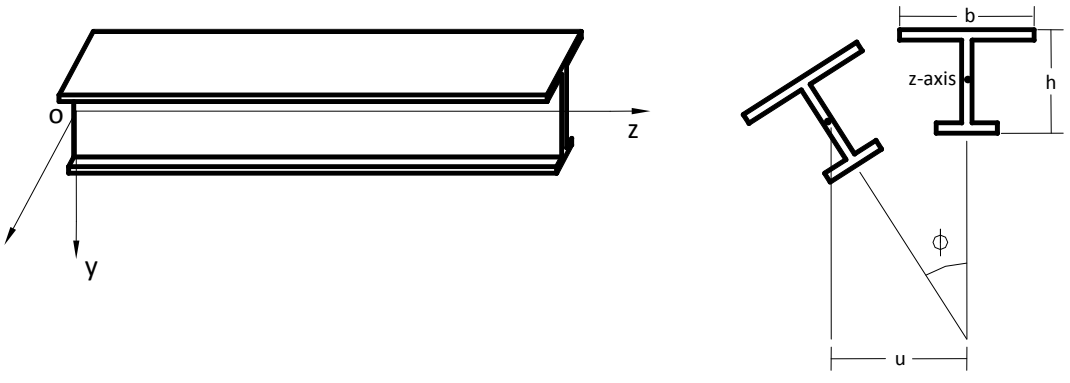

Figure 3.1 Coordinate System of Undeformed Monosymmetric Beam

The displacements in the *x*, *y*, and *z* directions are denoted as *u*, *v*, and *w*, respectively. If loading occurs in the *yz* plane, the member will have an in-plane displacement, *v*, in the *y*-direction and an in-plane rotation $\frac{dv}{dz}$. A member loaded along the *z*-axis will have a displacement, *w*. The result of lateral-torsional buckling is an out-of-plane displacement, *u*, in the *x*-direction, an out-of-plane rotation, $\frac{du}{dz}$, an out-of-plane twisting rotation, ϕ, and an out-of-plane torsional curvature, $\frac{d\phi}{dz}$. It is assumed in this chapter that in-plane deformations *w*, *v*, and $\frac{dv}{dz}$ are very small and therefore can be neglected. In the next chapter, the energy equations derived in this chapter will be expanded to include these displacements, which are known as prebuckling deformations.

The applied loads on the beam column include; (1) a distributed load, *q*, which acts at a height *a* above the centroidal axis (2) a concentrated load, *P*, which acts at a height *e* above the centroidal axis (3) a concentric axial load, *F* (4) end moments, M_1 and M_2, as shown below.

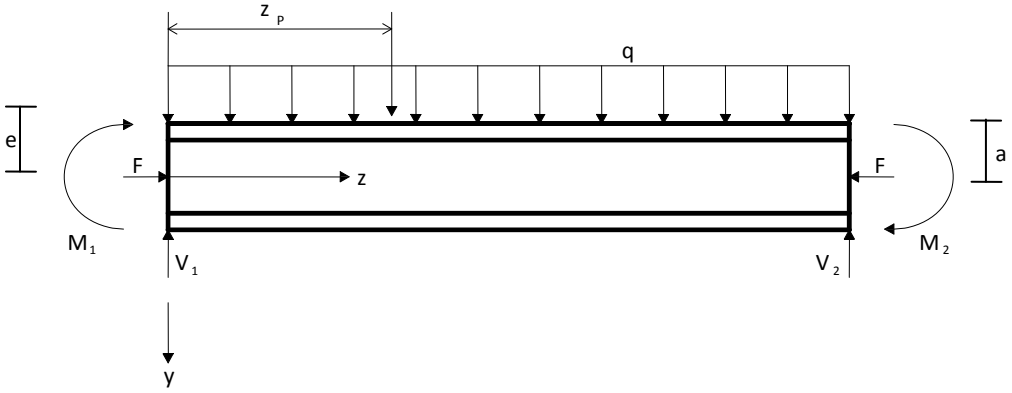

Figure 3.2 External Loads and Member End Actions of Beam Element

The energy equations for the lateral-torsional buckling of a member with a monosymmetric cross-section differ from those of a member with a double symmetric cross-section because the centroid and the shear center do not coincide on a monosymmetric beam-column, as shown in Figure 3.3. This introduces the term, $\hat{y}_o$, into the derivation representing the distance between the shear center, *s*, and the centroid, *o*.

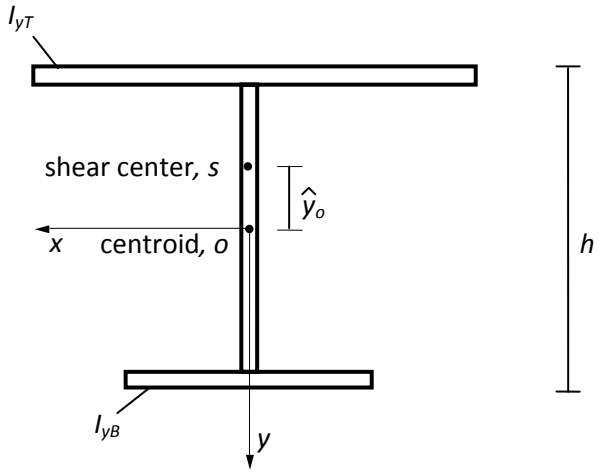

Figure 3.3 Cross-Section of Monosymmetric I-beam

The change in effective torsional stiffness of the member due to the components of bending compressive and tensile stresses that produce a torque in the beam as it twists during buckling is referred to as the Wagner effect (Anderson and Trahair, 1972). In a beam with a doubly-symmetric cross-section, these compressive and tensile stresses balance each other and do not affect the torsional stiffness of the beam. For the case of monosymmetry, these tensile and compressive stresses do not balance each other and the resulting torque causes a change in the effective torsional stiffness of the member from GJ to $(GJ + M_x \theta_x)$ (Wang and Kitipornchai, 1986). Because the smaller flange of the beam is farther away from the shear center than the

larger flange, it creates a larger moment arm and predominates in the Wagner effect. This means that when the smaller flange is in tension, the effective torsional stiffness of the beam is increased while the effective torsional stiffness is reduced when the smaller flange is in compression. This inconsistency adds to the complexity of the energy equation derivations for lateral torsional buckling.

The energy equation for an elastic thin-walled member is derived by considering the strain energy stored in the member, U, and the potential energy of the external loads, Ω, as

$$\Pi = U + \Omega \tag{3.1}$$

where Π represents the total potential energy of the member.

The strain energy present in the member is the potential energy of the internal stresses and strains present in the beam-column, while the potential energy of the loads represents the negative of the work done by external forces. The total potential energy increment may be written as

$$\Delta\Pi = \delta\Pi + \frac{1}{2!}\delta^2\Pi + \frac{1}{3!}\delta^3\Pi + \ldots \tag{3.2}$$

The theorem of stationary total potential energy states that *of all kinematically admissible deformations, the actual deformations (those which correspond to stresses which satisfy equilibrium) are the ones for which the total potential energy assumes a stationary value* (Pilkey and Wunderlich, 1994) or $\delta\Pi = 0$.

As previously discussed, the structure is unstable at buckling. The theorem of minimum total potential energy states that this stationary value of Π at an equilibrium position is minimum when the position is stable. Therefore the equilibrium position can be considered stable when

$$\frac{1}{2}\delta^2 \Pi > 0 \tag{3.3}$$

and likewise is unstable when

$$\frac{1}{2}\delta^2 \Pi < 0 \tag{3.4}$$

Therefore, the critical condition for buckling would be when the total potential energy is *equal* to zero, thus representing the transition from a stable to unstable state (Pi, et al., 1992).

$$\frac{1}{2}\delta^2 \Pi = 0 \tag{3.5}$$

Substituting Eq. (3.1) yields the critical condition for buckling as

$$\frac{1}{2}\left(\delta^2 U + \delta^2 \Omega\right) = 0 \tag{3.6}$$

3.1 STRAIN ENERGY

The strain energy portion of the total potential energy may be expressed as a function of the longitudinal and shear strains as well as stresses. Assume an arbitrary point P_o in the cross section of the thin walled member. The strain energy of the member can be expressed as

$$U = \frac{1}{2}\int_L \int_A \left(\varepsilon_p \sigma_p + \gamma_p \tau_p\right) dA\, dz \tag{3.7}$$

where

ε_p = longitudinal strain of point P_o

σ_p = longitudinal stress of point P_o

γ_p = shear strain of point P_o

τ_p = shear stress of point P_o

With its second variation being

$$\frac{1}{2}\delta^2 U = \frac{1}{2}\int_L\int_A \left(\delta\varepsilon_p\delta\sigma_p + \delta\gamma_p\delta\tau_p + \delta^2\varepsilon_p\sigma_p + \delta^2\gamma_p\tau_p\right)dA\ dz \tag{3.8}$$

ε_p, σ_p, γ_p, and τ_p and their variations will be expressed in terms of centroidal displacements in the following section in order to derive the energy equation for lateral-torsional buckling.

3.1.1 Displacements

In order to properly investigate deformations in a beam-column, two sets of coordinate systems are defined. In the fixed global coordinate system *oxyz*, the axis *oz* is fixed and coincides with the centroidal axis of the undeformed beam. The axes *ox* and *oy* represent the principle axes of the undeformed beam, as shown in Figure 3.4.

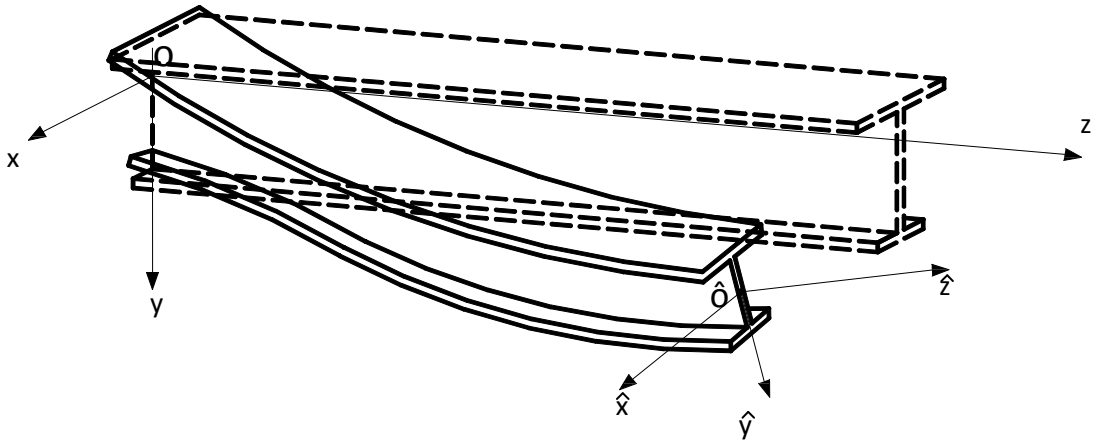

Figure 3.4 Deformed Beam

The second set of coordinate systems is a moving, right hand, local coordinate system, $\hat{o}\hat{x}\hat{y}\hat{z}$. The origin of this coordinate system is at point $\hat{o}$ located on the centroidal axis of the beam and moves with the beam during displacement, as shown in Figure 3.4. The axis $\hat{o}\hat{z}$ coincides with the tangent at $\hat{o}$ after the centroidal axis has been deformed. The principle axes of the deformed beam are $\hat{o}\hat{x}$ and $\hat{o}\hat{y}$.

When the beam column element buckles, point P_o on the beam moves to point P. This deformation occurs in two stages. Point P_o first translates to point P_t by the displacements u, v, and w. The point P_t then rotates through an angle θ to the point P about the line on where the line on passes through the points o and $\hat{o}$. After the rotation, the moving local coordinate system $\hat{o}\hat{x}\hat{y}\hat{z}$ becomes fixed. The transition of point P_o to point P can be seen in Figure 3.5. The directional cosines of the moving axes $\hat{o}\hat{x}$, $\hat{o}\hat{y}$, and $\hat{o}\hat{z}$ relative to the fixed global axes ox, oy, and oz can be determined by assuming rigid body rotation of the axes through an angle θ (Pi, et al., 1992).

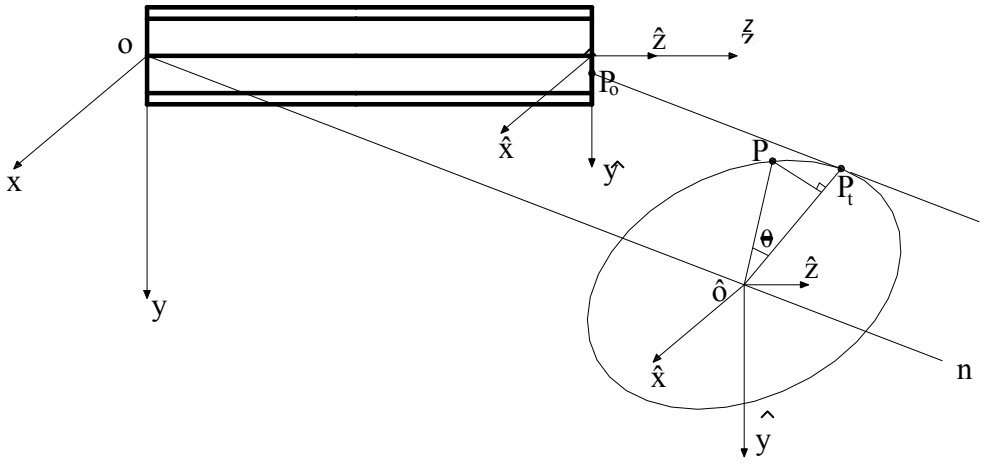

Figure 3.5 Translation of Point P_o to Point P

The displacements of point P_o can be expressed as (Pi, et al., 1992)

$$\begin{Bmatrix} u_p \\ v_p \\ w_p \end{Bmatrix} = \begin{Bmatrix} u \\ v \\ w \end{Bmatrix} + T_R \begin{Bmatrix} \hat{x} \\ \hat{y} - \hat{y}_o \\ -\omega k_z \end{Bmatrix} - \begin{Bmatrix} \hat{x} \\ \hat{y} - \hat{y}_o \\ 0 \end{Bmatrix} \tag{3.9}$$

Where u_p, v_p, and w_p are total displacements of general point $P_o(\hat{x},\hat{y},0)$. Note that *u, v,* and *w* are shear center displacements and $(\hat{y} - \hat{y}_o)$ is the distance between the centroid and the shear center, as seen in Figure 3.3. ω is the section warping function (Vlasov, 1961) and $-\omega k_z$ is the warping displacement and represents the deformation in the z-direction.

The first term on the right side of the equation contains the shear center displacement as the point P_o translates laterally to point P_t. The remaining terms on the right side of the equation represent the rotation of point P_t to its final destination at point *P*. T_R is defined as the rotational transformation matrix of the angle of rotation, θ. Assuming small angles of rotation

$$T_R = \begin{bmatrix} 1 - \frac{\theta_y^2}{2} - \frac{\theta_z^2}{2} & -\theta_z + \frac{\theta_x\theta_y}{2} & \theta_y + \frac{\theta_x\theta_z}{2} \\ \theta + \frac{\theta_x\theta_y}{2} & 1 - \frac{\theta_x^2}{2} - \frac{\theta_z^2}{2} & -\theta_x + \frac{\theta_y\theta_z}{2} \\ -\theta_y + \frac{\theta_x\theta_z}{2} & \theta_x + \frac{\theta_y\theta_z}{2} & 1 - \frac{\theta_x^2}{2} - \frac{\theta_y^2}{2} \end{bmatrix} \tag{3.10}$$

where θ_x, θ_y, and θ_z are components of the rotation θ in the *x*, *y*, and *z* directions, respectively (Torkamani, 1998).

Consider an undeformed element Δz and its deformed counterpart $\Delta z(1+\varepsilon)$, where ε represents the strain. $\Delta u, \Delta v,$ and $(\Delta z + \Delta w)$ are components of the deformed element length

$\Delta z(1+\varepsilon)$ on the *ox*, *oy*, and *oz* axes, respectively. The relationship between the deformed element and its components can be expressed as

$$\Delta z(1+\varepsilon)\vec{N}_z = \Delta u\,\vec{i} + \Delta v\,\vec{j} + (\Delta z + \Delta w)\vec{k} \tag{3.11}$$

where $\vec{N}_z$ is a unit vector in the $\hat{oz}$ direction.

$\Delta z(1+\varepsilon)\vec{N}_z$ is projected on the x and y axes as

$$\Delta u = \Delta z\,(1+\varepsilon)\,\vec{N}_z \cdot \vec{i} = \Delta z\,(1+\varepsilon) l_z \tag{3.12}$$

$$\Delta v = \Delta z\,(1+\varepsilon)\,\vec{N}_z \cdot \vec{j} = \Delta z(1+\varepsilon) m_z \tag{3.13}$$

where l_z, m_z, and n_z are directional cosines of the $\hat{oz}$ direction with respect to the *oxyz* fixed coordinate system.

Dividing the previous equations by Δz, and taking the limit as Δz goes to zero gives

$$\frac{du}{dz} = \lim_{\Delta z \to o} \frac{\Delta u}{\Delta z} = \lim_{\Delta z \to o} \frac{\Delta z(1+\varepsilon) l_z}{\Delta z} = (1+\varepsilon) l_z \tag{3.14}$$

$$\frac{dv}{dz} = \lim_{\Delta z \to o} \frac{\Delta v}{\Delta z} = \lim_{\Delta z \to o} \frac{\Delta z(1+\varepsilon) m_z}{\Delta z} = (1+\varepsilon) m_z \tag{3.15}$$

Where l_z and m_z are defined as . (Torkamani, 1998)

$$l_z = \theta_y + \frac{\theta_x \theta_z}{2} \tag{3.16}$$

$$m_z = -\theta_x + \frac{\theta_y \theta_z}{2} \tag{3.17}$$

Therefore

$$\frac{du}{dz} = \left(\theta_y + \frac{\theta_x \theta_z}{2}\right)(1+\varepsilon) \tag{3.18}$$

$$\frac{dv}{dz} = \left(-\theta_x + \frac{\theta_y \theta_z}{2}\right)(1+\varepsilon) \tag{3.19}$$

By disregarding higher order terms, strain is eliminated and Eqs. (3.18) and (3.19) become

$$\frac{du}{dz} \approx \left(\theta_y + \frac{\theta_x \theta_z}{2} \right) \tag{3.20}$$

$$\frac{dv}{dz} \approx \left(-\theta_x + \frac{\theta_y \theta_z}{2} \right) \tag{3.21}$$

Solving for θ_x and θ_y from the previous equations yields

$$\theta_x = -\frac{dv}{dz} + \frac{1}{2}\theta_z \frac{du}{dz} \tag{3.22}$$

$$\theta_y = \frac{du}{dz} + \frac{1}{2}\theta_z \frac{dv}{dz} \tag{3.23}$$

Projecting the unit lengths along the $\hat{o}\hat{x}$ axis onto the *oy* axis and the $\hat{o}\hat{y}$ axis onto the *ox* axis yield m_x and l_y respectively. (Torkamani, 1998)

$$l_y = -\theta_z + \frac{\theta_x \theta_y}{2} \tag{3.24}$$

$$m_x = \theta_z + \frac{\theta_x \theta_y}{2} \tag{3.25}$$

The projections $-\theta_z + \frac{\theta_x \theta_y}{2}$ and $\theta_z + \frac{\theta_x \theta_y}{2}$ of unit lengths along the $\hat{o}\hat{y}$ and $\hat{o}\hat{x}$ axes onto the ox and oy axes, respectively, can be used to define the the mean twist rotation, ϕ, of the $\hat{o}\hat{x}$ and $\hat{o}\hat{y}$ axes on the *oz* axis is

$$\phi = \frac{1}{2}\left[\left(\theta_z + \frac{\theta_x \theta_y}{2} \right) - \left(-\theta_z + \frac{\theta_x \theta_y}{2} \right) \right] \tag{3.26}$$

Which simplifies to

$$\phi = \theta_z \tag{3.27}$$

Substituting the expressions for θ_x, θ_y, and θ_z into the rotational transformation matrix, T_R, yields

$$T_R = \begin{bmatrix} l_x & l_y & l_z \\ m_x & m_y & m_z \\ n_x & n_y & n_z \end{bmatrix} \tag{3.28}$$

Where

$$l_x = 1 - \frac{1}{2}\left(\frac{du}{dz}\right)^2 - \frac{1}{2}\phi^2 - \frac{1}{2}\frac{du}{dz}\frac{dv}{dz}\phi \tag{3.29}$$

$$l_y = -\phi - \frac{1}{2}\frac{du}{dz}\frac{dv}{dz} + \frac{1}{4}\left(\frac{du}{dz}\right)^2\phi - \frac{1}{4}\left(\frac{dv}{dz}\right)^2\phi \tag{3.30}$$

$$l_z = \frac{du}{dz} \tag{3.31}$$

$$m_x = \phi - \frac{1}{2}\frac{du}{dz}\frac{dv}{dz} - \frac{1}{4}\left(\frac{dv}{dz}\right)^2\phi + \frac{1}{4}\left(\frac{du}{dz}\right)^2\phi \tag{3.32}$$

$$m_y = 1 - \frac{1}{2}\left(\frac{dv}{dz}\right)^2 - \frac{1}{2}\phi^2 + \frac{1}{2}\frac{du}{dz}\frac{dv}{dz}\phi \tag{3.33}$$

$$m_z = \frac{dv}{dz} \tag{3.34}$$

$$n_x = -\frac{du}{dz} - \frac{dv}{dz}\phi + \frac{1}{4}\frac{du}{dz}\phi^2 \tag{3.35}$$

$$n_y = -\frac{dv}{dz} + \frac{du}{dz}\phi + \frac{1}{4}\frac{dv}{dz}\phi^2 \tag{3.36}$$

$$n_z = 1 - \frac{1}{2}\left(\frac{du}{dz}\right)^2 - \frac{1}{2}\left(\frac{dv}{dz}\right)^2 \tag{3.37}$$

The torsional curvature is (Love, 1944)

$$k_z = \frac{dl_x}{dz}l_y + \frac{dm_x}{dz}m_y + \frac{dn_x}{dz}n_y \tag{3.38}$$

Substituting l_x through n_y into the previous expression yields a nonlinear expression for torsional curvature as

$$k_z = \frac{d\phi}{dz} + \frac{1}{2}\left(\frac{d^2u}{dz^2}\frac{dv}{dz} - \frac{d^2v}{dz^2}\frac{du}{dz}\right) \tag{3.39}$$

Eliminating second and higher order terms, the expression for torsional curvature may be simplified to

$$k_z = \frac{d\phi}{dz} \tag{3.40}$$

Substituting Eqs. (3.29) – (3.37) into Eq. (3.9) yield the displacement of an arbitrary point P_o in terms of shear center displacements, rotations, and the section warping. The total displacements u_p, v_p, and w_p can be considered the sum of linear and quadratic components of the form

$$\begin{Bmatrix} u_p \\ v_p \\ w_p \end{Bmatrix} = \begin{Bmatrix} u_{pl} \\ v_{pl} \\ w_{pl} \end{Bmatrix} + \begin{Bmatrix} u_{pn} \\ v_{pn} \\ w_{pn} \end{Bmatrix} \tag{3.41}$$

where

$$\begin{Bmatrix} u_{pl} \\ v_{pl} \\ w_{pl} \end{Bmatrix} = \begin{Bmatrix} u - (\hat{y} - \hat{y}_o)\phi \\ v + \hat{x}\phi \\ w - \hat{x}\dfrac{du}{dz} - \hat{y}\dfrac{dv}{dz} - \omega\dfrac{d\phi}{dz} \end{Bmatrix} \tag{3.42}$$

$$\begin{Bmatrix} u_{pn} \\ v_{pn} \\ w_{pn} \end{Bmatrix} = \begin{Bmatrix} -\frac{1}{2}\hat{x}\left(\left(\frac{du}{dz}\right)^2 + \phi^2 + \left(\frac{du}{dz}\right)\left(\frac{dv}{dz}\right)\phi\right) - \frac{1}{2}(\hat{y} - \hat{y}_o)\left(\frac{du}{dz}\frac{dv}{dz} - \frac{1}{2}\left(\frac{du}{dz}\right)^2\phi + \frac{1}{2}\left(\frac{dv}{dz}\right)^2\phi\right) - \omega\frac{du}{dz}\frac{d\phi}{dz} \\ -\frac{1}{2}\hat{x}\left(\frac{du}{dz}\frac{dv}{dz} + \frac{1}{2}\left(\frac{dv}{dz}\right)^2\phi - \frac{1}{2}\left(\frac{du}{dz}\right)^2\phi\right) - \frac{1}{2}(\hat{y} - \hat{y}_o)\left(\left(\frac{dv}{dz}\right)^2 + \phi^2 - \frac{du}{dz}\frac{dv}{dz}\phi\right) - \omega\frac{dv}{dz}\frac{d\phi}{dz} \\ -\hat{x}\left(\frac{dv}{dz}\phi - \frac{1}{4}\frac{du}{dz}\phi^2\right) + (\hat{y} - \hat{y}_o)\left(\frac{du}{dz}\phi + \frac{1}{4}\frac{dv}{dz}\phi^2\right) + \frac{1}{2}\omega\frac{d\phi}{dz}\left(\left(\frac{du}{dz^2}\right)^2 + \left(\frac{dv}{dz^2}\right)^2\right) \end{Bmatrix} \tag{3.43}$$

The relationship between the displacement of the shear center, w_s, and the displacement of the centroid, w, in the z-direction can be expressed as (Pi and Trahair, 1992a)

$$w_s = w - \hat{y}_o\left(\frac{dv}{dz} - \frac{1}{2}\frac{dv}{dz}\phi^2 - \frac{du}{dz}\phi\right) \tag{3.44}$$

The derivatives of u_p, v_p, and w_p with respect to z are

$$\frac{du_p}{dz} = \frac{du}{dz} - \hat{y}\frac{d\phi}{dz} + \hat{y}_o\frac{d\phi}{dz} + O_x\left(\frac{du}{dz}, \frac{dv}{dz}, \phi\right) \tag{3.45}$$

$$\frac{dv_p}{dz} = \frac{dv}{dz} - \hat{x}\frac{d\phi}{dz} + O_y\left(\frac{du}{dz}, \frac{dv}{dz}, \phi\right) \tag{3.46}$$

$$\frac{dw_p}{dz} = \frac{dw}{dz} - \hat{x}\frac{d^2u}{dz^2} - \hat{y}\frac{d^2v}{dz^2} - \omega\frac{d^2\phi}{dz^2} - \hat{x}\frac{d\phi}{dz}\frac{dv}{dz} - \hat{x}\phi\frac{d^2v}{dz^2} + \hat{y}\frac{d\phi}{dz}\frac{du}{dz} + \hat{y}\phi\frac{d^2u}{dz^2} + O_z\left(\frac{du}{dz}, \frac{dv}{dz}, \phi\right) \tag{3.47}$$

The terms O_x, O_y, and O_z represent terms that are second order or higher and may be disregarded.

3.1.2 Strains

The longitudinal normal strain ε_p of point P can be expressed in terms of the rates of change of the displacements of point P as

$$\varepsilon_p = \frac{dw_p}{dz} + \frac{1}{2}\left(\left(\frac{du_p}{dz}\right)^2 + \left(\frac{dv_p}{dz}\right)^2 + \left(\frac{dw_p}{dz}\right)^2\right) \tag{3.48}$$

For small strains, $\left(\frac{dw_p}{dz}\right)^2$ is small compared to $\left(\frac{du_p}{dz}\right)^2$ and $\left(\frac{dv_p}{dz}\right)^2$ and can be disregarded.

Therefore

$$\varepsilon_p = \frac{dw_p}{dz} + \frac{1}{2}\left(\left(\frac{du_p}{dz}\right)^2 + \left(\frac{dv_p}{dz}\right)^2\right) \tag{3.49}$$

Substituting in the derivatives of the displacements u_p, v_p, and w_p of point P_o yields

$$\varepsilon_p = \frac{dw}{dz} - \hat{x}\frac{d^2u}{dz^2} - \hat{y}\frac{d^2v}{dz^2} - \omega\frac{d^2\phi}{dz^2} + \frac{1}{2}\left(\left(\frac{du}{dz}\right)^2 + \left(\frac{dv}{dz}\right)^2\right) - \hat{x}\frac{d^2v}{dz^2}\phi + \hat{y}\frac{d^2u}{dz^2}\phi + \hat{y}_o\frac{du}{dz}\frac{d\phi}{dz}$$

$$+ \frac{1}{2}\left(\hat{x}^2 + \left(\hat{y} - \hat{y}_o\right)^2\right)\left(\frac{d\phi}{dz}\right)^2 \tag{3.50}$$

The first variation of the longitudinal strain is

$$\delta\varepsilon_p = \frac{d\delta w}{dz} - \hat{x}\frac{d^2\delta u}{dz^2} - \hat{y}\frac{d^2\delta v}{dz^2} - \omega\frac{d^2\delta\phi}{dz^2} + \frac{d\delta u}{dz}\frac{du}{dz} + \frac{d\delta v}{dz}\frac{dv}{dz} - \hat{x}\frac{d^2\delta v}{dz^2}\phi - \hat{x}\frac{d^2v}{dz^2}\delta\phi + \hat{y}\frac{d^2\delta u}{dz^2}\phi$$

$$+ \hat{y}\frac{d^2u}{dz^2}\delta\phi + \hat{y}_o\frac{d\delta u}{dz}\frac{d\phi}{dz} + \hat{y}_o\frac{du}{dz}\frac{d\delta\phi}{dz} + \left(\hat{x}^2 + \left(\hat{y} - \hat{y}_o\right)^2\right)\frac{d\delta\phi d\phi}{dz} \tag{3.51}$$

The second variation of the longitudinal strain is

$$\delta^2\varepsilon_p = \left(\frac{d\delta u}{dz}\right)^2 + \left(\frac{d\delta v}{dz}\right)^2 - 2\hat{x}\frac{d^2\delta v}{dz^2}\delta\phi + 2\hat{y}\frac{d^2\delta u}{dz^2}\delta\phi + 2\hat{y}_o\frac{d\delta u}{dz}\frac{d\delta\phi}{dz} + \left(\hat{x}^2 + \left(\hat{y} - \hat{y}_o\right)^2\right)\left(\frac{d\delta\phi}{dz}\right)^2 \tag{3.52}$$

It is assumed that the second variations of the displacements in Eq. (3.52) vanishes. The above equations contain a combination of the strains before and after buckling. In this case, the prebuckling displacements are defined as v and w. During buckling, the displacements are defined as δu and $\delta\phi$. Therefore, the displacements u, ϕ, δv, and δw are equal to zero and may be eliminated from the above equations.

The equations for longitudinal strain and its first and second variation thus become

$$\varepsilon_p = \frac{dw}{dz} - \hat{y}\frac{d^2v}{dz^2} + \frac{1}{2}\left(\frac{dv}{dz}\right)^2 \tag{3.53}$$

$$\delta\varepsilon_p = -\hat{x}\frac{d^2\delta u}{dz^2} - \omega\frac{d^2\delta\phi}{dz^2} - \hat{x}\frac{d^2v}{dz^2}\delta\phi \tag{3.54}$$

$$\delta^2\varepsilon_p = \left(\frac{d\delta u}{dz}\right)^2 + 2\hat{y}\frac{d^2\delta u}{dz^2}\delta\phi + 2\hat{y}_o\frac{d\delta u}{dz}\frac{d\delta\phi}{dz} + \left(\hat{x}^2 + \left(\hat{y} - \hat{y}_o\right)^2\right)\left(\frac{d\delta\phi}{dz}\right)^2 \tag{3.55}$$

The shear strains due to bending and warping of the thin walled section are neglected. The shear strain at point P_o due to uniform torsion is (Pi and Trahair, 1992a)

$$\gamma_p = -2t_p\frac{d\phi}{dz} \tag{3.56}$$

Where t_p represents the distance of P_o from the midthickness line of the cross-section.

The first variation of the shear strain is

$$\delta\gamma_p = -2t_p\frac{d\delta\phi}{dz} \tag{3.57}$$

And the second variation of the shear strain is assumed to be zero.

$$\delta^2\gamma_p = 0 \tag{3.58}$$

3.1.3 Stresses and Stress Resultants

The stresses at point P_o can be related to the strains by Hooke's Law as

$$\begin{Bmatrix}\sigma_p\\ \tau_p\end{Bmatrix} = \begin{bmatrix}E & 0\\ 0 & G\end{bmatrix}\begin{Bmatrix}\varepsilon_p\\ \gamma_p\end{Bmatrix} \tag{3.59}$$

The stress resultants for a beam bending are:

$$M_x = \int_A \hat{y}\sigma_p dA \tag{3.60}$$

$$F = \int_A \sigma_p dA \tag{3.61}$$

So that

$$\sigma_p = \frac{F}{A} + \frac{M_x \hat{y}}{I_x} \tag{3.62}$$

3.1.4 Section Properties

$$\int_A \hat{x} dA = \int_A \hat{y} dA = 0 \tag{3.63}$$

$$\int_A \hat{x}\hat{y} dA = 0 \tag{3.64}$$

$$A = \int dA \tag{3.65}$$

$$I_x = \int_A \hat{y}^2 dA \tag{3.66}$$

$$I_y = \int_A \hat{x}^2 dA \tag{3.67}$$

These section properties are valid for not only monosymmetric beams, but doubly symmetric ones as well. To solve the energy equation for monosymmetric beams, additional section properties must be introduced.

$$\rho = \frac{I_{yC}}{I_{yT} + I_{yC}} = \frac{I_{yC}}{I_y} \tag{3.68}$$

Where I_{yT} and I_{yC} are the minor axis second moments of area of the tension and compression flanges, respectively (Kitipornchai and Trahair, 1980). The value of ρ can range from 0 to 1, with doubly symmetric I-beams having a value of 0.5. The warping moment of inertia given in Eq. (3.69), with other section properties listed below.

$$I_w = \rho(1-\rho) I_y h^2 \tag{3.69}$$

$$J = \sum \frac{bt^3}{3} \tag{3.70}$$

$$r_o^{\,2} = \frac{I_x + I_y}{A} + \hat{y}_o^{\,2} \tag{3.71}$$

$$\beta_x = \frac{1}{I_x}\left(\int_A \hat{x}^2 y \, dA + \int_A \hat{y}^3 \, dA \right) - 2\hat{y}_o \tag{3.72}$$

where r_o is the polar radius of gyration for the beam about the shear center. β_x is known as the monosymmetric parameter (Trahair and Nethercot, 1984) . The term β_x arises from the Wagner effect discussed previously in this chapter when the compressive stresses do not equally oppose the tensile stresses in a member. In the case of doubly symmetric beams, the stresses balance each other and β_x is equal to zero. When the smaller flange of a monosymmetric beam is in compression, there is a reduction in the effective torsional stiffness and β_x is negative. Conversely, when the smaller flange is in tension, the effective torsional stiffness is greater and β_x is positive.

3.2 STRAIN ENERGY EQUATION FOR MONOSYMMETRIC BEAM-COLUMN

With the newly introduced section properties, the second variation of the strain energy of the monosymmetric beam can now be derived to its accepted form. Substituting $\varepsilon_p, \delta\varepsilon_p, \delta^2\varepsilon_p, \gamma_p, \delta\gamma_p$ and $\delta^2\gamma_p$ as well as the stress resultants M_x and F and the section properties into Eq. (3.8) yields

$$\frac{1}{2}\delta^2 U = \frac{1}{2}\int_L \left\{ EI_y\left(\frac{d^2(\delta u)}{dz^2}\right)^2 + GJ\left(\frac{d\ (\delta\phi)}{dz}\right)^2 + EI_\omega\left(\frac{d^2(\delta\phi)}{dz^2}\right)^2 \right.$$

$$+ F\left[\left(\frac{d(\delta u)}{dz}\right)^2 + 2\hat{y}_o\left(\frac{d(\delta u)}{dz}\right)\left(\frac{d(\delta\phi)}{dz}\right) + \left(r_o^{\,2} + \hat{y}_o^{\,2}\right)\left(\frac{d\ (\delta\phi)}{dz}\right)^2\right]$$

$$\left. + M_x(z)\left[2\left(\frac{d^2(\delta u)}{dz^2}\right)\delta\phi + \beta_x\left(\frac{d(\delta\phi)}{dz}\right)^2\right]\right\} dz \qquad (3.73)$$

3.3 POTENTIAL ENERGY OF THE EXTERNAL LOADS

The equations for the potential energy possessed by the loads, or the work done by external forces, are derived by multiplying the loads by their corresponding displacements, and summing them up.

$$\Omega = -\int_L (v_q q)dz - \sum (v_P P - \frac{dv_M}{dz} M + w_F F) \tag{3.74}$$

With its second variation being

$$\frac{1}{2}\delta^2\Omega = -\int_L \left(\delta^2 v_q q\right)dz - \sum\left(\delta^2 v_P P - \frac{d\delta^2 v_M}{dz} M + \delta^2 w_F F\right) \tag{3.75}$$

Where

v_q = vertical displacement which transverse distributed load q acts

q = transverse distributed load in y-direction

v_P = vertical displacement which transverse concentrated load P acts

P = transverse concentrated load in y-direction

v_M = vertical displacement which moment M acts

$\frac{dv_M}{dz}$ = rotation caused by moment M

M = applied moment in x-direction

w_F = longitudinal displacement which load F acts

F = concentric load in z-direction

3.3.1 Displacements and Rotations of Load Points

The longitudinal displacement, w_F, is considered to be relatively small. Therefore, $w_F = 0$.

The vertical displacement of a point $\left(\hat{x} = 0, \hat{y} = a, \omega = 0\right)$ at which a transverse distributed load q acts may be found by

$$v_q = v + m_y a - a \tag{3.76}$$

Where

$$m_y = 1 - \frac{1}{2}\left(\frac{dv}{dz}\right)^2 - \frac{1}{2}\phi^2 + \frac{1}{2}\frac{du}{dz}\frac{dv}{dz}\phi \tag{3.77}$$

Therefore,

$$v_q = v - \frac{1}{2}\left(a - \hat{y}_o\right)\left[\left(\frac{dv}{dz}\right)^2 + \phi^2 - \frac{du}{dz}\frac{dv}{dz}\phi\right] \tag{3.78}$$

Similarly, the vertical displacement of a point $\left(\hat{x} = 0, \hat{y} = e, \omega = 0\right)$ at which a transverse concentrated load, *P*, acts is expressed as

$$v_P = v - \frac{1}{2}\left(e - \hat{y}_o\right)\left[\left(\frac{dv}{dz}\right)^2 + \phi^2 - \frac{du}{dz}\frac{dv}{dz}\phi\right] \tag{3.79}$$

The rotation about an axis parallel to the original axis *ox* at a point $\left(\hat{x} = 0, \hat{y} = y_M, \omega = 0\right)$ at which concentrated moment M_x acts is

$$\frac{dv_M}{dz} = \frac{dv}{dz} \tag{3.80}$$

Because the effects of prebuckling are negected, the deformation *v* and its derivatives are reduced to zero. These effects will be implemented in a later section. The displacements corresponding to the external loads then simplify to

$$v_q = -\frac{1}{2}\left(a - \hat{y}_o\right)\phi^2 \tag{3.81}$$

$$v_P = -\frac{1}{2}\left(e - \hat{y}_o\right)\phi^2 \tag{3.82}$$

$$\frac{dv_M}{dz} = 0 \tag{3.83}$$

The second variations of the displacements are

$$\delta^2 v_q = -\frac{1}{2}\left(a - \hat{y}_o\right)\left(\delta\phi\right)^2 \tag{3.84}$$

$$\delta^2 v_P = -\frac{1}{2}\left(e - \hat{y}_o\right)\left(\delta\phi\ \right)^2 \tag{3.85}$$

$$\frac{dv_M}{dz} = 0 \tag{3.86}$$

Substituting Eqs. (3.84) – (3.86) into Eq. (3.75) yields

$$\frac{1}{2}\delta^2\Omega = \frac{1}{2}\int_L q\left(a - \hat{y}_o\right)\left(\delta\phi\right)^2 dz + \frac{1}{2}\sum P\left(e - \hat{y}_o\right)\left(\delta\phi\right)^2 \tag{3.87}$$

3.4 ENERGY EQUATION FOR LATERAL TORSIONAL BUCKLING OF MONOSYMMETRIC BEAMS

The second variation of the total potential energy equation for lateral torsional buckling of monosymmetric beams is the sum of the second variation of the strain energy equation given in Eq. (3.74) and the second variation of the potential energy of the loads given in Eq. (3.87), as shown below.

$$\frac{1}{2}\delta^2\Pi = \frac{1}{2}\int_L \left\{ EI_y\left(\frac{d^2(\delta u)}{dz^2}\right)^2 + GJ\left(\frac{d\ (\delta\phi)}{dz}\right)^2 + EI_\omega\left(\frac{d^2(\delta\phi)}{dz^2}\right)^2 \right.$$

$$+ F\left[\left(\frac{d(\delta u)}{dz}\right)^2 + 2\hat{y}_o\left(\frac{d(\delta u)}{dz}\right)\left(\frac{d(\delta\phi)}{dz}\right) + \left(r_o^{\,2} + \hat{y}_o^{\,2}\right)\left(\frac{d\ (\delta\phi)}{dz}\right)^2\right]$$

$$\left. + M_x(z)\left[2\left(\frac{d^2(\delta u)}{dz^2}\right)\delta\phi + \beta_x\left(\frac{d(\delta\phi)}{dz}\right)^2\right]\right\} dz$$

$$+ \frac{1}{2}\int_L q\left(a - \hat{y}_o\right)(\delta\phi)^2\, dz + \frac{1}{2}\sum P\left(e - \hat{y}_o\right)(\delta\phi)^2 = 0 \qquad (3.88)$$

Where

$$M_x = M_1 + V_1 z - q\frac{z^2}{2} \text{ for } 0 < z < z_p$$

$$M_x = M_1 + V_1 z - q\frac{z^2}{2} - P\left(z - z_p\right) \text{ for } z_p < z < L$$

z_p = distance along beam in z-direction of applied concentrated load, P

The terms in the energy equation can be separated into three groups. The first group consists of the terms that contain the buckling rigidities EI_y, GJ, and EI_ω and represent strain energy stored during buckling. The second group consists of the terms that contain the stress resultants F and M_x, which represent the work done by the applied loads at the shear center. The third group consists of the remaining terms which represent the work done by transverse forces q and P.

3.5 NON-DIMENSIONAL ENERGY EQUATION FOR LATERAL-TORSIONAL BUCKLING

The energy equation presented in the previous section has limitations in predicting a lateral-torsional buckling parameter obtained from the solution of the eigenvalue problem because it depends on beam properties such as *E*, *G*, *L*, etc. Elimination of these properties through a non-dimensional analysis will provide more general results to determine critical loads and moments for lateral-torsional buckling.

The stiffness parameter, K, of the beam is defined as

$$K = \sqrt{\frac{\pi^2 EI_\omega}{GJL^2}} \approx \sqrt{\frac{\pi^2 EI_y h^2}{4GJL^2}} \tag{3.89}$$

The loading parameters are

$$\gamma_P = \frac{PL^2}{\sqrt{EI_y GJ}} \tag{3.90}$$

$$\gamma_q = \frac{qL^3}{\sqrt{EI_y GJ}} \tag{3.91}$$

The monosymmetry parameters are (Kitipornchai, et al.1980)

$$\bar{\beta}_x = \frac{\beta_x}{L}\sqrt{\frac{EI_y}{GJ}} \tag{3.92}$$

$$\bar{r}_o = \frac{r_o}{L}\sqrt{\frac{EI_y}{GJ}} \tag{3.93}$$

$$\bar{y}_o = \frac{2\hat{y}_o}{h} \tag{3.94}$$

Other useful parameters for the non-dimensional analysis are

$$\delta\bar{u} = \frac{\delta u}{L}\sqrt{\frac{EI_y}{GJ}} \tag{3.95}$$

$$\bar{F} = \frac{FL^2}{EI_y} \tag{3.96}$$

$$\bar{M}_1 = \frac{M_1 L}{\sqrt{EI_y GJ}} \tag{3.97}$$

$$\bar{V}_1 = \frac{V_1 L^2}{\sqrt{EI_y GJ}} \tag{3.98}$$

$$\bar{z} = \frac{z}{L} \tag{3.99}$$

$$\bar{z}_p = \frac{z_p}{L} \tag{3.100}$$

$$\bar{a} = \frac{2a}{h} \tag{3.101}$$

$$\bar{e} = \frac{2e}{h} \tag{3.102}$$

where

h = the distance between the centroids of the flanges

The application of these parameters to the energy equation derived in the previous section yield a non-dimensional energy equation that provides a buckling parameter for lateral torsional buckling of a beam-column with a monosymmetric cross-section. The multiplication factor used to change the energy equation to a non-dimensional form is

$$\overline{\Pi} = \frac{2\Pi L}{GJ} \tag{3.103}$$

The second variation of the non-dimensional total potential energy equation is

$$\frac{1}{2}\delta^2\overline{\Pi} = \frac{1}{2}\int_0^1 \left\{ \left(\frac{d^2(\delta\overline{u})}{d\overline{z}^2} \right)^2 + \left(\frac{d\ (\delta\phi)}{d\overline{z}} \right)^2 + \frac{K^2}{\pi^2}\left(\frac{d^2(\delta\phi)}{dz^2} \right)^2 \right\} d\overline{z}$$

$$+ \overline{F}\int_0^1 \left[\left(\frac{d(\delta\overline{u})}{d\overline{z}} \right)^2 + 2\overline{y}_o \left(\frac{d(\delta\overline{u})}{d\overline{z}} \right)\left(\frac{d(\delta\phi)}{d\overline{z}} \right) + \left(\overline{r}_o{}^2 + \overline{y}_o{}^2 \right)\left(\frac{d\ (\delta\phi)}{d\overline{z}} \right)^2 \right] d\overline{z}$$

$$+ \overline{M}\int_0^1 \left[\left(\frac{d^2(\delta\overline{u})}{d\overline{z}^2} \right)\delta\phi + \overline{\beta}_x \left(\frac{d(\delta\phi)}{d\overline{z}} \right)^2 \right] d\overline{z}$$

$$+ \frac{K}{\pi}\left[\int_0^1 \overline{q}\left(\overline{a} - \overline{y}_o \right)\left(\delta\phi \right)^2 d\overline{z} + \sum \overline{P}_i \left(\overline{e} - \overline{y}_o \right)\left(\delta\phi_i \right)^2 \right] \tag{3.104}$$

where

$$\overline{M}_x = \overline{M}_1 + \overline{V}_1\overline{z} - \overline{q}\frac{\overline{z}^2}{2} \quad \text{for } 0 < \overline{z} < \overline{z}_p$$

$$\overline{M}_x = \overline{M}_1 + \overline{V}_1\overline{z} - \overline{q}\frac{\overline{z}^2}{2} - \overline{P}\left(\overline{z} - \overline{z}_p \right) \quad \text{for } \overline{z}_p < \overline{z} < 1$$

4.0 LATERAL-TORSIONAL BUCKLING OF MONOSYMMETRIC BEAMS CONSIDERING PREBUCKLING DEFLECTIONS

In the previous chapter, the effects of prebuckling deflections were ignored. These effects are ignored assuming that the thin-walled object is almost perfectly straight and any deformation is so small that it may be disregarded. This assumption is only valid when the ratios of minor axis flexural stiffness and torsional stiffness to the major axis flexural stiffness are very small. In the case where the ratios are not small, the effects of prebuckling deflections may significantly alter buckling loads and therefore cannot be ignored.

4.1 STRAIN ENERGY CONSIDERING PREBUCKLING DEFLECTIONS

4.1.1 Displacements

In the previous chapter, the expression for torsional curvature was simplified to include just the first term because the other terms in the expression were deemed to be relatively small. To consider the effects of prebuckling deflections, the torsional curvature, k_z, must be represented by:

$$k_z = \phi^2 + \frac{1}{2}\left(\frac{d^2u}{dz^2}\frac{dv}{dz} - \frac{du}{dz}\frac{d^2v}{dz^2}\right) \tag{4.1}$$

Which creates a longitudinal displacement of

$$w_p = \left[w - \hat{x}\frac{du}{dz} - \hat{y}\frac{dv}{dz} - \omega\frac{d\phi}{dz}\right] + \left[-\hat{x}\left(\frac{dv}{dz}\phi - \frac{1}{4}\frac{du}{dz}\phi^2\right) + \hat{y}\left(\frac{du}{dz}\phi + \frac{1}{4}\frac{dv}{dz}\phi^2\right)\right.$$

$$\left. - \omega\left(\frac{1}{2}\left(\frac{d^2u}{dz^2}\frac{dv}{dz} - \frac{d^2v}{dz^2}\frac{du}{dz}\right) - \frac{1}{2}\left(\frac{d\phi}{dz} + \frac{1}{2}\left(\frac{d^2u}{dz^2}\frac{dv}{dz} - \frac{d^2v}{dz}\frac{du}{dz}\right)\right)\left(\left(\frac{du}{dz}\right)^2 + \left(\frac{dv}{dz}\right)^2\right)\right)\right] \tag{4.2}$$

with the first derivative of w_p being

$$\frac{dw_p}{dz} = \frac{dw}{dz} - \hat{x}\frac{d^2u}{dz^2} - \hat{y}\frac{d^2v}{dz^2} - \omega\frac{d^2\phi}{dz^2} - \frac{\omega}{2}\left[\frac{d^3u}{dz^3}\frac{dv}{dz} - \frac{d^3v}{dz^3}\frac{du}{dz}\right] - \hat{x}\left[\frac{d\phi}{dz}\frac{dv}{dz} + \phi\frac{d^2v}{dz^2} - \frac{1}{2}\phi\frac{d\phi}{dz}\frac{du}{dz}\right.$$

$$\left. - \frac{1}{4}\phi^2\frac{d^2u}{dz^2}\right] + \hat{y}\left[\frac{d\phi}{dz}\frac{du}{dz} + \phi\frac{d^2u}{dz^2} + \frac{1}{2}\phi\frac{d\phi}{dz}\frac{dv}{dz} + \frac{1}{4}\phi^2\frac{d^2v}{dz^2}\right] + O_z\left(\frac{du}{dz}, \frac{dv}{dz}, \phi\right) \tag{4.3}$$

where O_z represents functions which are 4th order or higher and disregarded for simplicity.

4.1.2 Longitudinal Strain

The longitudinal strain in the previous chapter is give as

$$\varepsilon_p \approx \frac{dw_p}{dz} + \frac{1}{2}\left(\left(\frac{du_p}{dz}\right)^2 + \left(\frac{dv_p}{dz}\right)^2\right) \tag{4.4}$$

Substituting the displacements $\frac{du_p}{dz}$ and $\frac{dv_p}{dz}$ derived in the previous chapter and the new expression for $\frac{dw_p}{dz}$ considering prebuckling deflections yields

$$\varepsilon_p = \frac{dw}{dz} - \hat{x}\frac{d^2u}{dz^2} - \hat{y}\frac{d^2v}{dz^2} - \omega\frac{d^2\phi}{dz^2} - \frac{\omega}{2}\left[\frac{d^3u}{dz^3}\frac{dv}{dz} - \frac{d^3v}{dz^3}\frac{du}{dz}\right] - \hat{x}\left[\frac{d\phi}{dz}\frac{dv}{dz} + \phi\frac{d^2v}{dz^2} - \frac{1}{2}\phi\frac{d\phi}{dz}\frac{du}{dz}\right.$$

$$\left. - \frac{1}{4}\phi^2\frac{d^2u}{dz^2}\right] + \hat{y}\left[\frac{d\phi}{dz}\frac{du}{dz} + \phi\frac{d^2u}{dz^2} + \frac{1}{2}\phi\frac{d\phi}{dz}\frac{dv}{dz} + \frac{1}{4}\phi^2\frac{d^2v}{dz^2}\right] + \frac{1}{2}\left(\left(\frac{du}{dz}\right)^2 + \left(\frac{dv}{dz}\right)^2\right)$$

$$+ \frac{1}{2}\left(\frac{d\phi}{dz}\right)^2\left(\left(\hat{y} - \hat{y}_o\right)^2 + \hat{x}^2\right) + \hat{y}_o\frac{du}{dz}\frac{d\phi}{dz} \tag{4.5}$$

The first variation of ε_p would then become

$$\delta\varepsilon_p = \frac{d\delta w}{dz} - \hat{x}\frac{d^2\delta u}{dz^2} - \hat{y}\frac{d^2\delta v}{dz^2} - \omega\frac{d^2\delta\phi}{dz^2} - \hat{x}\left[\frac{d^2v}{dz^2}\delta\phi + \phi\frac{d^2\delta v}{dz^2} - \frac{1}{2}\delta\phi\frac{d\phi}{dz}\frac{du}{dz} - \frac{1}{2}\phi\frac{d\delta\phi}{dz}\frac{du}{dz}\right.$$

$$\left. - \frac{1}{2}\phi\frac{d\phi}{dz}\frac{d\delta u}{dz} - \frac{1}{2}\phi\delta\phi\frac{d^2u}{dz^2} - \frac{1}{4}\phi^2\frac{d^2\delta u}{dz^2}\right] + \hat{y}\left[\frac{d^2u}{dz^2}\delta\phi + \frac{d^2\delta u}{dz^2}\phi + \frac{1}{2}\delta\phi\frac{d\phi}{dz}\frac{dv}{dz}\right.$$

$$\left. + \frac{1}{2}\phi\frac{d\delta\phi}{dz}\frac{dv}{dz} + \frac{1}{2}\phi\frac{d\phi}{dz}\frac{d\delta v}{dz} + \frac{1}{2}\phi\delta\phi\frac{d^2v}{dz^2} + \frac{1}{4}\phi^2\frac{d^2\delta v}{dz^2}\right] + \hat{y}_o\frac{d\delta u}{dz}\frac{d\phi}{dz} + \hat{y}_o\frac{du}{dz}\frac{d\delta\phi}{dz}$$

$$+ \left(\hat{x}^2 + \left(\hat{y} - \hat{y}_o\right)^2\right)\frac{d\delta\phi}{dz}\frac{d\phi}{dz} - \frac{\omega}{2}\left[\frac{d^3\delta u}{dz^3}\frac{dv}{dz} + \frac{d^3u}{dz^3}\frac{d\delta v}{dz} - \frac{d^3v}{dz}\frac{d\delta u}{dz} - \frac{d^3\delta v}{dz^3}\frac{du}{dz}\right]$$

$$+ \frac{d\delta u}{dz}\frac{du}{dz} + \frac{d\delta v}{dz}\frac{dv}{dz} \tag{4.6}$$

The second variation of ε_p is

$$\delta^2\ \varepsilon_p = \left(\frac{d\delta u}{dz}\right)^2 + \left(\frac{d\delta v}{dz}\right)^2 - \hat{x}\left[2\delta\phi\frac{d^2\delta v}{dz^2} - \delta\phi\frac{d\delta\phi}{dz}\frac{du}{dz} - \delta\phi\frac{d\phi}{dz}\frac{d\delta u}{dz} - \phi\frac{d\delta\phi}{dz}\frac{d\delta u}{dz}\right.$$

$$\left. - \frac{1}{2}(\delta\phi)^2\frac{d^2u}{dz^2} - \phi\delta\phi\frac{d^2\delta u}{dz^2}\right] + \hat{y}\left[2\delta\phi\frac{d^2\delta u}{dz^2} + \delta\phi\frac{d\delta\phi}{dz}\frac{dv}{dz} + \delta\phi\frac{d\phi}{dz}\frac{d\delta v}{dz}\right.$$

$$\left. + \frac{d\delta\phi}{dz}\frac{d\delta v}{dz} + \frac{1}{2}(\delta\phi)^2\frac{d^2v}{dz^2} + \phi\delta\phi\frac{d^2\delta v}{dz^2} + 2\hat{y}_o\frac{d\delta u}{dz}\frac{d\delta\phi}{dz} + \left(\hat{x}^2 + (\hat{y} - \hat{y}_o)^2\right)\left(\frac{d\delta\phi}{dz}\right)^2\right.$$

$$\left. - \omega\left[\frac{d^3\delta u}{dz^3}\frac{d\delta v}{dz} - \frac{d^3\delta v}{dz^3}\frac{d\delta u}{dz}\right]\right. \tag{4.7}$$

The deformations are assumed to occur in two stages; a prebuckling state $\{0, v, w, 0\}$ followed by a lateral buckling state $\{\delta u, 0, 0, \delta\phi\}$. This allows for the following simplication to be applied to the expression for longitudinal strain and it variations (Pi et al., 1992)

$$u, \phi, \delta v, \delta w = 0$$

The simplified expressions are as follows

$$\varepsilon_p = \frac{dw}{dz} - \hat{y}\frac{d^2v}{dz} + \frac{1}{2}\left(\frac{dv}{dz}\right)^2 \tag{4.8}$$

$$\delta\varepsilon_p = -\hat{x}\left[\frac{d^2\delta u}{dz^2} + \frac{d^2v}{dz^2}\delta\phi\right] - \omega\left[\frac{d^2\delta\phi}{dz^2} + \frac{1}{2}\left(\frac{d^3\delta u}{dz^3}\frac{dv}{dz} - \frac{d^3v}{dz^3}\frac{d\delta u}{dz}\right)\right] \tag{4.9}$$

$$\delta^2\ \varepsilon_p = \left(\frac{d\delta u}{dz}\right)^2 + \hat{y}\left[2\delta\phi\frac{d^2\delta u}{dz^2} + \frac{1}{2}(\delta\phi)^2\frac{d^2v}{dz^2} + \delta\phi\frac{d\delta\phi}{dz}\frac{dv}{dz}\right] + 2\hat{y}_o\frac{d\delta u}{dz}\frac{d\delta\phi}{dz}$$

$$+ \left(\hat{x}^2 + (\hat{y} - \hat{y}_o)^2\right)\left(\frac{d\delta\phi}{dz}\right)^2 \tag{4.10}$$

4.1.3 Shear Strain

The effects of shear strain due to bending and warping are neglected. The shear strain due to uniform torsion is

$$\gamma_p = -2t_p k_z \tag{4.11}$$

Substituting the unsimplified expression for torsional curvature, γ_p becomes (Vlasov, 1961)

$$\gamma_p = -2t_p\left(\frac{d\phi}{dz} + \frac{1}{2}\left(\frac{d^2u}{dz^2}\frac{dv}{dz} - \frac{d^2v}{dz^2}\frac{du}{dz}\right)\right) \tag{4.12}$$

The first variation of γ_p

$$\delta\gamma_p = -2t_p\left(\frac{d\delta\phi}{dz} + \frac{1}{2}\left(\frac{d^2\delta u}{dz^2}\frac{dv}{dz} - \frac{d^2v}{dz^2}\frac{d\delta u}{dz}\right)\right) \tag{4.13}$$

The second variation of γ_p is assumed to be zero.

$$\delta^2\gamma_p = 0 \tag{4.14}$$

4.2 STRAIN ENERGY EQUATION CONSIDERING PREBUCKLING DEFLECTIONS

Substituting the revised expressions for longitudinal and shear stress and their variations into the strain energy equation given in Chapter 3 with the linearized stress resultants

$$F = EA\frac{dw}{dz} \tag{4.15}$$

$$M_x = -EI\frac{d^2v}{dz^2} \tag{4.16}$$

yield the strain energy equation for monosymmetric beam-columns considering prebuckling deflections as shown below.

$$\frac{1}{2}\delta^2 U = \frac{1}{2}\int_L \left\{ EI_y\left[\frac{d^2(\delta u)}{dz^2} + \frac{d^2v}{dz^2}\delta\phi\right]^2 + GJ\left[\frac{d\ (\delta\phi)}{dz} + \frac{1}{2}\left(\frac{dv}{dz}\frac{d^2(\delta u)}{dz^2} - \frac{d^2v}{dz^2}\frac{d(\delta u)}{dz}\right)\right]^2 \right.$$

$$+ EI_w\left[\frac{d^2\delta\phi}{dz^2} + \frac{1}{2}\left(\frac{dv}{dz}\frac{d^3(\delta u)}{dz^3} - \frac{d^3v}{dz^3}\frac{d(\delta u)}{dz}\right)\right]^2 + F\left[\left(\frac{d(\delta u)}{dz}\right)^2\right.$$

$$\left. + 2\hat{y}_o\left(\frac{d(\delta u)}{dz}\frac{d(\delta\phi)}{dz} + \frac{dv}{dz}\frac{d\delta\phi}{dz}\delta\phi\right) + \left(r_o^{\,2} + \hat{y}_o^{\,2}\right)\left(\frac{d\delta\phi}{dz}\right)^2\right]$$

$$\left. + M_x\left[2\left(\frac{d^2(\delta u)}{dz^2}\right)\delta\phi + \beta_x\left(\frac{d(\delta\phi)}{dz}\right)^2 + \left(\frac{d^2v}{dz^2}\right)\delta\phi^2\right]\right\}dz \tag{4.17}$$

4.3 POTENTIAL ENERGY OF THE LOADS CONSIDERING PREBUCKLING DEFLECTIONS

4.3.1 Displacements and Rotations of Load Points

The displacements and rotations of load points must be re-derived considering prebuckling deflections. The second variations of the displacements due to the distributed and concentrated loads, v_q and v_P respectively, considering prebuckling deflections are given as

$$\delta^2 v_P = -\left(e - \hat{y}_o\right)\left(\left(\delta\phi\right)^2 - \frac{d\delta u}{dz}\frac{dv}{dz}\delta\phi\right) \tag{4.18}$$

$$\delta^2 v_q = -\left(a - \hat{y}_o\right)\left(\left(\delta\phi\right)^2 - \frac{d\delta u}{dz}\frac{dv}{dz}\delta\phi\right) \tag{4.19}$$

Substituting the new expressions for the second variations of the displacements of the loads into the potential energy equation given in Chapter 3 yields the new potential energy of the loads equation as

$$\frac{1}{2}\delta^2\Omega = \frac{1}{2}\int_L q\left(a - \hat{y}_o\right)\left(\left(\delta\phi\right)^2 - \frac{d\delta u}{dz}\frac{dv}{dz}\delta\phi\right)dz + \frac{1}{2}\sum P\left(e - \hat{y}_o\right)\left(\left(\delta\phi\right)^2 - \frac{d\delta u}{dz}\frac{dv}{dz}\delta\phi\right) \tag{4.20}$$

4.4 ENERGY EQUATION CONSIDERING PREBUCKLING DEFORMATIONS

The energy equation for lateral torsional buckling of monosymmetric beam-columns considering prebuckling deformations is determined by substituting Eq. (4.17) and Eq. (4.20) into Eq. (3.6) as

$$\frac{1}{2}\delta^2\Pi = \frac{1}{2}\int_L \left\{ EI_y\left[\frac{d^2(\delta u)}{dz^2} + \frac{d^2 v}{dz^2}\delta\phi\right]^2 + GJ\left[\frac{d\ (\delta\phi)}{dz} + \frac{1}{2}\left(\frac{dv}{dz}\frac{d^2(\delta u)}{dz^2} - \frac{d^2 v}{dz^2}\frac{d(\delta u)}{dz}\right)\right]^2 \right.$$

$$+ EI_w\left[\frac{d^2\delta\phi}{dz^2} + \frac{1}{2}\left(\frac{dv}{dz}\frac{d^3(\delta u)}{dz^3} - \frac{d^3 v}{dz^3}\frac{d(\delta u)}{dz}\right)\right]^2$$

$$+ F\left[\left(\frac{d(\delta u)}{dz}\right)^2 + 2\hat{y}_o\left(\frac{d(\delta u)}{dz}\frac{d(\delta\phi)}{dz} + \frac{dv}{dz}\frac{d\delta\phi}{dz}\delta\phi\right) + \left(r_o^{\,2} + \hat{y}_o^{\,2}\right)\left(\frac{d\delta\phi}{dz}\right)^2\right]$$

$$\left. + M_x\left[2\left(\frac{d^2(\delta u)}{dz^2}\right)\delta\phi + \beta_x\left(\frac{d(\delta\phi)}{dz}\right)^2 + \left(\frac{d^2 v}{dz^2}\right)\delta\phi^2\right]\right\} dz$$

$$+ \frac{1}{2}\int_L q\left(a - \hat{y}_o\right)\left((\delta\phi)^2 - \frac{d\delta u}{dz}\frac{dv}{dz}\delta\phi\right) dz$$

$$+ \frac{1}{2}\sum P\left(e - \hat{y}_o\right)\left((\delta\phi)^2 - \frac{d\delta u}{dz}\frac{dv}{dz}\delta\phi\right) \qquad (4.21)$$

The first two lines on the right side of the equation contain terms involving buckling rigidities EI_y, GJ, and EI_ω and represent the strain energy stored during prebuckling and buckling. The third and fourth line of the equation contain terms involving the stress resultants F and M_x, which represent the work done by the applied loads at the shear center, considering the effects of prebuckling. The final two lines of the equation represent the work done by the distributed load, q, and the concentrated load, P, considering prebuckling deflections.

In order to linearize the new energy equation, the second order in-plane displacements are neglected in order to avoid a quadratic eigenvalue equation (Roberts, 2004). The new energy equation, disregarding these second order displacements, is

$$\frac{1}{2}\delta^2\Pi = \frac{1}{2}\int_L \Bigg[EI_y \left(\frac{d^2(\delta u)}{dz^2} \right)^2 + 2EI_y \frac{d^2(\delta u)}{dz^2}\frac{d^2 v}{dz^2}\delta\phi + GJ\left(\frac{d(\delta\phi)}{dz} \right)^2$$

$$+ GJ\frac{d(\delta\phi)}{dz}\left(\frac{dv}{dz}\frac{d^2(\delta u)}{dz^2} - \frac{d^2 v}{dz^2}\frac{d(\delta u)}{dz} \right) + EI_\omega \left(\frac{d^2(\delta\phi)}{dz^2} \right)^2$$

$$+ EI_\omega \frac{d^2(\delta\phi)}{dz^2}\left(\frac{dv}{dz}\frac{d^3(\delta u)}{dz^3} - \frac{d^3 v}{dz^3}\frac{d(\delta u)}{dz} \right)$$

$$+ F\left[\left(\frac{d(\delta u)}{dz} \right)^2 + 2\hat{y}_o \left(\frac{d(\delta u)}{dz}\frac{d(\delta\phi)}{dz} \right) + \left(r_o^{\,2} + \hat{y}_o^{\,2} \right)\left(\frac{d\delta\phi}{dz} \right)^2 \right]$$

$$+ M_x \left[2\left(\frac{d^2(\delta u)}{dz^2} \right)\delta\phi + \beta_x \left(\frac{d(\delta\phi)}{dz} \right)^2 \right] \Bigg\} dz + \frac{1}{2}\int q\left(a - \hat{y}_o \right)(\delta\phi)^2 dz$$

$$+ \frac{1}{2}\sum P\left(e - \hat{y}_o \right)(\delta\phi)^2 = 0 \tag{4.22}$$

Comparing this equation to Eq. (3.88) in the previous chapter, the only terms that differ are

$$\frac{1}{2}\int_L \Bigg[2EI_y \frac{d^2(\delta u)}{dz^2}\frac{d^2 v}{dz^2}\delta\phi + GJ\frac{d(\delta\phi)}{dz}\left(\frac{dv}{dz}\frac{d^2(\delta u)}{dz^2} - \frac{d^2 v}{dz^2}\frac{d(\delta u)}{dz} \right)$$

$$+ EI_\omega \frac{d^2(\delta\phi)}{dz^2}\left(\frac{dv}{dz}\frac{d^3(\delta u)}{dz^3} - \frac{d^3 v}{dz^3}\frac{d(\delta u)}{dz} \right) \Bigg] dz \tag{4.23}$$

The in-plane curvature is

$$\frac{d^2 v}{dz^2} = -\frac{M_x}{EI_x} \tag{4.24}$$

Likewise,

$$\frac{dv}{dz} = \int -\frac{M_x}{EI_x} dz + C \tag{4.25}$$

$$\frac{d^3v}{dz^3} = -\frac{1}{EI_x}\frac{dM_x}{dz} = -\frac{V_y}{EI_x} \tag{4.26}$$

The constant C is a function of $\frac{dv}{dz}$ and is calculated at $z = 0$ as $C = \frac{dv\,(0)}{dz}$.

Substituting these equations into Eq. (4.23) yields

$$\frac{1}{2}\int_L -2\frac{I_y}{I_x}M_x\frac{d^2(\delta u)}{dz^2}\delta\phi + GJ\left(\int -\frac{M_x}{EI_x}dz + C\right)\frac{d(\delta\phi)}{dz}\frac{d^2(\delta u)}{dz^2}$$

$$+ GJ\frac{M_x}{EI_x}\frac{d(\delta\phi)}{dz}\frac{d(\delta u)}{dz} + EI_\omega\left(\int -\frac{M_x}{EI_x}dz + C\right)\frac{d^2(\delta\phi)}{dz^2}\frac{d^3(\delta u)}{dz^3}$$

$$\frac{I_\omega}{I_x}V_y\frac{d^2(\delta\phi)}{dz^2}\frac{d(\delta u)}{dz}\Bigg]dz \tag{4.27}$$

5.0 APPLICATIONS

This chapter will present examples using the buckling equation derived in Section 3.4 (Eq. (3.88)) to determine approximate solutions for specific loading and boundary conditions. These solutions will be obtained by assuming suitable shape functions for the displacement u and rotation ϕ during buckling. The solutions will then be compared to examples presented in other literature that used different methods, including differential equilibrium equation method for the first example and the method of finite differences for the remaining examples, to obtain buckling results to demonstrate the validity of the buckling equations presented in this paper.

5.1 SIMPLY-SUPPORTED MONOSYMMETRIC BEAM SUBJECTED TO EQUAL END MOMENTS, M

This example will derive the lateral-torsional buckling moment, M_{cr}, for a simply-supported beam whose ends are restrained from twist subjected to equal end moments, as shown in Figure 5.1.

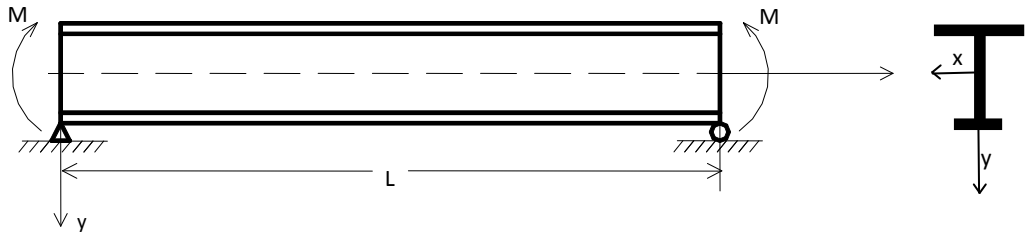

Figure 5.1 Monosymmetric Beam with Subjected to Equal End Moments

The lateral torsional buckling equation derived in Chapter 3 is

$$\frac{1}{2}\delta^2\Pi = \frac{1}{2}\int_L \left\{ EI_y\left(\frac{d^2(\delta u)}{dz^2}\right)^2 + GJ\left(\frac{d\ (\delta\phi)}{dz}\right)^2 + EI_\omega\left(\frac{d^2(\delta\phi)}{dz^2}\right)^2 \right.$$

$$+ F\left[\left(\frac{d(\delta u)}{dz}\right)^2 + 2\hat{y}_o\left(\frac{d(\delta u)}{dz}\right)\left(\frac{d(\delta\phi)}{dz}\right) + \left(r_o^{\,2} + \hat{y}_o^{\,2}\right)\left(\frac{d\ (\delta\phi)}{dz}\right)^2\right]$$

$$\left. + M_x(z)\left[2\left(\frac{d^2(\delta u)}{dz^2}\right)\delta\phi + \beta_x\left(\frac{d(\delta\phi)}{dz}\right)^2\right]\right\} dz$$

$$+ \frac{1}{2}\int_L q\left(a - \hat{y}_o\right)(\delta\phi)^2\, dz + \frac{1}{2}\sum P\left(e - \hat{y}_o\right)(\delta\phi)^2 = 0 \qquad (5.1)$$

Since $M_x = M$ and there is no axial force or transverse loading in this example, $F = 0$, $q = 0$, and $P = 0$, Eq. (5.1) reduces to

$$\frac{1}{2}\delta^2\Pi = \frac{1}{2}\int_L \left\{ EI_y\left(\frac{d^2(\delta u)}{dz^2}\right)^2 + GJ\left(\frac{d\ (\delta\phi)}{dz}\right)^2 + EI_\omega\left(\frac{d^2(\delta\phi)}{dz^2}\right)^2 \right.$$

$$\left. + M_x(z)\left[2\left(\frac{d^2(\delta u)}{dz^2}\right)\delta\phi + \beta_x\left(\frac{d(\delta\phi)}{dz}\right)^2\right]\right\} dz \qquad (5.2)$$

For a simply-supported beam, the following shape functions can be used to solve this problem.

$$u(z) = A\sin\left(\frac{\pi z}{L}\right) \qquad (5.3)$$

$$\phi(z) = B\sin\left(\frac{\pi z}{L}\right) \qquad (5.4)$$

The first variation of u and ϕ, as well as their first and second derivatives are needed to solve this problem and are shown below as

$$\delta u = \delta A\sin\left(\frac{\pi z}{L}\right) \qquad (5.5)$$

$$\delta\phi = \delta B\sin\left(\frac{\pi z}{L}\right) \qquad (5.6)$$

$$\frac{d(\delta u)}{dz} = \left(\frac{\pi}{L}\right)\delta A\cos\left(\frac{\pi z}{L}\right) \qquad (5.7)$$

$$\frac{d(\delta\phi)}{dz} = \left(\frac{\pi}{L}\right)\delta B\cos\left(\frac{\pi z}{L}\right) \qquad (5.8)$$

$$\frac{d^2(\delta u)}{dz^2} = -\left(\frac{\pi}{L}\right)^2 \delta A \sin\left(\frac{\pi z}{L}\right) \tag{5.9}$$

$$\frac{d^2(\delta \phi)}{dz^2} = -\left(\frac{\pi}{L}\right)^2 \delta B \sin\left(\frac{\pi z}{L}\right) \tag{5.10}$$

Substituting Eqs. (5.3) – (5.10) into Eq. (5.1) yields

$$\begin{aligned}\frac{1}{2}\delta^2\Pi = \frac{1}{2}\int_0^L \Bigg\{ & \left(\frac{\pi}{L}\right)^4 EI_y(\delta A)^2 \sin^2\left(\frac{\pi z}{L}\right) + \left(\frac{\pi}{L}\right)^2 GJ(\delta B)^2 \cos^2\left(\frac{\pi z}{L}\right) \\ & + \left(\frac{\pi}{L}\right)^4 EI_\omega(\delta B)^2 \sin^2\left(\frac{\pi z}{L}\right) \\ & + M\left[-2\left(\frac{\pi}{L}\right)^2\left(\delta A \sin\left(\frac{\pi z}{L}\right)\right)\left(\delta B \sin\left(\frac{\pi z}{L}\right)\right) + \beta_x\left(\frac{\pi}{L}\right)^2(\delta B)^2 \cos^2\left(\frac{\pi z}{L}\right)\right]\Bigg\} dz\end{aligned} \tag{5.11}$$

The following integrations will be necessary to evaluate Eq. (5.11)

$$\int_0^L \sin^2\left(\frac{\pi z}{L}\right) dz = \frac{L}{2} \tag{5.12}$$

$$\int_0^L \cos^2\left(\frac{\pi z}{L}\right) dz = \frac{L}{2} \tag{5.13}$$

Integrating Eq. (5.11) with respect to z gives

$$\begin{aligned}\frac{1}{2}\delta^2\Pi = \frac{1}{2}\Bigg\{ & \left(\frac{L}{2}\right)\left(\frac{\pi}{L}\right)^4 EI_y(\delta A)^2 + \left(\frac{L}{2}\right)\left(\frac{\pi}{L}\right)^2 GJ(\delta B)^2 + \left(\frac{L}{2}\right)\left(\frac{\pi}{L}\right)^4 EI_\omega(\delta B)^2 \\ & + M\left[-2\left(\frac{L}{2}\right)\left(\frac{\pi}{L}\right)^2(\delta A)(\delta B) + \beta_x\left(\frac{L}{2}\right)\left(\frac{\pi}{L}\right)^2(\delta B)^2\right]\Bigg\} dz\end{aligned} \tag{5.14}$$

The critical buckling load occurs when the second variation of total potential energy is equal to zero. Eq. (5.14) can then be written as

$$\frac{1}{2}\delta^2\Pi = \frac{1}{2}\frac{L}{2}\left(\frac{\pi}{L}\right)^2 \begin{Bmatrix}\delta A \\ \delta B\end{Bmatrix}^T \begin{bmatrix}\left(\frac{\pi}{L}\right)^2 EI_y & -M \\ -M & GJ + \left(\frac{\pi}{L}\right)^2 EI_\omega + M\beta_x\end{bmatrix} \begin{Bmatrix}\delta A \\ \delta B\end{Bmatrix} = 0 \tag{5.15}$$

Since δA and δB are not equal to zero

$$\begin{bmatrix}\left(\frac{\pi}{L}\right)^2 EI_y & -M \\ -M & GJ + \left(\frac{\pi}{L}\right)^2 EI_\omega + M\beta_x\end{bmatrix} \begin{Bmatrix}\delta A \\ \delta B\end{Bmatrix} = 0 \tag{5.16}$$

If the deformed configuration of the beam is to yield a nontrivial solution, the determinant of the coefficients δA and δB in Eq. (5.16) must vanish leaving

$$M^2 - \left(\frac{\pi}{L}\right)^2 EI_y\beta_x M - \left(\frac{\pi}{L}\right)^2 EI_y\left(GJ + \left(\frac{\pi}{L}\right)^2 EI_\omega\right) = 0 \tag{5.17}$$

Solving Eq. (5.17) for M gives the critical moment for lateral torsional buckling of a monosymmetric I-beam subjected to equal end moments as

$$M_{cr} = \frac{1}{2}\left(\frac{\pi}{L}\right)^2 EI_y\beta_x + \sqrt{\left(\frac{\pi}{L}\right)^4 \frac{\left(EI_y\right)^2\beta_x^2}{4} + \left(\frac{\pi}{L}\right)^2 EI_y GJ + \left(\frac{\pi}{L}\right)^4 EI_y EI_\omega} \tag{5.18}$$

The beam stiffness parameter and the monosymmetric parameter were given in Section 3.5 under non-dimensional analysis as

$$K = \sqrt{\frac{\pi^2 EI_\omega}{GJL^2}} \tag{5.19}$$

$$\overline{\beta}_x = \frac{\beta_x}{L}\sqrt{\frac{EI_y}{GJ}} \tag{5.20}$$

Rewriting Eq. (5.18) in terms of K and $\overline{\beta}_x$ yields the elastic critical moment as

$$M_{cr} = \frac{\pi}{L}\sqrt{EI_y GJ}\left[\sqrt{1 + K^2 + \left(\frac{\pi\overline{\beta}}{2}\right)^2} + \frac{\pi\overline{\beta}}{2}\right] \tag{5.21}$$

This result for the lateral torsional buckling moment of monosymmetric I-beams under a uniform moment matches the solution given by (Kitipornchai, et al. 1986) for $F = 0$ when the elastic critical moment was derived using the differential equilibrium method illustrated in Chapter 2 Eq. (2.53).

5.2 SIMPLY-SUPPORTED MONOSYMMETRIC BEAM SUBJECTED TO CONCENTRATED CENTRAL LOAD, P

This example will present the lateral-torsional buckling load, P_{cr}, for a simply-supported beam whose ends are restrained from twist subjected to a concentrated central load that is applied to the shear center of the beam, as shown in Figure 5.2.

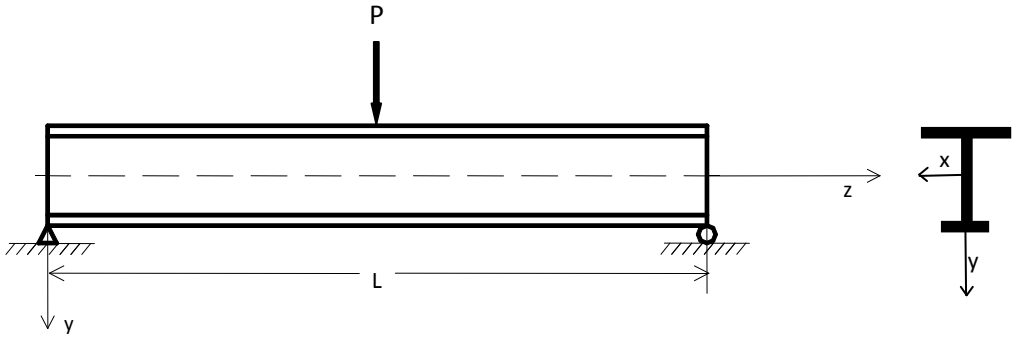

Figure 5.2 Monosymmetric Beam Subjected to Concentrated Central Load

There is no axial force or uniformly distributed load acting on the beam. Therefore, $F = 0$ and $q = 0$. Since the concentrated load, P, is applied at the beam's shear center, $\left(e - \hat{y}_o\right) = 0$.

Therefore, Eq. (5.1) reduces to

$$\frac{1}{2}\delta^2\Pi = \frac{1}{2}\int_L \left\{ EI_y\left(\frac{d^2(\delta u)}{dz^2}\right)^2 + GJ\left(\frac{d\ (\delta\phi)}{dz}\right)^2 + EI_\omega\left(\frac{d^2(\delta\phi)}{dz^2}\right)^2 \right.$$

$$\left. + M_x(z)\left[2\left(\frac{d^2(\delta u)}{dz^2}\right)\delta\phi + \beta_x\left(\frac{d(\delta\phi)}{dz}\right)^2\right]\right\} dz \qquad (5.22)$$

Since this beam is also simply supported, the same buckling modes shapes will be used as in Section 5.1. The moment along the beam, $M_x(z)$, for a beam with a concentrated central load can be expressed as

$$M_x(z) = \frac{P}{2}z \qquad \text{for} \qquad 0 \le z \le \frac{L}{2} \qquad (5.23)$$

$$M_x(z) = \frac{P}{2}(L - z) \qquad \text{for} \qquad \frac{L}{2} \le z \le L \qquad (5.24)$$

Substituting Eqs. (5.3) – (5.10) and Eqs. (5.23) – (5.24) into Eq. (5.22) yields

$$\frac{1}{2}\delta^2\Pi = \frac{1}{2}\int_0^L \left\{ \left(\frac{\pi}{L}\right)^4 EI_y(\delta A)^2 \sin^2\left(\frac{\pi z}{L}\right) + \left(\frac{\pi}{L}\right)^2 GJ(\delta B)^2 \cos^2\left(\frac{\pi z}{L}\right) \right.$$

$$\left. + \left(\frac{\pi}{L}\right)^4 EI_\omega(\delta B)^2 \sin^2\left(\frac{\pi z}{L}\right)\right\} dz$$

$$+ \frac{1}{2}\int_0^{\frac{L}{2}} \left\{ \frac{-2P}{P} z\left(\frac{\pi}{L}\right)^2 \left(\delta A \sin\left(\frac{\pi z}{L}\right)\right)\left(\delta B \sin\left(\frac{\pi z}{L}\right)\right) \right.$$

$$\left. + \frac{P}{2} z\beta_x \left(\frac{\pi}{L}\right)^2 (\delta B)^2 \cos^2\left(\frac{\pi z}{L}\right)\right\} dz$$

$$+ \frac{1}{2}\int_{\frac{L}{2}}^L \left\{ \frac{-2P}{P}(L - z)\left(\frac{\pi}{L}\right)^2 \left(\delta A \sin\left(\frac{\pi z}{L}\right)\right)\left(\delta B \sin\left(\frac{\pi z}{L}\right)\right) \right.$$

$$+\frac{P}{2}(L-z)\beta_x\left(\frac{\pi}{L}\right)^2(\delta B)^2\cos^2\left(\frac{\pi z}{L}\right)\Bigg\}dz \tag{5.25}$$

The following integrations will be necessary to evaluate Eq. (5.25)

$$\int_0^{\frac{L}{2}} z\sin^2\left(\frac{\pi z}{L}\right)dz = \frac{L^2}{16}+\frac{L^2}{4\pi^2} \tag{5.26}$$

$$\int_0^{\frac{L}{2}} \frac{z}{2}\cos^2\left(\frac{\pi z}{L}\right)dz = \frac{L^2}{32}-\frac{L^2}{8\pi^2} \tag{5.27}$$

$$\int_{\frac{L}{2}}^{L} (L-z)\sin^2\left(\frac{\pi z}{L}\right)dz = \frac{L^2}{16}+\frac{L^2}{4\pi^2} \tag{5.28}$$

$$\int_{\frac{L}{2}}^{L} \frac{(L-z)}{2}\cos^2\left(\frac{\pi z}{L}\right)dz = \frac{L^2}{32}-\frac{L^2}{8\pi^2} \tag{5.29}$$

Therefore integrating Eq. (5.25) with respect to z gives

$$\begin{aligned}\frac{1}{2}\delta^2\Pi = \frac{1}{2}\Bigg\{&\left(\frac{L}{2}\right)\left(\frac{\pi}{L}\right)^2 EI_y(\delta A)^2+\left(\frac{L}{2}\right)\left(\frac{\pi}{L}\right)^2 GJ(\delta B)^2+\left(\frac{L}{2}\right)\left(\frac{\pi}{L}\right)^2 EI_\omega(\delta B)^2\\ &+\left[-\left(\frac{\pi}{L}\right)^2 P\left(\frac{L^2}{16}+\frac{L^2}{4\pi^2}\right)(\delta A)(\delta B)+\left(\frac{\pi}{L}\right)^2 P\beta_x\left(\frac{L^2}{32}-\frac{L^2}{8\pi^2}\right)(\delta B)^2\right]\\ &+\left[-\left(\frac{\pi}{L}\right)^2 P\left(\frac{L^2}{16}+\frac{L^2}{4\pi^2}\right)(\delta A)(\delta B)+\left(\frac{\pi}{L}\right)^2 P\beta_x\left(\frac{L^2}{32}-\frac{L^2}{8\pi^2}\right)(\delta B)^2\right]\Bigg\}\end{aligned} \tag{5.30}$$

Which simplifies to

$$\frac{1}{2}\delta^2\Pi = \frac{1}{2}\frac{L}{2}\left(\frac{\pi}{L}\right)^2\left[\left(\frac{\pi}{L}\right)^2 EI_y(\delta A)^2 + GJ(\delta B)^2 + \left(\frac{\pi}{L}\right)^2 EI_\omega(\delta B)^2 - PL\left(\frac{\pi^2+4}{4\pi^2}\right)(\delta A)(\delta B) + PL\beta_x\left(\frac{\pi^2-4}{8\pi^2}\right)(\delta B)^2\right] \tag{5.31}$$

The critical buckling load occurs when the second variation of total potential energy is equal to zero, as

$$\frac{1}{2}\delta^2\Pi = \frac{1}{2}\frac{L}{2}\left(\frac{\pi}{L}\right)^2\begin{Bmatrix}\delta A\\ \delta B\end{Bmatrix}^T\begin{bmatrix}\left(\frac{\pi}{L}\right)^2 EI_y & -PL\left(\frac{\pi^2+4}{8\pi^2}\right)\\ -PL\left(\frac{\pi^2+4}{8\pi^2}\right) & GJ+\left(\frac{\pi}{L}\right)^2 EI_\omega + PL\beta_x\left(\frac{\pi^2-4}{8\pi^2}\right)\end{bmatrix}\begin{Bmatrix}\delta A\\ \delta B\end{Bmatrix} = 0 \tag{5.32}$$

Since δA and δB are not equal to zero

$$\begin{bmatrix}\left(\frac{\pi}{L}\right)^2 EI_y & -PL\left(\frac{\pi^2+4}{8\pi^2}\right)\\ -PL\left(\frac{\pi^2+4}{8\pi^2}\right) & GJ+\left(\frac{\pi}{L}\right)^2 EI_\omega + PL\beta_x\left(\frac{\pi^2-4}{8\pi^2}\right)\end{bmatrix}\begin{Bmatrix}\delta A\\ \delta B\end{Bmatrix} = 0 \tag{5.33}$$

If the deformed configuration of the beam is to yield a nontrivial solution, the determinant of the coefficients δA and δB in Eq. (5.33) must vanish leaving

$$\left(\frac{\pi^2+4}{8\pi^2}\right)^2 L^2P^2 - \left(\frac{\pi}{L}\right)^2 EI_y\beta_x\left(\frac{\pi^2-4}{8\pi^2}\right)LP - \left(\frac{\pi}{L}\right)^2 EI_y\left(GJ+\left(\frac{\pi}{L}\right)^2 EI_\omega\right) = 0 \tag{5.34}$$

Solving Eq. (5.34) for P gives the critical buckling load for lateral torsional buckling of a monosymmetric I-beam subjected to a concentrated central load as

$$P_{cr} = \frac{1}{\left(\pi^2 + 4\right)^2 L^3}\left\{4\left[16\left(EI_y\right)^2 \beta_x{}^2 \pi^8 - 8\left(EI_y\right)^2 \beta_x{}^2 \pi^{10} + \left(EI_y\right)^2 \beta_x{}^2 \pi^{12}\right.\right.$$

$$+ 4\left(EI_y\right)GJL^2\pi^{10} + 32\left(EI_y\right)GJL^2\pi^8 + 64\left(EI_y\right)GJL^2\pi^6 + 4\left(EI_y\right)\left(EI_\omega\right)\pi^{12}$$

$$\left.\left. + 32\left(EI_y\right)\left(EI_\omega\right)\pi^{10} + 64\left(EI_y\right)\left(EI_\omega\right)\pi^8\right]^{\frac{1}{2}} + 4\left(EI_y\right)\beta_x\pi^6 - 16\left(EI_y\right)\beta_x\pi^4\right\} \quad (5.35)$$

The non-dimensional loading parameter, γ_P, was given in section 3.5 as

$$\gamma_P = \frac{PL^2}{\sqrt{EI_y GJ}} \quad (5.36)$$

Rewriting Eq. (5.35) in terms of the non-dimensional beam stiffness parameter, K, given in Eq. (5.19) and the monosymmetric parameter, $\overline{\beta}_x$, given in Eq. (5.20), as well as the loading parameter, γ_P, shown in Eq. (5.36) yields the elastic critical load parameter for a simply-supported monosymmetric beam with a concentrated point load as

$$\gamma_P = \frac{1}{\left(\pi^2 + 4\right)^2}\left\{4\left[\left(\pi^{12} - 8\pi^{10} + 16\pi^8\right)\overline{\beta}_x{}^2 + \left(4\pi^{10} + 32\pi^8 + 64\pi^6\right)\right.\right.$$

$$\left.\left. + \left(4\pi^{10} + 32\pi^8 + 64\pi^6\right)K^2\right]^{\frac{1}{2}} + \left(4\pi^6 - 16\pi^4\right)\beta_x\right\} \quad (5.37)$$

This result can then be compared to the results given in (Anderson and Trahair, 1972) where the critical load parameters were obtained using the method of finite differences. Figures 5.3 – 5.9 compare the solution presented in Eq. (5.37) with the results given by Anderson and Trahair at various values of K and $\overline{\beta}_x$. The results obtained by this research using approximate shape functions are more accurate as the values for $\overline{\beta}_x$ become closer to zero, representing a doubly-

symmetric beam. Thus, the shape functions used in this example more accurately predict the buckled shape of simply-supported beams with doubly-symmetric cross-sections.

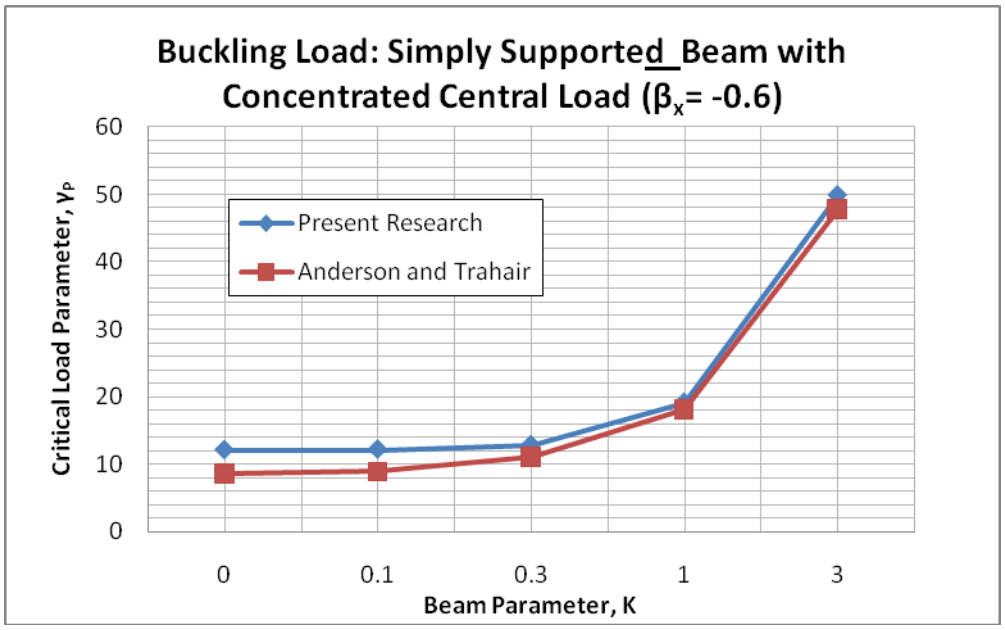

Figure 5.3 Buckling Load: Simply Supported Beam with Monosymmetric Cross-Section Subjected to a Concentrated Central Load $\left(\overline{\beta}_x = -0.6\right)$

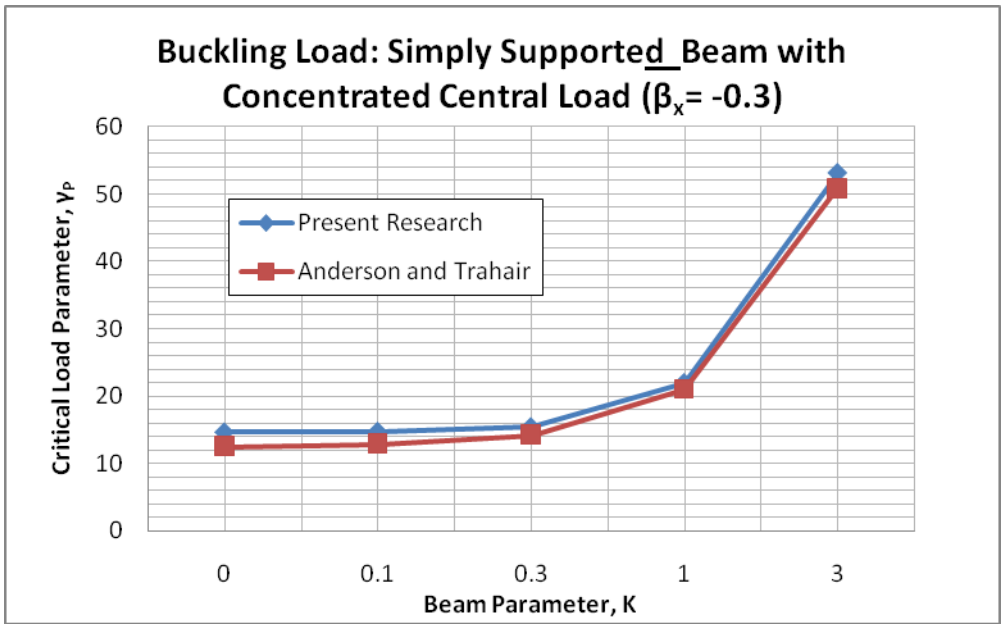

Figure 5.4 Buckling Load: Simply Supported Beam with Monosymmetric Cross-Section Subjected to a Concentrated Central Load $\left(\overline{\beta}_x = -0.3\right)$

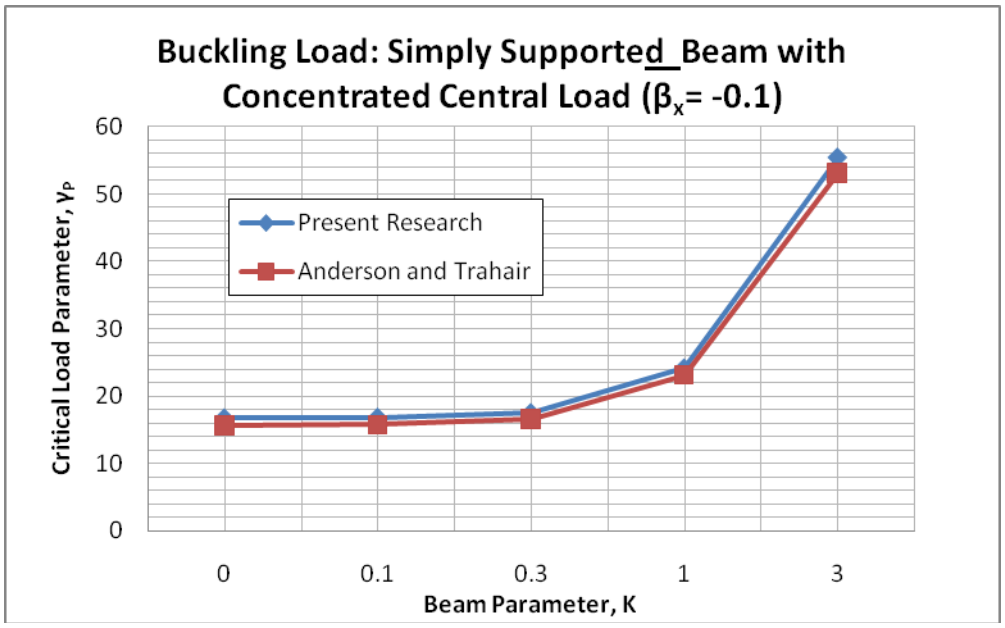

Figure 5.5 Buckling Load: Simply Supported Beam with Monosymmetric Cross-Section Subjected to a Concentrated Central Load $\left(\overline{\beta}_x = -0.1\right)$

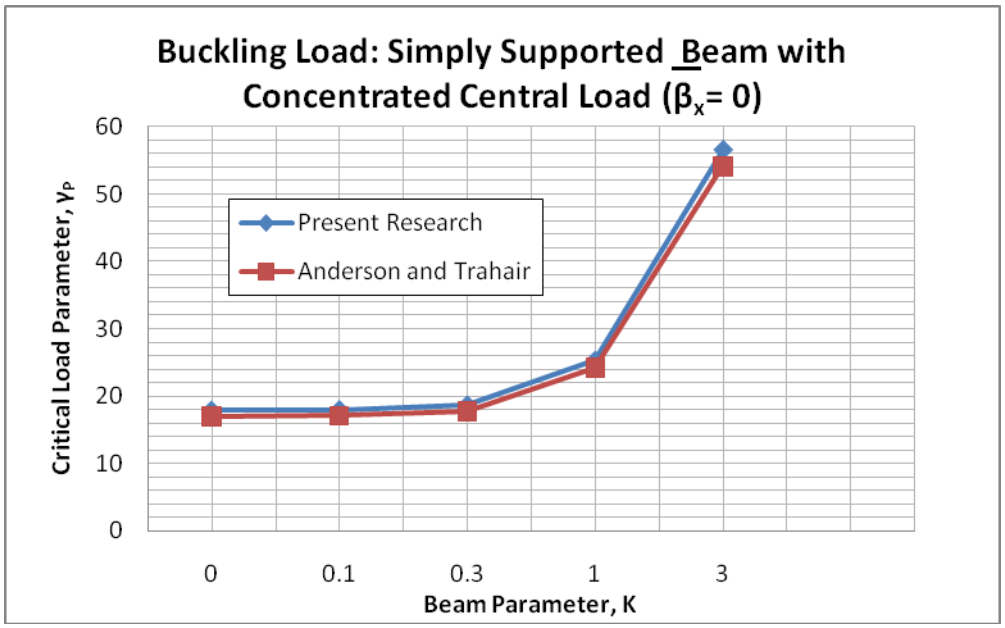

Figure 5.6 Buckling Load: Simply Supported Beam with Monosymmetric Cross-Section Subjected to a Concentrated Central Load $\left(\overline{\beta}_x = 0\right)$

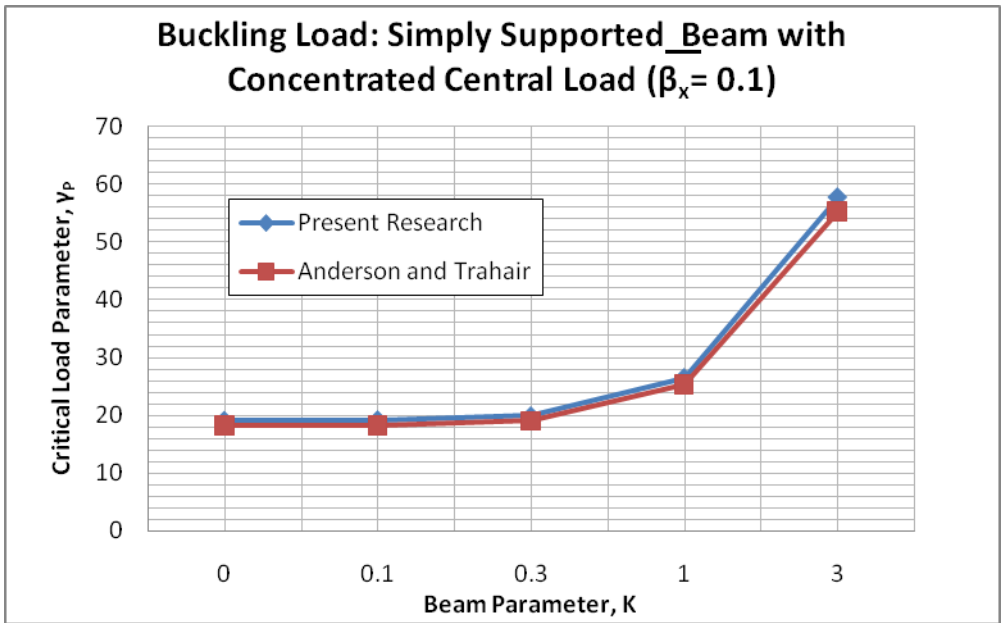

Figure 5.7 Buckling Load: Simply Supported Beam with Monosymmetric Cross-Section Subjected to a Concentrated Central Load $\left(\overline{\beta}_x = 0.1\right)$

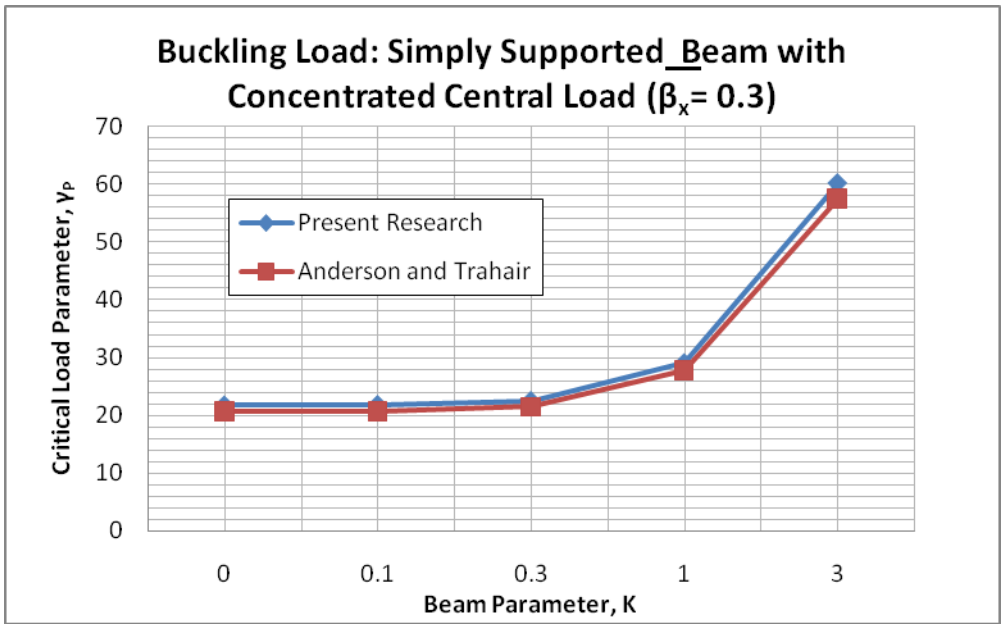

Figure 5.8 Buckling Load: Simply Supported Beam with Monosymmetric Cross-Section Subjected to a Concentrated Central Load $\left(\overline{\beta}_x = 0.3\right)$

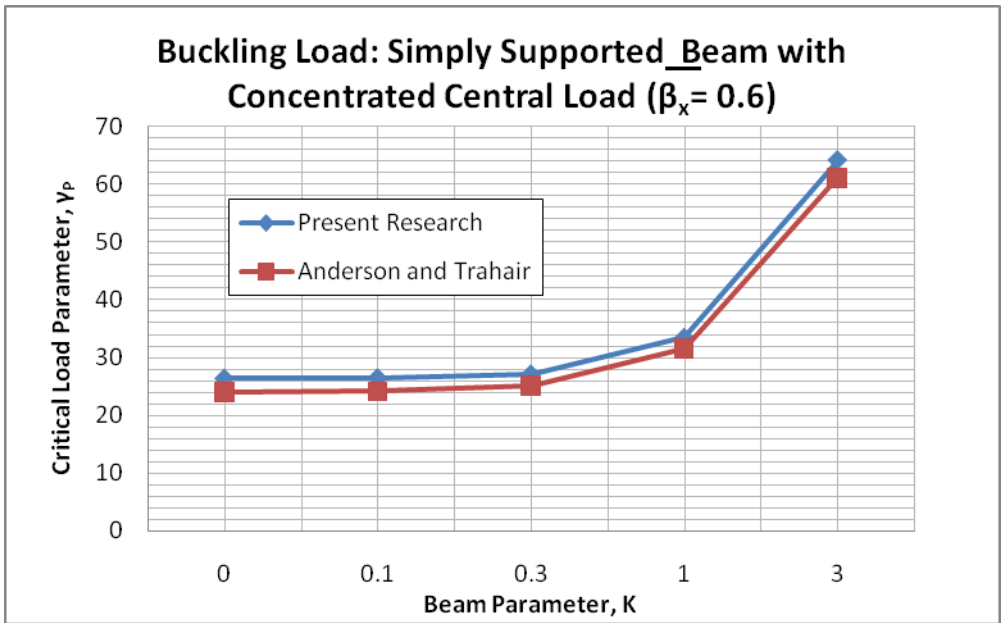

Figure 5.9 Buckling Load: Simply Supported Beam with Monosymmetric Cross-Section Subjected to a Concentrated Central Load $\left(\overline{\beta}_x = 0.6\right)$

5.3 SIMPLY-SUPPORTED MONOSYMMETRIC BEAM SUBJECTED TO UNIFORMLY DISTRIBUTED LOAD, *q*

This example will present the lateral-torsional buckling load, q_{cr}, for a simply-supported beam whose ends are restrained from twist subjected to a uniformly distributed load that is applied to the shear center of the beam, as shown in Figure 5.10

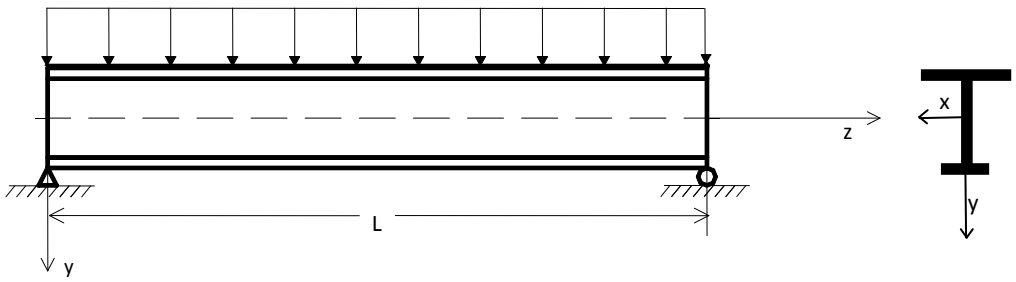

Figure 5.10 Monosymmetric Beam Subjected to Uniformly Distributed Load

There is no axial force or concentrated load acting on the beam. Therefore, $F = 0$ and $P = 0$. Since the uniformly distributed load, q, is applied at the beam's shear center, $\left(a - \hat{y}_0\right) = 0$.

Therefore, Eq. (5.1) reduces to

$$\frac{1}{2}\delta^2\Pi = \frac{1}{2}\int_L \left\{ EI_y\left(\frac{d^2(\delta u)}{dz^2}\right)^2 + GJ\left(\frac{d\ (\delta\phi)}{dz}\right)^2 + EI_\omega\left(\frac{d^2(\delta\phi)}{dz^2}\right)^2 \right.$$

$$\left. + M_x(z)\left[2\left(\frac{d^2(\delta u)}{dz^2}\right)\delta\phi + \beta_x\left(\frac{d(\delta\phi)}{dz}\right)^2\right]\right\} dz \qquad (5.38)$$

Since this beam is also simply supported, the same buckling modes shapes will be used as in section 5.1. The moment along the beam, $M_x(z)$, for a beam with a uniformly distributed load can be expressed as

$$M_x = \frac{qz}{2}(L - z) \qquad \text{for} \qquad 0 \le z \le L \qquad (5.39)$$

Substituting Eqs. (5.3) – (5.10) and Eq. (5.39) into Eq. (5.38) yields

$$\frac{1}{2}\delta^2\Pi = \frac{1}{2}\int_0^L \left\{ \left(\frac{\pi}{L}\right)^4 EI_y(\delta A)^2 \sin^2\left(\frac{\pi z}{L}\right) + \left(\frac{\pi}{L}\right)^2 GJ(\delta B)^2 \cos^2\left(\frac{\pi z}{L}\right) \right.$$

$$\left. + \left(\frac{\pi}{L}\right)^4 EI_\omega(\delta B)^2 \sin^2\left(\frac{\pi z}{L}\right)\right\} dz$$

$$+ \frac{1}{2}\int_0^L \left\{ \frac{-2qz}{2}(L - z)\left(\frac{\pi}{L}\right)^2 \left(\delta A \sin\left(\frac{\pi z}{L}\right)\right)\left(\delta B \sin\left(\frac{\pi z}{L}\right)\right) \right.$$

$$\left. + \frac{qz}{2}(L - z)\beta_x\left(\frac{\pi}{L}\right)^2 (\delta B)^2 \cos^2\left(\frac{\pi z}{L}\right)\right\} dz \qquad (5.40)$$

The following integrations will be necessary to evaluate Eq. (5.40).

$$\int_0^L \left(zL - z^2\right)\sin^2\left(\frac{\pi z}{L}\right)dz = \frac{L^3}{12} + \frac{L^3}{4\pi^2} \tag{5.41}$$

$$\int_0^L \frac{\left(zL - z^2\right)}{2}\cos^2\left(\frac{\pi z}{L}\right)dz = \frac{L^3}{24} - \frac{L^3}{8\pi^2} \tag{5.42}$$

Therefore, integrating Eq. (5.40) with respect to z yields

$$\frac{1}{2}\delta^2\Pi = \frac{1}{2}\left\{\left(\frac{L}{2}\right)\left(\frac{\pi}{L}\right)^4 EI_y\left(\delta A\right)^2 + \left(\frac{L}{2}\right)\left(\frac{\pi}{L}\right)^2 GJ\left(\delta B\right)^2 + \left(\frac{L}{2}\right)\left(\frac{\pi}{L}\right)^4 EI_\omega\left(\delta B\right)^2 + \left[-\left(\frac{\pi}{L}\right)^2 q\left(\frac{L^3}{12} + \frac{L^3}{4\pi^2}\right)\left(\delta A\right)\left(\delta B\right) + \left(\frac{\pi}{L}\right)^2 q\beta_x\left(\frac{L^3}{24} - \frac{L^3}{8\pi^2}\right)\left(\delta B\right)^2\right]\right\} \tag{5.43}$$

Which simplifies to

$$\frac{1}{2}\delta^2\Pi = \frac{1}{2}\frac{L}{2}\left(\frac{\pi}{L}\right)^2\left[\left(\frac{\pi}{L}\right)^2 EI_y\left(\delta A\right)^2 + GJ\left(\delta B\right)^2 + \left(\frac{\pi}{L}\right)^2 EI_\omega\left(\delta B\right)^2 - qL^2\left(\frac{\pi^2 + 3}{6\pi^2}\right)\left(\delta A\right)\left(\delta B\right) + qL^2\beta_x\left(\frac{\pi^2 - 3}{12\pi^2}\right)\left(\delta B\right)^2\right] \tag{5.44}$$

The critical buckling load occurs when the second variation of total potential energy is equal to zero, as

$$\frac{1}{2}\delta^2\Pi = \frac{1}{2}\frac{L}{2}\left(\frac{\pi}{L}\right)^2\begin{Bmatrix}\delta A\\ \delta B\end{Bmatrix}^T\begin{bmatrix}\left(\frac{\pi}{L}\right)^2 EI_y & -qL^2\left(\frac{\pi^2 + 3}{12\pi^2}\right)\\ -qL^2\left(\frac{\pi^2 + 3}{12\pi^2}\right) & GJ + \left(\frac{\pi}{L}\right)^2 EI_\omega + qL^2\beta_x\left(\frac{\pi^2 - 3}{12\pi^2}\right)\end{bmatrix}\begin{Bmatrix}\delta A\\ \delta B\end{Bmatrix} = 0 \tag{5.45}$$

Since δA and δB are not equal to zero

$$\begin{bmatrix} \left(\frac{\pi}{L}\right)^2 EI_y & -qL^2\left(\frac{\pi^2+3}{12\pi^2}\right) \\ -qL^2\left(\frac{\pi^2+3}{12\pi^2}\right) & GJ+\left(\frac{\pi}{L}\right)^2 EI_\omega + qL^2\beta_x\left(\frac{\pi^2-3}{12\pi^2}\right) \end{bmatrix} \begin{Bmatrix} \delta A \\ \delta B \end{Bmatrix} = 0 \tag{5.46}$$

If the deformed configuration of the beam is to yield a nontrivial solution, the determinant of the coefficients δA and δB in Eq. (5.46) must vanish leaving

$$\left(\frac{\pi^2+3}{12\pi^2}\right)^2 L^4 q^2 - \left(\frac{\pi}{L}\right)^2 EI_y\beta_x\left(\frac{\pi^2-3}{12\pi^2}\right) L^2 q - \left(\frac{\pi}{L}\right)^2 EI_y\left(GJ+\left(\frac{\pi}{L}\right)^2 EI_\omega\right) = 0 \tag{5.47}$$

Solving Eq. (5.47) for q gives the critical buckling load for lateral torsional buckling of a monosymmetric I-beam subjected to a uniformly distributed load as

$$\begin{aligned} q_{cr} = \frac{1}{\left(\pi^2+3\right)^2 L^4}\Big\{ 6\Big[& 9\left(EI_y\right)^2\beta_x{}^2\pi^8 - 6\left(EI_y\right)^2\beta_x{}^2\pi^{10} + \left(EI_y\right)^2\beta_x{}^2\pi^{12} \\ & + 4\left(EI_y\right)GJL^2\pi^{10} + 24\left(EI_y\right)GJL^2\pi^8 + 36\left(EI_y\right)GJL^2\pi^6 + 4\left(EI_y\right)\left(EI_\omega\right)\pi^{12} \\ & + 24\left(EI_y\right)\left(EI_\omega\right)\pi^{10} + 36\left(EI_y\right)\left(EI_\omega\right)\pi^8\Big]^{\frac{1}{2}} + 4\left(EI_y\right)\beta_x\pi^6 - 12\left(EI_y\right)\beta_x\pi^4\Big\} \end{aligned} \tag{5.48}$$

The non-dimensional loading parameter, γ_q, was given in section 3.5 as

$$\gamma_q = \frac{qL^3}{\sqrt{EI_y GJ}} \tag{5.49}$$

Rewriting Eq. (5.48) in terms of the non-dimensional beam stiffness parameter, K, given in Eq. (5.19) and the monosymmetric parameter, β_x, given in Eq. (5.20), as well as the loading

parameter, γ_q, shown in Eq. (5.49) yields the elastic critical load parameter for a simply-supported monosymmetric beam with a uniformly distributed load as

$$\gamma_q = \frac{1}{\left(\pi^2 + 3\right)^2}\left\{4\left[\left(\pi^{12} - 6\pi^{10} + 9\pi^8\right)\overline{\beta}_x^{\,2} + \left(4\pi^{10} + 24\pi^8 + 36\pi^6\right) + \left(4\pi^{10} + 24\pi^8 + 36\pi^6\right)K^2\right]^{\frac{1}{2}} + \left(4\pi^6 - 12\pi^4\right)\beta_x\right\} \tag{5.50}$$

As in section 5.1, this result can then be compared to the results given in (Anderson and Trahair, 1972) where the critical load parameters were obtained using the method of finite differences. Figures 5.11 – 5.17 compare the solution presented in Eq. (5.50) with the results given by Anderson and Trahair at various values of K and $\overline{\beta}_x$. As in the example in Section 5.2, the results obtained by this research using approximate shape functions are more accurate as the values for $\overline{\beta}_x$ become closer to zero, representing a doubly-symmetric beam.

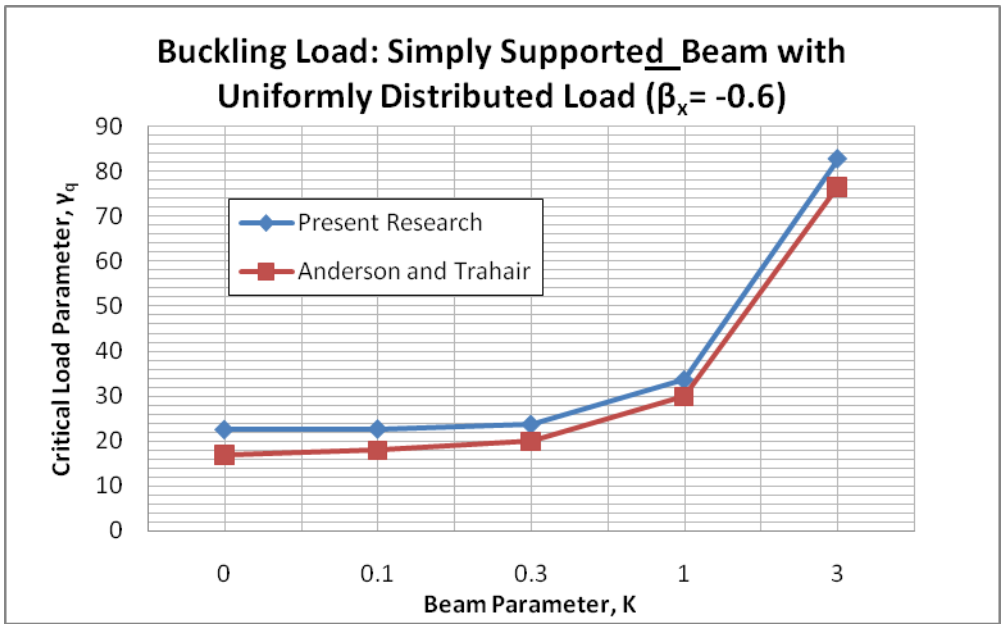

Figure 5.11 Buckling Load: Simply Supported Beam with Monosymmetric Cross-Section Subjected to a Uniformly Distributed Load $\left(\overline{\beta}_x = -0.6\right)$

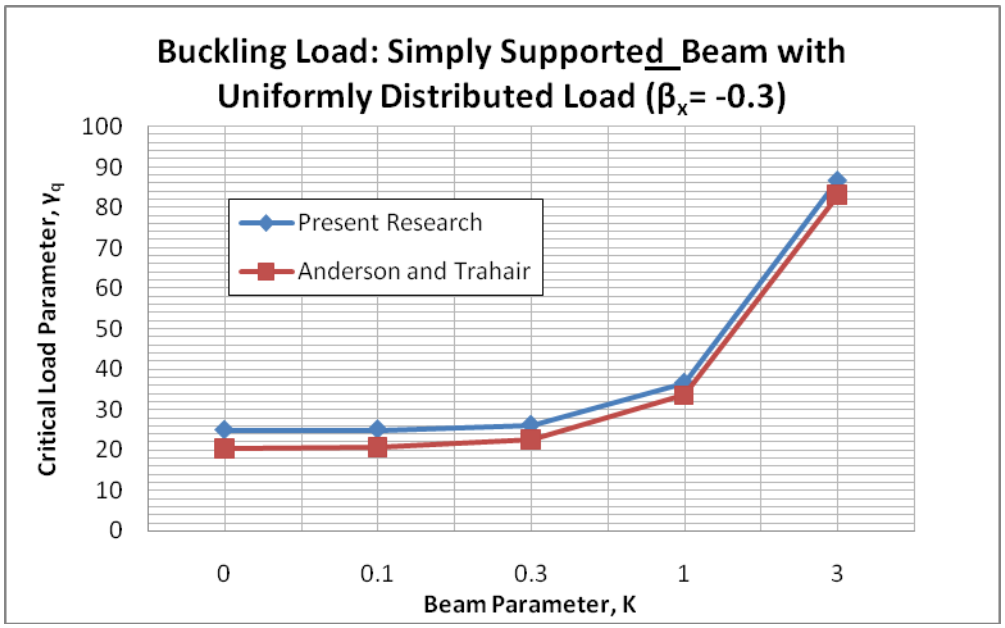

Figure 5.12 Buckling Load: Simply Supported Beam with Monosymmetric Cross-Section Subjected to a Uniformly Distributed Load $\left(\overline{\beta}_x = -0.3\right)$

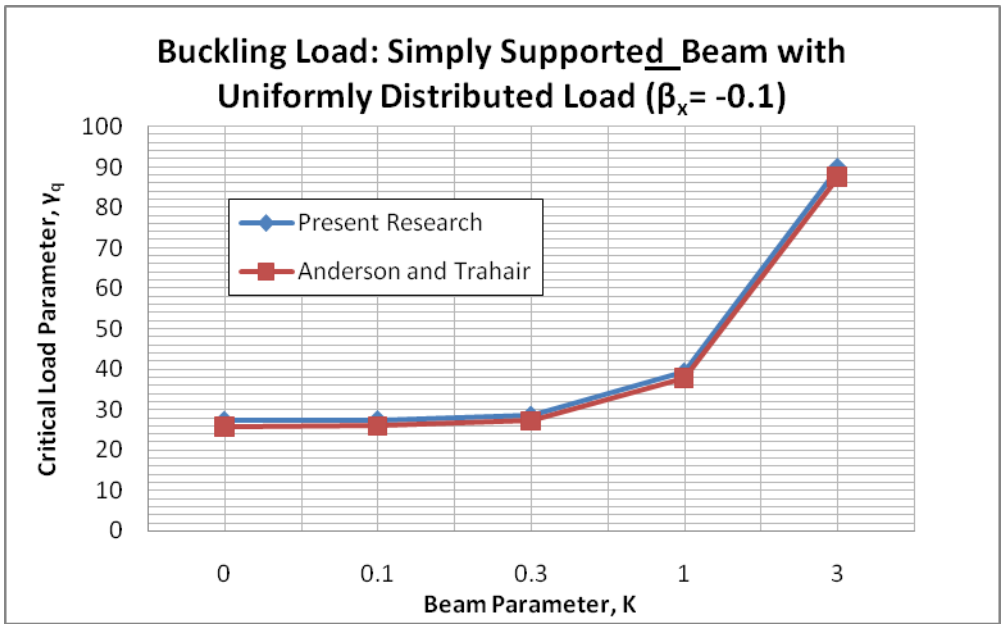

Figure 5.13 Buckling Load: Simply Supported Beam with Monosymmetric Cross-Section Subjected to a Uniformly Distributed Load $\left(\overline{\beta}_x = -0.1\right)$

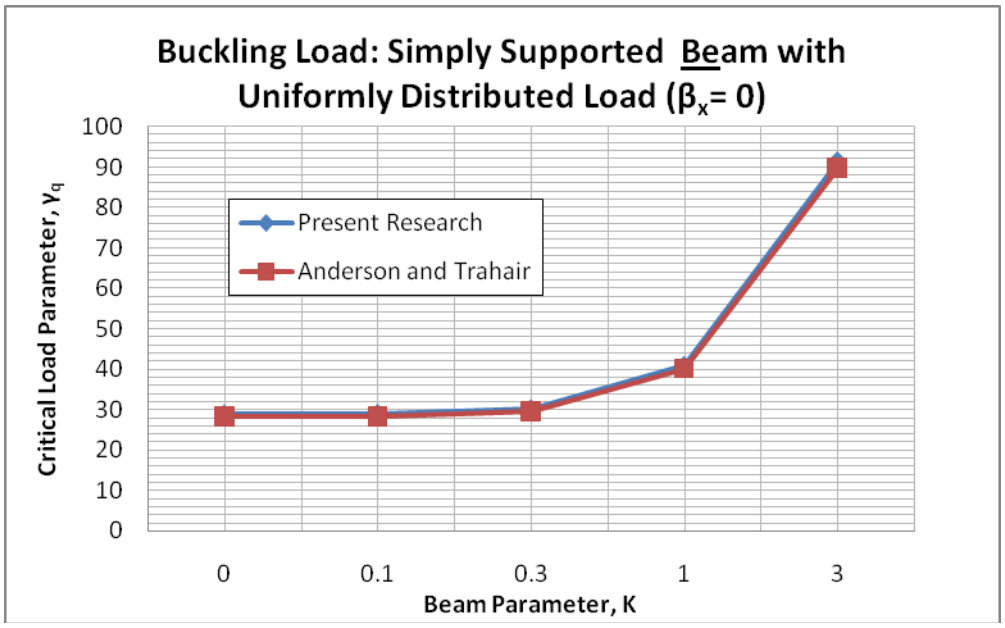

Figure 5.14 Buckling Load: Simply Supported Beam with Monosymmetric Cross-Section Subjected to a Uniformly Distributed Load $\left(\overline{\beta}_x = 0\right)$

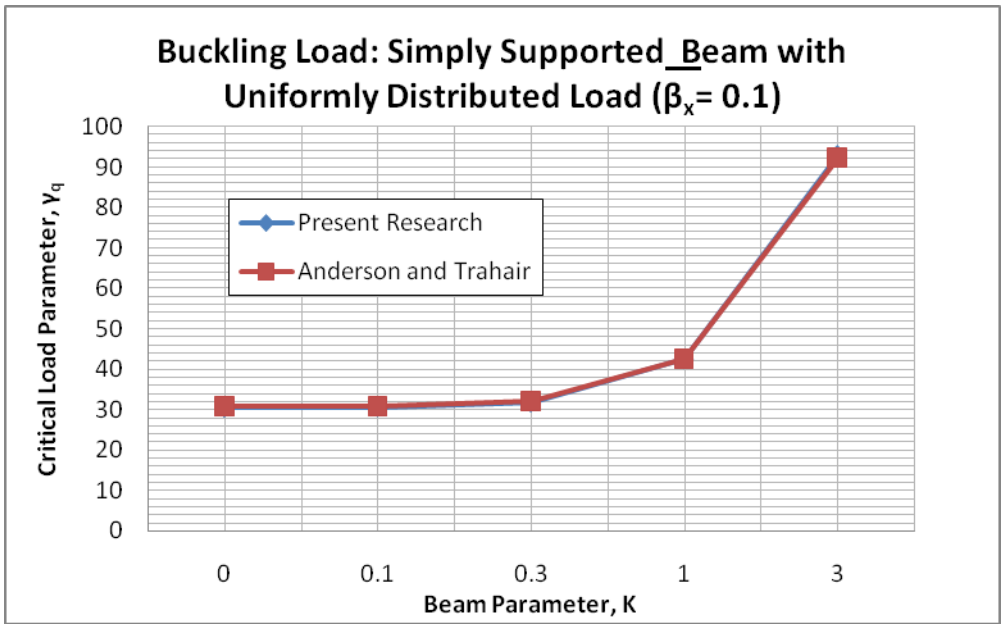

Figure 5.15 Buckling Load: Simply Supported Beam with Monosymmetric Cross-Section Subjected to a Uniformly Distributed Load $\left(\overline{\beta}_x = 0.1\right)$

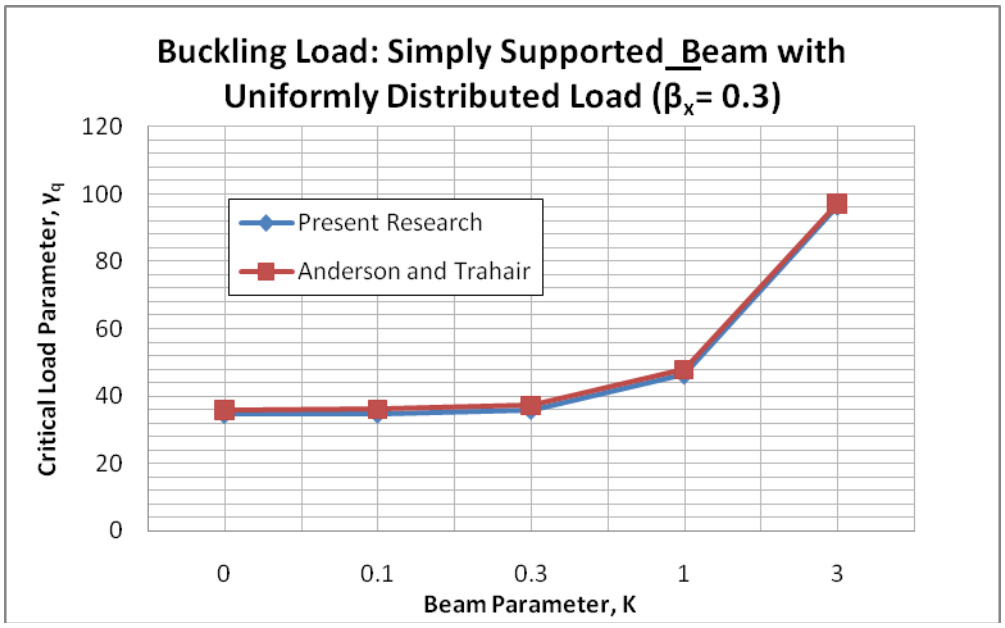

Figure 5.16 Buckling Load: Simply Supported Beam with Monosymmetric Cross-Section Subjected to a Uniformly Distributed Load $\left(\overline{\beta}_x = 0.3\right)$

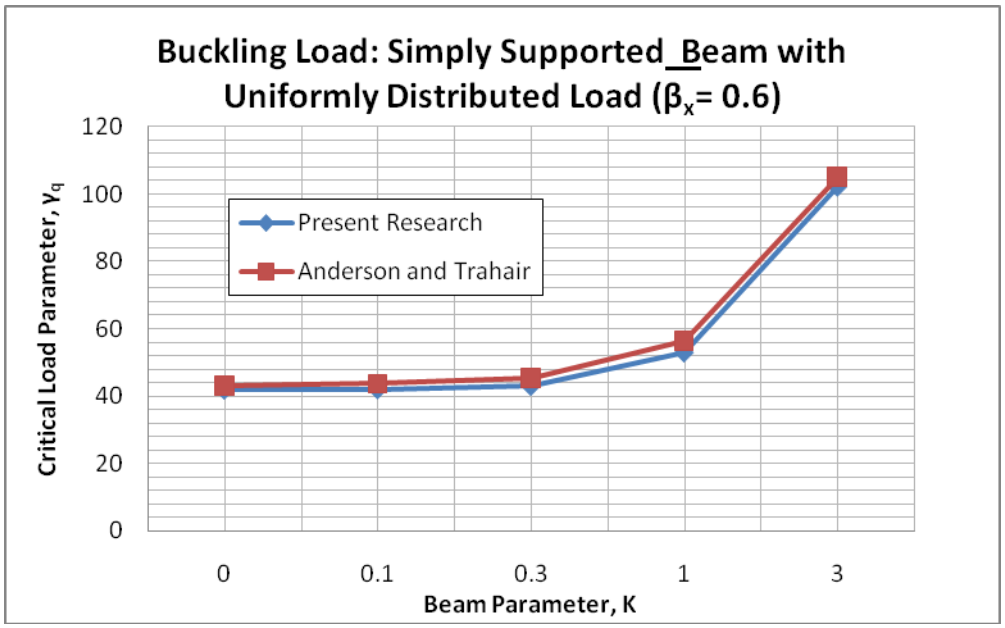

Figure 5.17 Buckling Load: Simply Supported Beam with Monosymmetric Cross-Section Subjected to a Uniformly Distributed Load $\left(\overline{\beta}_x = 0.6\right)$

5.4 CANTILEVER WITH END POINT LOAD, P

This example will present the lateral-torsional buckling load, P_{cr}, for a cantilever beam subjected to a concentrated central load that is applied at the end of the beam to its shear center, as shown in Figure 5.18.

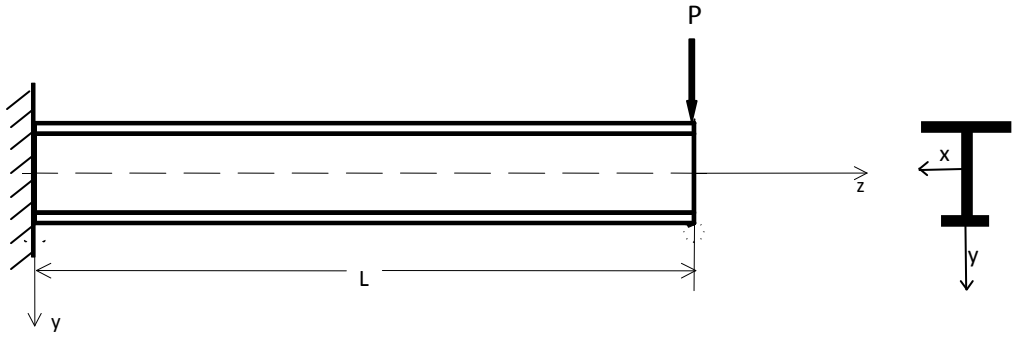

Figure 5.18 Monosymmetric Cantilever Beam Subjected to Concentrated End Load

There is no axial force or uniformly distributed load acting on the beam. Therefore, $F = 0$ and $q = 0$. Since the concentrated load, P, is applied at the beam's shear center, $\left(e - \hat{y}_0\right) = 0$.

Therefore, Eq. (5.1) reduces to

$$\frac{1}{2}\delta^2\Pi = \frac{1}{2}\int_L \left\{ EI_y\left(\frac{d^2(\delta u)}{dz^2}\right)^2 + GJ\left(\frac{d\ (\delta\phi)}{dz}\right)^2 + EI_\omega\left(\frac{d^2(\delta\phi)}{dz^2}\right)^2 \right.$$

$$\left. + M_x(z)\left[2\left(\frac{d^2(\delta u)}{dz^2}\right)\delta\phi + \beta_x\left(\frac{d(\delta\phi)}{dz}\right)^2\right]\right\} dz \qquad (5.51)$$

The moment along the beam, $M_x(z)$, for a beam with a concentrated central load can be expressed as

$$M_x(z) = -P(L-z) \qquad \text{for} \qquad 0 \le z \le L \qquad (5.52)$$

Several shape functions including $u(z) = A\left(1-\cos\frac{\pi z}{2L}\right)$ and $\phi(z) = B\left(1-\cos\frac{\pi z}{2L}\right)$ were experimented with to accurately predict the buckled shape of a cantilever beam. It was determined that in order to obtain acceptable results, a more complicated shape function in the form of a trigonometric series must be used (Wang and Kitipornchai, 1986).

$$u(z) = \sum_{r=1}^{n} \Delta_r\left[1-\cos\frac{(2r-1)\pi z}{2L}\right] \qquad (5.53)$$

$$\phi(z) = \sum_{r=1}^{n} \theta_r\left[1-\cos\frac{(2r-1)\pi z}{2L}\right] \qquad (5.54)$$

The first variation of u and ϕ, as well as their first and second derivatives are needed to solve this problem and are shown below as

$$\delta u = \sum_{r=1}^{n} \delta\Delta_r\left[1-\cos\frac{(2r-1)\pi z}{2L}\right] \qquad (5.55)$$

$$\delta\phi = \sum_{r=1}^{n} \delta\theta_r \left[1 - \cos\frac{(2r-1)\pi z}{2L} \right] \tag{5.56}$$

$$\frac{d(\delta u)}{dz} = \sum_{r=1}^{n} \left(\frac{1}{2} \delta\Delta_r \sin\left(\frac{1}{2} \frac{2r-1}{L} \pi z \right) \frac{2r-1}{L} \pi \right) \tag{5.57}$$

$$\frac{d(\delta \phi)}{dz} = \sum_{r=1}^{n} \left(\frac{1}{2} \delta\theta_r \sin\left(\frac{1}{2} \frac{2r-1}{L} \pi z \right) \frac{2r-1}{L} \pi \right) \tag{5.58}$$

$$\frac{d^2(\delta u)}{dz^2} = \sum_{r=1}^{n} \left(\frac{1}{4} \delta\Delta_r \cos\left(\frac{1}{2} \frac{2r-1}{L} \pi z \right) \frac{(2r-1)^2}{L^2} \pi^2 \right) \tag{5.59}$$

$$\frac{d^2(\delta \phi)}{dz^2} = \sum_{r=1}^{n} \left(\frac{1}{4} \delta\theta_r \cos\left(\frac{1}{2} \frac{2r-1}{L} \pi z \right) \frac{(2r-1)^2}{L^2} \pi^2 \right) \tag{5.60}$$

Substituting Eqs. (5.52) – (5.60) into Eq. (5.51) yields

$$\frac{1}{2}\delta^2\Pi = \frac{1}{2}\int_L \left\{ EI_y\left(\sum_{r=1}^{n}\left(\frac{1}{4}\delta\Delta_r\cos\left(\frac{1}{2}\frac{2r-1}{L}\pi z\right)\frac{(2r-1)^2}{L^2}\pi^2\right)\right)^2 \right.$$

$$+ GJ\left(\sum_{r=1}^{n}\left(\frac{1}{2}\delta\theta_r\sin\left(\frac{1}{2}\frac{2r-1}{L}\pi z\right)\frac{2r-1}{L}\pi\right)\right)^2$$

$$EI_\omega\left(\sum_{r=1}^{n}\left(\frac{1}{4}\delta\theta_r\cos\left(\frac{1}{2}\frac{2r-1}{L}\pi z\right)\frac{(2r-1)^2}{L^2}\pi^2\right)\right)^2$$

$$- P(L-z)\left[2\left(\sum_{r=1}^{n}\left(\frac{1}{4}\delta\Delta_r\cos\left(\frac{1}{2}\frac{2r-1}{L}\pi z\right)\frac{(2r-1)^2}{L^2}\pi^2\right)\right)\left(\sum_{r=1}^{n}\delta\theta_r\left[1-\cos\frac{(2r-1)\pi z}{2L}\right]\right)\right.$$

$$\left.\left. + \beta_x\left(\sum_{r=1}^{n}\left(\frac{1}{2}\delta\theta_r\sin\left(\frac{1}{2}\frac{2r-1}{L}\pi z\right)\frac{2r-1}{L}\pi\right)\right)^2\right]\right\}dz \qquad (5.61)$$

Therefore integrating Eq. (5.51) with respect to z gives

$$\frac{1}{2}\delta^2\Pi = \frac{\pi^4 EI_y}{64L^3}\left[\sum_{r=1}^{n}\left((2r-1)^4\delta\Delta_r{}^2\right)\right] + \frac{GJ\pi^2}{16L}\left[\sum_{r=1}^{n}\left((2r-1)^4\left(1+\frac{(2r-1)^2\pi^2 EI_\omega}{4GJL^2}\right)\delta\theta_r^2\right)\right]$$

$$+ \frac{P\pi^2}{4}\left[\sum_{r=1}^{n}\left(\left(\frac{1}{4}-\frac{3}{(2r-1)^2\pi^2}\right)(2r-1)^2\delta\theta_r\ \delta\Delta_r\right)\right]$$

$$+ \frac{P}{4}\left[\sum_{r=1}^{n}\left((2r-1)^2\ \delta\Delta_r\left(\sum_{s=1,\,s\neq r}^{n}\delta\theta_s\left(\frac{1-(-1)^{r+s-1}}{2(r+s-1)^2}+\frac{1-(-1)^{r-s}}{2(r-s)^2}-\frac{4}{(2r-1)^2}\right)\right)\right)\right]$$

$$+ \frac{P\beta_x\pi^2}{8}\left[\sum_{r=1}^{n}\left(\left(\frac{1}{(2r-1)^2\pi^2}-\frac{1}{4}\right)(2r-1)^2\delta\theta_r{}^2\right)\right] \qquad (5.62)$$

Taking the derivative of Eq. (5.62) with respect to $\delta\Delta_r$ and $\delta\theta_r$ yields the following set of homogeneous linear equations.

$$\frac{d\left(\frac{1}{2}\delta^2\Pi\right)}{d\delta\Delta_r} = \frac{\pi^2(2r-1)^4}{32}\delta\Delta_r + \frac{\gamma_c(2r-1)^2}{4}\left(\frac{1}{4} - \frac{3}{(2r-1)^2\pi^2}\right)\delta\theta_r$$

$$+ \frac{\gamma_c(2r-1)^2}{4\pi^2}\left[\sum_{s=1,\, s\neq r}^{n}\left(\left(\frac{1-(-1)^{r+s-1}}{2(r+s-1)^2} + \frac{1-(-1)^{r-s}}{2(r-s)^2} - \frac{4}{(2r-1)^2}\right)\delta\theta_s\right)\right] = 0$$

(5.63)

for r = 1, ..., n.

And

$$\frac{d\left(\frac{1}{2}\delta^2\Pi\right)}{d\delta\theta_r} = \left[\frac{(2r-1)^2}{8} + \frac{(2r-1)^4K^2}{32} + \frac{\gamma_c(2r-1)^2}{4}\overline{\beta}\left(\frac{1}{(2r-1)^2\pi^2} - \frac{1}{4}\right)\right]\delta\theta_r$$

$$+ \frac{\gamma_c(2r-1)^2}{4}\left[\frac{1}{4} - \frac{3}{(2r-1)^2\pi^2}\right]\delta\Delta_r$$

$$+ \frac{\gamma_c}{4\pi^2}\left[\sum_{s=1,\, s\neq r}^{n}\left((2s-1)^2\left(\frac{1-(-1)^{r+s-1}}{2(r+s-1)^2} + \frac{1-(-1)^{r-s}}{2(r-s)^2} - \frac{4}{(2r-1)^2}\right)\delta\Delta_s\right)\right]$$

$$+ \frac{\gamma_c}{\pi^2}\left[\sum_{s=1,\, s\neq r}^{n}\left(\left(\frac{1}{4}(2r-1)(2s-1)\overline{\beta}\frac{1-(-1)^{r+s-1}}{2(r+s-1)^2} - \frac{1-(-1)^{r-s}}{2(r-s)^2}\right)\delta\theta_s\right)\right] = 0$$

(5.64)

for $r = 1, ..., n$.

where the non-dimensional critical load is defined as

$$\gamma_P = \frac{PL^2}{\sqrt{EI_y GJ}} \tag{5.65}$$

Eqs. (5.63) and (5.64) are evaluated at $n = 7$ with the results in the form

$$[A]\begin{Bmatrix} \Delta_1 \\ \theta_1 \\ \vdots \\ \vdots \\ \Delta_7 \\ \theta_7 \end{Bmatrix} - \gamma_P [B]\begin{Bmatrix} \Delta_1 \\ \theta_1 \\ \vdots \\ \vdots \\ \Delta_7 \\ \theta_7 \end{Bmatrix} = 0 \tag{5.66}$$

which can be rearranged to the form

$$[D]\{\alpha\} = \lambda\{\alpha\} \tag{5.67}$$

Where

$$[D] = [A]^{-1}[B] \tag{5.68}$$

$$\alpha = \begin{Bmatrix} \Delta_1 \\ \theta_1 \\ \vdots \\ \vdots \\ \Delta_7 \\ \theta_7 \end{Bmatrix} \tag{5.69}$$

$$\lambda = \frac{1}{\gamma_P} \tag{5.70}$$

Where [A] and [B] are 14 by 14 matrices with the terms of each matrix given in Appendix B. The eigenvalues, λ, can be derived from Eq. (5.67), which yield the critical load, as shown in Eq. (5.70).

This result can then be compared to the results given in (Anderson and Trahair, 1972) where the critical load parameters were obtained using the method of finite differences. Figures 5.19 – 5.25 compare the results obtained using Eqs. 5.63 and 5.64 at values of n = 3, 5, and 7 with the results given by Anderson and Trahair at various values of K and $\overline{\beta}_x$. The shape functions using trigonometric series appear to have the same limitations as the ones used for the simply-supported beams where the predicted buckling moment is more accurate when the beam is closer to being doubly-symmetric, with the best predicted result occurring for higher values of n.

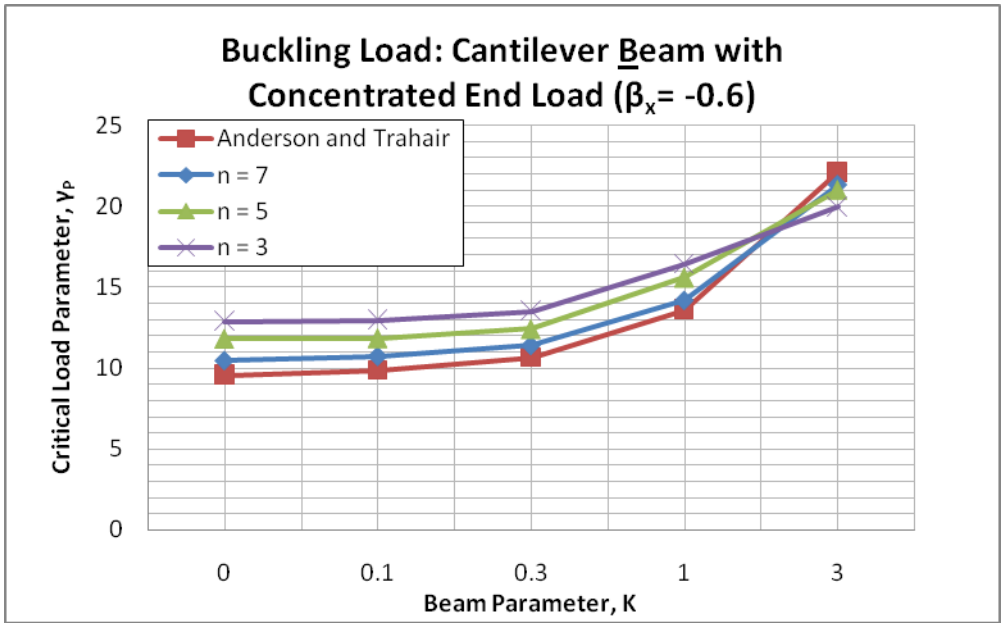

Figure 5.19 Buckling Load: Cantilever Beam with Monosymmetric Cross-Section Subjected to a Concentrated End Load $\left(\overline{\beta}_x = -0.6\right)$

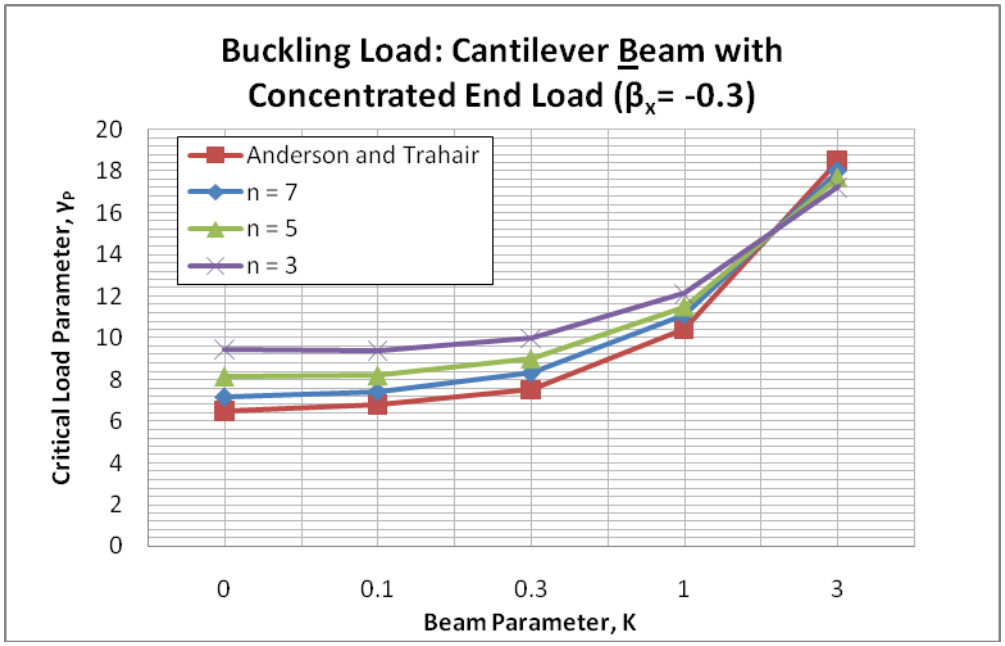

Figure 5.20 Buckling Load: Cantilever Beam with Monosymmetric Cross-Section Subjected to a Concentrated End Load $\left(\bar{\beta}_x = -0.3\right)$

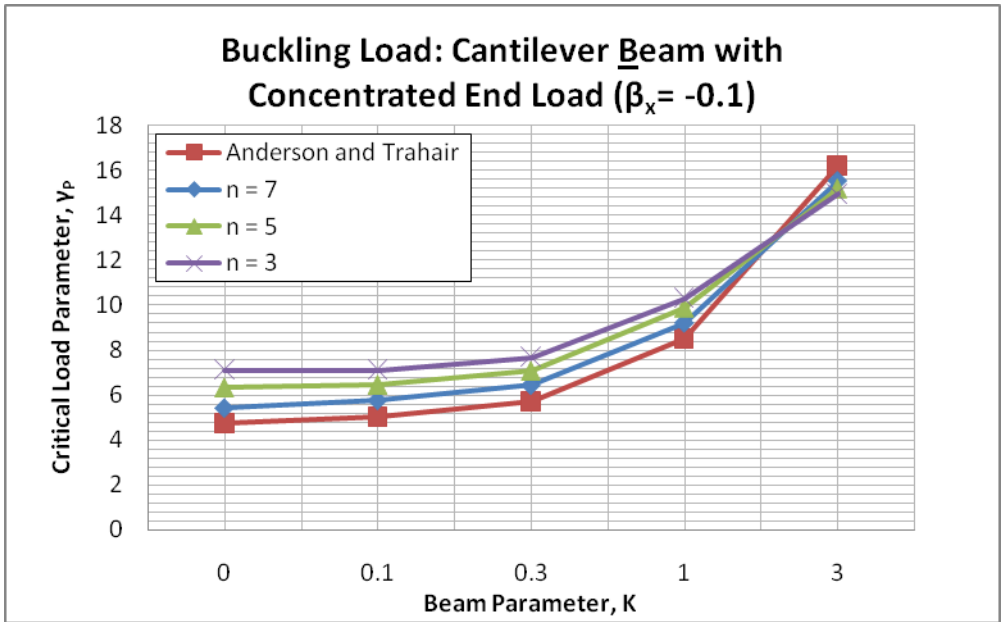

Figure 5.21 Buckling Load: Cantilever Beam with Monosymmetric Cross-Section Subjected to a Concentrated End Load $\left(\bar{\beta}_x = -0.1\right)$

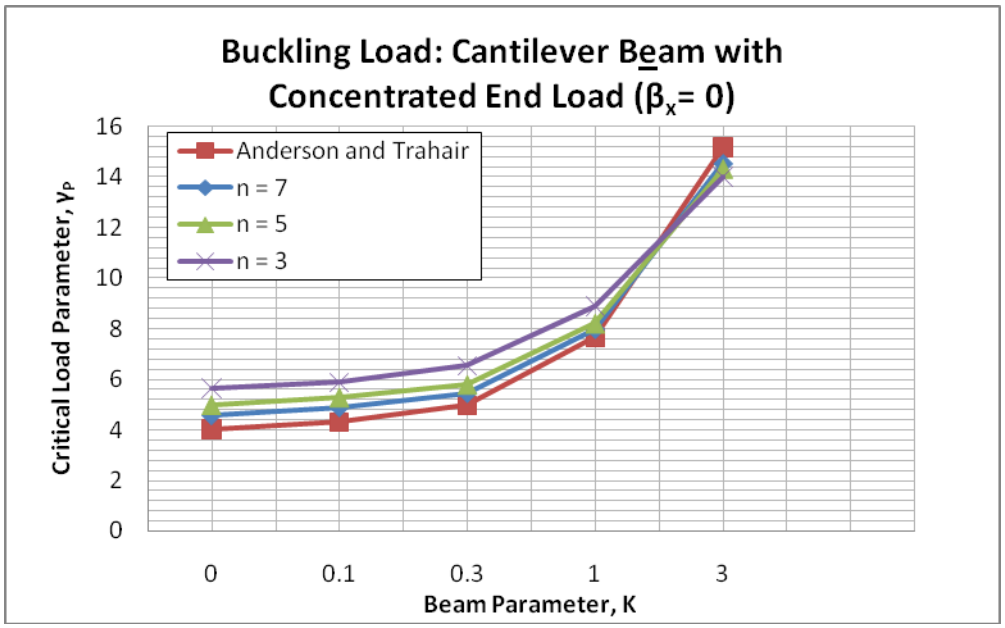

Figure 5.22 Buckling Load: Cantilever Beam with Monosymmetric Cross-Section Subjected to a Concentrated End Load $\left(\overline{\beta}_x = 0\right)$

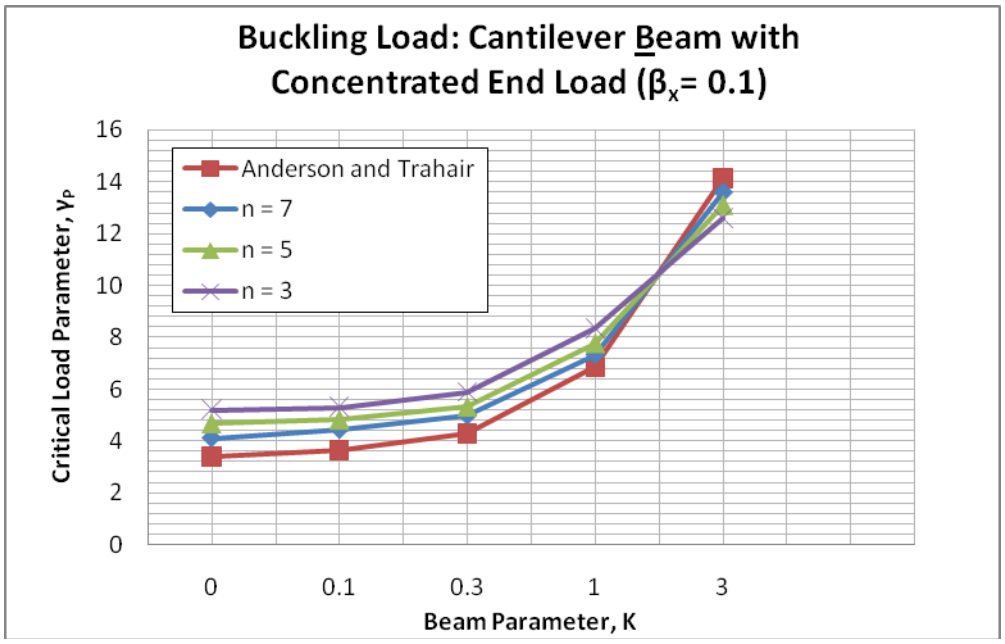

Figure 5.23 Buckling Load: Cantilever Beam with Monosymmetric Cross-Section Subjected to a Concentrated End Load $\left(\overline{\beta}_x = 0.1\right)$

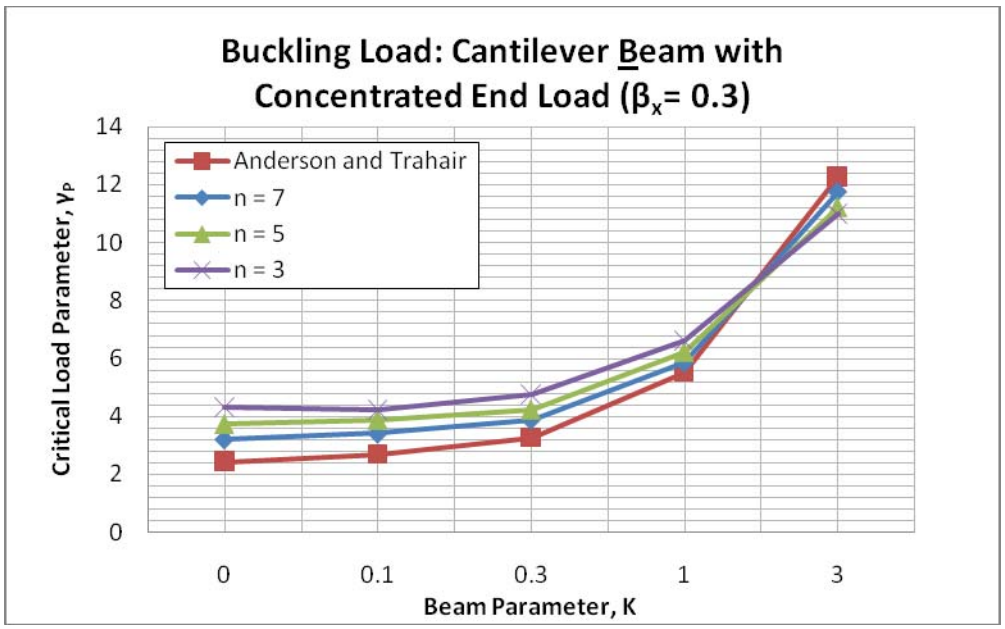

Figure 5.24 Buckling Load: Cantilever Beam with Monosymmetric Cross-Section Subjected to a Concentrated End Load $\left(\overline{\beta}_x = 0.3\right)$

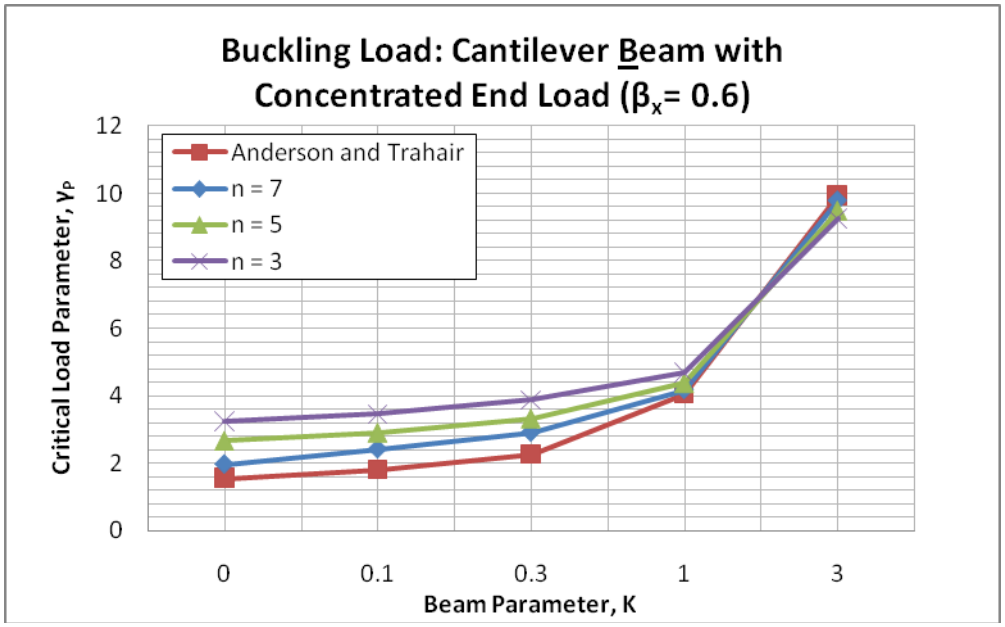

Figure 5.25 Buckling Load: Cantilever Beam with Monosymmetric Cross-Section Subjected to a Concentrated End Load $\left(\overline{\beta}_x = 0.6\right)$

6.0 FINITE ELEMENT METHOD

The finite element method is a numerical technique used to solve problems that may be otherwise difficult to solve analytically. In this chapter, the finite element method will be used in conjunction with the energy method to establish finite element equations that can be used to solve for the elastic lateral buckling load. The basic concept behind the finite element method is to model a continuum with infinite degrees of freedom and as a system of elements having finite degrees of freedom. These elements are assembled to accurately approximate the behavior of the entire system.

The first step toward formulating a finite element solution is to divide the system into a number of discrete elements. These elements are connected by nodes, which are common points shared by adjacent elements that establish the continuity of the system. The size of the elements are arbitrary and should be selected to closely model the behavior of the entire system. After the elements have been defined and nodes selected, a displacement function is established for each element. A displacement function is normally a linear combination of shape functions. Shape functions are usually polynomial functions representing a unit displacement of a particular node and zero for the other nodes. The number of polynomial functions used to describe each element is based on the number of degrees of freedom of that element. A strain-displacement relationship and a stress-strain relationship are then defined for each element from the shape functions.

The principle of minimum total potential energy will be used to derive the element stiffness matrix and an element geometric stiffness matrix. Once these matrices are obtained, they can be converted to the global coordinate system and assembled into a global stiffness matrix to represent the entire system. The matrix can then be partitioned into free and restrained degrees of freedom by the application of boundary conditions. The section of the global stiffness matrix and geometric stiffness matrix containing the free degrees of freedom can then be used to obtain the buckling loads for lateral-torsional buckling.

In this project, the structural system that the finite element method is being applied to is any plane frame. Each frame element has six nodal degrees of freedom, which means twelve total degrees of freedom for each element. The coordinate system for the beam-column elements of the plane frame is shown in Figures 6.1 – 6.3**.**

Figure 6.1 shows the top view of the element with a displacement *u(z)* at a distance *z* along the element, which is the lateral bending in the *x* direction. Of the four out-of-plane nodal coordinates shown, u_1 and u_3 are the out-of-plane nodal displacements at nodes 1 and 2, respectively, and u_2 and u_4 are the out-of-plane nodal rotations of nodes 1 and 2, respectively.

Figure 6.2 shows the elevation view of the element with a displacement *v(z)* at a distance *z* along the element, which is the in-plane bending in the *y* direction. Of the four in-plane nodal coordinates shown, v_1 and v_3 are the in-plane nodal displacements at nodes 1 and 2, respectively, and v_2 and v_4 are the in-plane nodal rotations of nodes 1 and 2, respectively.

Figure 6.3 shows the elevation view of the element with a displacement $\phi(z)$ at a distance *z* along the element, which is the torsional rotation in the z-direction. Of the four nodal coordinates shown, ϕ_1 and ϕ_3 are the torsional rotations at nodes 1 and 2, respectively, and ϕ_2 and ϕ_4 are the torsional curvatures of nodes 1 and 2, respectively.

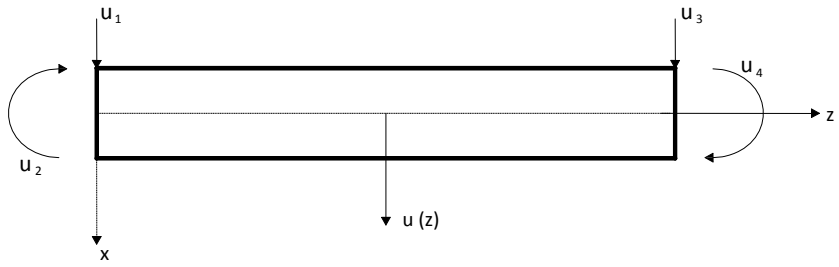

Figure 6.1 Element Degrees of Freedom with Nodal Displacements *u*

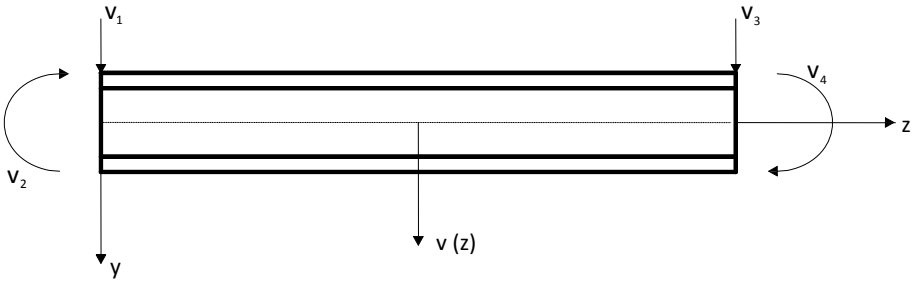

Figure 6.2 Element Degrees of Freedom with Nodal Displacements *v*

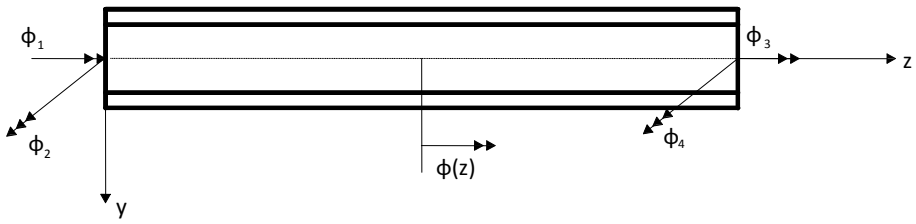

Figure 6.3 Element Degrees of Freedom with Nodal Displacements ϕ

The displacement functions for the generalized displacements *u(z)*, *v(z)*, and *φ(z)* are assumed to be cubic polynomials. These displacement functions are expressed below as (Roberts, 2004)

$$u(z) = [N]\{u\} \tag{6.1}$$

$$v(z) = [N]\{v\} \tag{6.2}$$

$$\phi(z) = [N]\{\phi\} \tag{6.3}$$

where

$$N = \left[\frac{1}{L^3}\left(2z^3 - 3z^2L + L^3\right) \quad \frac{1}{L^3}\left(z^3L - 2z^2L^2 + zL^3\right) \quad \frac{1}{L^3}\left(-2z^3 + 3z^2L\right) \quad \frac{1}{L^3}\left(z^3L - z^2L^2\right) \right] \tag{6.4}$$

and

$$\{u\} = \begin{Bmatrix} u_1 & u_2 & u_3 & u_4 \end{Bmatrix}^T \tag{6.5}$$

$$\{v\} = \begin{Bmatrix} v_1 & v_2 & v_3 & v_4 \end{Bmatrix}^T \tag{6.6}$$

$$\{\phi\} = \begin{Bmatrix} \phi_1 & \phi_2 & \phi_3 & \phi_4 \end{Bmatrix}^T \tag{6.7}$$

The matrix [*N*] is the shape function matrix for each element. Each term in the shape function matrix represents the shape of the displacement function when the element degree of freedom corresponding to the shape function has a unit value and all other degrees of freedom are equal to zero.

The first variation of the displacement functions are

$$\delta u(z) = [N]\{\delta u\} \tag{6.8}$$

$$\delta v(z) = [N]\{\delta v\} \tag{6.9}$$

$$\delta\phi(z) = [N]\{\delta\phi\} \tag{6.10}$$

The element stiffness matrix for the structure is derived using the principle of minimum total potential energy. In order to apply the finite element method, the structure must be separated into a finite number of elements. The total potential energy for the system may be expressed as

$$\frac{1}{2}\delta^2\Pi = \frac{1}{2}\sum\left(\delta^2 U_e + \lambda\delta^2\Omega_e\right) = 0 \tag{6.11}$$

where $\frac{1}{2}\delta^2 U_e$ and $\frac{1}{2}\lambda\delta^2\Omega_e$ are the second variation of the strain energy stored in each element and the work done on each element, respectively. The term λ represents the buckling load factor which the initial load set has to be multiplied by to obtain the buckling load.

The strain energy stored and the work done on each individual element may be expressed as

$$\frac{1}{2}\delta^2\Pi = \frac{1}{2}\left\{\delta d_e\right\}^T\left(\left[k_e\right] + \lambda\left[g_e\right]\right)\left\{\delta d_e\right\} \tag{6.12}$$

where

$$\left\{d_e\right\} = \begin{Bmatrix} u_1 \\ u_2 \\ \phi_1 \\ \phi_2 \\ u_3 \\ u_4 \\ \phi_3 \\ \phi_4 \end{Bmatrix} = \text{the local nodal displacement vector for each element} \tag{6.13}$$

λ = the buckling parameter for each element

$\left[k_e\right]$ = the element local stiffness matrix

$\left[g_e\right]$ = the element local geometric stiffness matrix corresponding with the initial load set

The element local stiffness matrix and geometric stiffness matrix are both 8 by 8 matrices representing eight local displacements for each element corresponding to the displacements when buckling occurs. The arrangement of each matrix is shown below with both matrices being symmetric about the main diagonal.

$$\begin{array}{c} \\ u_1 \\ u_2 \\ \phi_1 \\ \phi_2 \\ u_3 \\ u_4 \\ \phi_3 \\ \phi_4 \\ \\ \end{array} \begin{bmatrix} k_{11} & k_{12} & k_{13} & k_{14} & k_{15} & k_{16} & k_{17} & k_{18} \\ & k_{22} & k_{23} & k_{24} & k_{25} & k_{26} & k_{27} & k_{28} \\ & & k_{33} & k_{34} & k_{35} & k_{36} & k_{37} & k_{38} \\ & & & k_{44} & k_{45} & k_{46} & k_{47} & k_{48} \\ & & & & k_{55} & k_{56} & k_{57} & k_{58} \\ & & & & & k_{66} & k_{67} & k_{68} \\ & & & & & & k_{77} & k_{78} \\ & & & & & & & k_{88} \end{bmatrix} \begin{array}{c} \\ u_1 \\ u_2 \\ \phi_1 \\ \phi_2 \\ u_3 \\ u_4 \\ \phi_3 \\ \phi_4 \\ \\ \end{array} \qquad (6.14)$$

$$\begin{array}{c} \\ u_1 \\ u_2 \\ \phi_1 \\ \phi_2 \\ u_3 \\ u_4 \\ \phi_3 \\ \phi_4 \\ \\ \end{array} \begin{bmatrix} g_{11} & g_{12} & g_{13} & g_{14} & g_{15} & g_{16} & g_{17} & g_{18} \\ & g_{22} & g_{23} & g_{24} & g_{25} & g_{26} & g_{27} & g_{28} \\ & & g_{33} & g_{34} & g_{35} & g_{36} & g_{37} & g_{38} \\ & & & g_{44} & g_{45} & g_{46} & g_{47} & g_{48} \\ & & & & g_{55} & g_{56} & g_{57} & g_{58} \\ & & & & & g_{66} & g_{67} & g_{68} \\ & & & & & & g_{77} & g_{78} \\ & & & & & & & g_{88} \end{bmatrix} \begin{array}{c} \\ u_1 \\ u_2 \\ \phi_1 \\ \phi_2 \\ u_3 \\ u_4 \\ \phi_3 \\ \phi_4 \\ \\ \end{array} \qquad (6.15)$$

To obtain the stiffness matrices, the lateral torsional buckling equation must be re-written in terms of the initial load set. The second variation of total potential energy then becomes

$$\frac{1}{2}\delta^2\Pi = \frac{1}{2}\int_L \left\{ EI_y\left(\frac{d^2(\delta u)}{dz^2}\right)^2 + GJ\left(\frac{d\ (\delta\phi)}{dz}\right)^2 + EI_\omega\left(\frac{d^2(\delta\phi)}{dz^2}\right)^2 \right.$$

$$+ \lambda F\left[\left(\frac{d(\delta u)}{dz}\right)^2 + 2\hat{y}_o\left(\frac{d(\delta u)}{dz}\right)\left(\frac{d(\delta\phi)}{dz}\right) + \left(r_o^{\,2} + \hat{y}_o^{\,2}\right)\left(\frac{d\ (\delta\phi)}{dz}\right)^2\right]$$

$$\left. + \lambda M_x(z)\left[2\left(\frac{d^2(\delta u)}{dz^2}\right)\delta\phi + \beta_x\left(\frac{d(\delta\phi)}{dz}\right)^2\right]\right\} dz$$

$$+ \frac{1}{2}\lambda\int_L q\left(a - \hat{y}_o\right)\left(\delta\phi\right)^2 dz + \frac{1}{2}\lambda\sum P\left(e - \hat{y}_o\right)\left(\delta\phi\right)^2 = 0 \qquad (6.16)$$

where the first three terms will contribute to the element elastic stiffness matrix, $\left[k_e\right]$, and the rest of the equation will contribute to the element geometric stiffness matrix, $\left[g_e\right]$.

6.1 ELASTIC STIFFNESS MATRIX

The first three terms of the buckling equation, Eq. (3.88), that will contribute to the element stiffness matrix are

$$\frac{1}{2}\int_L \left\{ EI_y\left(\frac{d^2(\delta u)}{dz^2}\right)^2 + GJ\left(\frac{d\ (\delta\phi)}{dz}\right)^2 + EI_\omega\left(\frac{d^2(\delta\phi)}{dz^2}\right)^2 \right\} dz \tag{6.17}$$

which can be expressed as

$$\frac{1}{2}\int_L \{\delta\varepsilon\}^T [D]\{\delta\varepsilon\}\, dz \tag{6.18}$$

where the generalized strain vector is

$$\{\delta\varepsilon\} = \left\{ \frac{d^2(\delta u)}{dz^2} \quad \frac{d(\delta\phi)}{dz} \quad -\frac{d^2(\delta\phi)}{dz^2} \right\}^T \tag{6.19}$$

and the generalized elasticity matrix is

$$[D] = \begin{bmatrix} EI_y & 0 & 0 \\ 0 & GJ & 0 \\ 0 & 0 & EI_w \end{bmatrix} \tag{6.20}$$

Substituting the first variation of the displacement functions into the generalized strain vector yields

$$\{\delta\varepsilon\} = \begin{bmatrix} [N,zz] & [0] \\ [0] & [N,z] \\ [0] & -[N,zz] \end{bmatrix} \begin{Bmatrix} \{\delta u\} \\ \{\delta\phi\} \end{Bmatrix} \tag{6.21}$$

which is substituted into Eq. (6.17) as follows.

$$\frac{1}{2}\int_L \begin{Bmatrix} \{\delta u\} \\ \{\delta\phi\} \end{Bmatrix}^T \begin{bmatrix} [N,zz] & [0] \\ [0] & [N,z] \\ [0] & -[N,zz] \end{bmatrix}^T [D] \begin{bmatrix} [N,zz] & [0] \\ [0] & [N,z] \\ [0] & -[N,zz] \end{bmatrix} \begin{Bmatrix} \{\delta u\} \\ \{\delta\phi\} \end{Bmatrix} dz \tag{6.22}$$

The stiffness matrix can then be expressed as

$$\left[k_e\right] = \int_L \begin{bmatrix} \left[N,zz\right] & [0] \\ [0] & \left[N,z\right] \\ [0] & -\left[N,zz\right] \end{bmatrix}^T [D] \begin{bmatrix} \left[N,zz\right] & [0] \\ [0] & \left[N,z\right] \\ [0] & -\left[N,zz\right] \end{bmatrix} dz \tag{6.23}$$

Eq. (6.23) yields an 8 by 8 matrix with the following arrangement.

$$\begin{array}{c} u_1 \\ u_2 \\ u_3 \\ u_4 \\ \phi_1 \\ \phi_2 \\ \phi_3 \\ \phi_4 \end{array} \begin{bmatrix} k_{11} & k_{12} & k_{13} & k_{14} & k_{15} & k_{16} & k_{17} & k_{18} \\ & k_{22} & k_{23} & k_{24} & k_{25} & k_{26} & k_{27} & k_{28} \\ & & k_{33} & k_{34} & k_{35} & k_{36} & k_{37} & k_{38} \\ & & & k_{44} & k_{45} & k_{46} & k_{47} & k_{48} \\ & & & & k_{55} & k_{56} & k_{57} & k_{58} \\ & & & & & k_{66} & k_{67} & k_{68} \\ & & & & & & k_{77} & k_{78} \\ & & & & & & & k_{88} \end{bmatrix} \begin{array}{cccccccc} u_1 & u_2 & u_3 & u_4 & \phi_1 & \phi_2 & \phi_3 & \phi_4 \end{array} \tag{6.24}$$

The terms of the elastic stiffness matrix are then rearranged to their appropriate locations as shown in Eq. (6.14) and listed in Appendix A.

6.2 GEOMETRIC STIFFNESS MATRIX

The contribution of the lateral torsional buckling equation in terms of the initial load set to the geometric stiffness matrix is

$$\frac{1}{2}\lambda\int_L F\left\{\left[\left(\frac{d(\delta u)}{dz}\right)^2 + 2\hat{y}_o\left(\frac{d(\delta u)}{dz}\right)\left(\frac{d(\delta\phi)}{dz}\right) + \left(r_o^{\,2} + \hat{y}_o^{\,2}\right)\left(\frac{d\ (\delta\phi)}{dz}\right)^2\right]\right.$$

$$\left. + M_x(z)\left[2\left(\frac{d^2(\delta u)}{dz^2}\right)\delta\phi + \beta_x\left(\frac{d(\delta\phi)}{dz}\right)^2\right]\right\}dz$$

$$+ \frac{1}{2}\lambda\int_L q\left(a - \hat{y}_o\right)\left(\delta\phi\right)^2 dz + \frac{1}{2}\lambda\sum P\left(e - \hat{y}_o\right)\left(\delta\phi\right)^2 = 0 \qquad (6.25)$$

which can be expressed as

$$\frac{1}{2}\int_L \{\delta\varepsilon\}^T [D]\{\delta\varepsilon\}dz + \frac{1}{2}\lambda\sum P\left(e - \hat{y}_o\right)\left(\delta\phi\right)^2 \qquad (6.26)$$

where the generalized strain vector is

$$\{\delta\varepsilon\} = \left\{\frac{d(\delta u)}{dz} \quad \frac{d^2(\delta u)}{dz^2} \quad \delta\phi \quad \frac{d(\delta\phi)}{dz}\right\}^T \qquad (6.27)$$

and the generalized elasticity matrix is

$$[D] = \begin{bmatrix} F & 0 & 0 & \hat{y}_o F \\ 0 & 0 & M_x(z) & 0 \\ 0 & M_x(z) & q\left(a - \hat{y}_o\right) & 0 \\ \hat{y}_o F & 0 & 0 & F\left(r_o^{\,2} + \hat{y}_o^{\,2}\right) + \left(M_x(z)\,\beta_x\right) \end{bmatrix} \qquad (6.28)$$

Substituting the first variation of the displacement functions into the generalized strain vector yields

$$\{\delta\varepsilon\} = \begin{bmatrix} [N,z] & [0] \\ [N,zz] & [0] \\ [0] & [N] \\ [0] & [N,z] \end{bmatrix} \begin{Bmatrix} \{\delta u\} \\ \{\delta\phi\} \end{Bmatrix} \tag{6.29}$$

which is substituted into Eq. (6.26) as follows.

$$\frac{1}{2}\int_L \begin{Bmatrix} \{\delta u\} \\ \{\delta\phi\} \end{Bmatrix}^T \begin{bmatrix} [N,z] & [0] \\ [N,zz] & [0] \\ [0] & [N] \\ [0] & [N,z] \end{bmatrix}^T [D] \begin{bmatrix} [N,z] & [0] \\ [N,zz] & [0] \\ [0] & [N] \\ [0] & [N,z] \end{bmatrix} \begin{Bmatrix} \{\delta u\} \\ \{\delta\phi\} \end{Bmatrix} dz$$

$$+ \frac{1}{2}\lambda \begin{Bmatrix} \{\delta u\} \\ \{\delta\phi\} \end{Bmatrix}^T [[0] \quad [N]]^T P(e - y_o)[[0] \quad [N]] \begin{Bmatrix} \{\delta u\} \\ \{\delta\phi\} \end{Bmatrix} \Bigg|_{z=z_p} \tag{6.30}$$

The geometric stiffness matrix can then be expressed as

$$[g_e] = \int_L \begin{bmatrix} [N,z] & [0] \\ [N,zz] & [0] \\ [0] & [N] \\ [0] & [N,z] \end{bmatrix}^T [D] \begin{bmatrix} [N,z] & [0] \\ [N,zz] & [0] \\ [0] & [N] \\ [0] & [N,z] \end{bmatrix} dz$$

$$+ \frac{1}{2}[[0] \quad [N]]^T P(e - y_o)[[0] \quad [N]] \Big|_{z=z_p} \tag{6.31}$$

The previous equation yields an 8 by 8 matrix with the following arrangement.

$$\begin{array}{c} \\ u_1 \\ u_2 \\ u_3 \\ u_4 \\ \phi_1 \\ \phi_2 \\ \phi_3 \\ \phi_4 \\ \\ \end{array} \begin{array}{c} \begin{array}{cccccccc} u_1 & u_2 & u_3 & u_4 & \phi_1 & \phi_2 & \phi_3 & \phi_4 \end{array} \\ \begin{bmatrix} g_{11} & g_{12} & g_{13} & g_{14} & g_{15} & g_{16} & g_{17} & g_{18} \\ & g_{22} & g_{23} & g_{24} & g_{25} & g_{26} & g_{27} & g_{28} \\ & & g_{33} & g_{34} & g_{35} & g_{36} & g_{37} & g_{38} \\ & & & g_{44} & g_{45} & g_{46} & g_{47} & g_{48} \\ & & & & g_{55} & g_{56} & g_{57} & g_{58} \\ & & & & & g_{66} & g_{67} & g_{68} \\ & & & & & & g_{77} & g_{78} \\ & & & & & & & g_{88} \end{bmatrix} \end{array} \tag{6.32}$$

The terms of the geometric stiffness matrix are then rearranged to their appropriate locations as shown in Eq. (6.15) and listed in Appendix A.

6.3 FINITE ELEMENT METHOD CONSIDERING PREBUCKLING DEFLECTIONS

The terms of the second variation of the total potential energy equation that account for prebuckling are

$$\frac{1}{2}\int_L \left[-2\frac{I_y}{I_x}M_x(z)\frac{d^2(\delta u)}{dz^2}\delta\phi + GJ\left(\int_0^z -\frac{M_x(z)}{EI_x}dz + C\right)\frac{d(\delta\phi)}{dz}\frac{d^2(\delta u)}{dz^2}\right.$$

$$+ GJ\frac{M_x(z)}{EI_x}\frac{d(\delta\phi)}{dz}\frac{d(\delta u)}{dz} + EI_\omega\left(\int_0^z -\frac{M_x(z)}{EI_x}dz + C\right)\frac{d^2(\delta\phi)}{dz^2}\frac{d^3(\delta u)}{dz^3}$$

$$\left. + \frac{I_\omega}{I_x}V_y\frac{d^2(\delta\phi)}{dz^2}\frac{d(\delta u)}{dz}\right]dz \qquad (6.33)$$

When integrating $\left(\int_0^z -\frac{M_x(z)}{EI_x}dz\right)$, $M_x(z)$ will be redefined as

$$H_x(z) = \int_0^z M_x(\eta)d\eta \qquad (6.34)$$

Further substituting the definitions given for $M_x(z)$ in Chapter 4 yields

$$H_x(z) = M_1 z + \frac{1}{2}V_1 z^2 - \frac{1}{6}qz^3 \qquad \text{for} \qquad 0 \le z \le z_p \qquad (6.35)$$

$$H_x(z) = M_1 z + \frac{1}{2}V_1 z^2 - \frac{1}{6}qz^3 - P(\frac{1}{2}z^2 - zz_p) \qquad \text{for} \qquad z_p \le z \le L \qquad (6.36)$$

Substituting $H_x(z)$ into the prebuckling energy equation and rearranging in terms of initial load set gives

$$\frac{1}{2}\int_L \left[EI_\omega C \frac{d^2(\delta\phi)}{dz^2}\frac{d^3(\delta u)}{dz^3} + GJC\frac{d(\delta\phi)}{dz}\frac{d^2(\delta u)}{dz^2}\right]dz + \frac{1}{2}\lambda\int_L \left[-2\frac{I_y}{I_x}M_x(z)\frac{d^2(\delta u)}{dz^2}\delta\phi \right.$$

$$-\frac{I_\omega}{I_x}H_x(z)\frac{d^2(\delta\phi)}{dz^2}\frac{d^3(\delta u)}{dz^3} - \frac{GJ}{EI_x}H_x(z)\frac{d(\delta\phi)}{dz}\frac{d^2(\delta u)}{dz^2} + \frac{GJ}{EI_x}M_x(z)\frac{d(\delta\phi)}{dz}\frac{d(\delta u)}{dz}$$

$$\left. +\frac{I_\omega}{I_x}V_y\frac{d^2(\delta\phi)}{dz^2}\frac{d(\delta u)}{dz}\right]dz \qquad (6.37)$$

where the first bracketed term of this equation contributes to the elastic stiffness matrix and the remaining terms contribute to the geometric stiffness matrix. Eq. (6.12) can then be expressed as

$$\frac{1}{2}\{\delta d_e\}^T\left([k_e]+[k_e]_P+\lambda([g_e]+[g_e]_P)\right)\{\delta d_e\} \qquad (6.38)$$

where $[k_e]$ and the $[g_e]$ are the same elastic and geometric stiffness matrices, respectively, that were derived in the previous two sections and $[k_e]_P$ and $[g_e]_P$ represent the prebuckling effects and are added to the previously derived matrices.

6.4 ELASTIC STIFFNESS MATRIX CONSIDERING PREBUCKLING DEFLECTIONS

The terms from the prebuckling energy equation (Eq. 4.27) that contribute to the elastic stiffness matrix, $[k_e]_P$, are

$$\frac{1}{2}\int_L \left[EI_\omega C \frac{d^2(\delta\phi)}{dz^2}\frac{d^3(\delta u)}{dz^3} + GJC\frac{d(\delta\phi)}{dz}\frac{d^2(\delta u)}{dz^2}\right] dz \tag{6.39}$$

which can be expressed as

$$\frac{1}{2}\int_L \{\delta\varepsilon\}^T [D]\{\delta\varepsilon\}\, dz \tag{6.40}$$

where the generalized strain vector is

$$\{\delta\varepsilon\} = \left\{ \frac{d^2(\delta u)}{dz^2} \quad \frac{d^3(\delta u)}{dz^3} \quad \frac{d(\delta\phi)}{dz} \quad \frac{d^2(\delta\phi)}{dz^2} \right\}^T \tag{6.41}$$

and the generalized elasticity matrix is

$$[D] = \begin{bmatrix} 0 & 0 & \frac{GJ}{2} & 0 \\ 0 & 0 & 0 & \frac{EI_\omega}{2} \\ \frac{GJ}{2} & 0 & 0 & 0 \\ 0 & \frac{EI_\omega}{2} & 0 & 0 \end{bmatrix} \tag{6.42}$$

Substituting the first variation of the displacement functions into the generalized strain vector yields

$$\{\delta\varepsilon\} = \begin{bmatrix} [N,zz] & 0 \\ [N,zzz] & 0 \\ 0 & [N,z] \\ 0 & [N,zz] \end{bmatrix} \begin{Bmatrix} \{\delta u\} \\ \{\delta\phi\} \end{Bmatrix} \tag{6.43}$$

which is substituted into Eq. (6.40) as follows.

$$\frac{1}{2}C\int_L \begin{Bmatrix} \{\delta u\} \\ \{\delta \phi\} \end{Bmatrix}^T \begin{bmatrix} [N,zz] & 0 \\ [N,zzz] & 0 \\ 0 & [N,z] \\ 0 & [N,zz] \end{bmatrix}^T [D] \begin{bmatrix} [N,zz] & 0 \\ [N,zzz] & 0 \\ 0 & [N,z] \\ 0 & [N,zz] \end{bmatrix} \begin{Bmatrix} \{\delta u\} \\ \{\delta \phi\} \end{Bmatrix} dz \qquad (6.44)$$

The stiffness matrix can then be expressed as

$$[k_e]_P = C\int_L \begin{bmatrix} [N,zz] & 0 \\ [N,zzz] & 0 \\ 0 & [N,z] \\ 0 & [N,zz] \end{bmatrix}^T [D] \begin{bmatrix} [N,zz] & 0 \\ [N,zzz] & 0 \\ 0 & [N,z] \\ 0 & [N,zz] \end{bmatrix} dz \qquad (6.45)$$

The elastic stiffness matrix considering prebuckling deflections, $[k_e]_P$, is again an 8 by 8 matrix. The terms of $[k_e]_P$ are then rearranged to their appropriate locations as shown in Eq. (6.14) and listed in Appendix A.

6.5 GEOMETRIC STIFFNESS MATRIX CONSIDERING PREBUCKLING DEFLECTIONS

The terms from the prebuckling energy equation Eq. (4.27) in terms of the initial load set that contribute to the geometric stiffness matrix, $[g_e]_P$, are

$$\frac{1}{2}\lambda\int_L\left[-2\frac{I_y}{I_x}M_x(z)\frac{d^2(\delta u)}{dz^2}\delta\phi-\frac{I_\omega}{I_x}H_x(z)\frac{d^2(\delta\phi)}{dz^2}\frac{d^3(\delta u)}{dz^3}-\frac{GJ}{EI_x}H_x(z)\frac{d(\delta\phi)}{dz}\frac{d^2(\delta u)}{dz^2}\right.$$

$$\left.+\frac{GJ}{EI_x}M_x(z)\frac{d(\delta\phi)}{dz}\frac{d(\delta u)}{dz}+\frac{I_\omega}{I_x}V_y\frac{d^2(\delta\phi)}{dz^2}\frac{d(\delta u)}{dz}\right]dz \tag{6.46}$$

which can be expressed as

$$\frac{1}{2}\lambda\int_L\{\delta\varepsilon\}^T[D]\{\delta\varepsilon\}\,dz \tag{6.47}$$

where the generalized strain vector is

$$\{\delta\varepsilon\}=\left\{\frac{d(\delta u)}{dz}\quad\frac{d^2(\delta u)}{dz^2}\quad\frac{d^3(\delta u)}{dz^3}\quad\delta\phi\quad\frac{d(\delta\phi)}{dz}\quad\frac{d^2(\delta\phi)}{dz^2}\right\}^T \tag{6.48}$$

and the generalized elasticity matrix is

$$[D]=\begin{bmatrix}0&0&0&0&\frac{GJM_x(z)}{2EI_x}&\frac{I_\omega V_y}{2I_x}\\0&0&0&-\frac{I_yM_x(z)}{I_x}&-\frac{GJH_x(z)}{2EI_x}&0\\0&0&0&0&0&-\frac{I_\omega H_x(z)}{2I_x}\\0&-\frac{I_yM_x(z)}{I_x}&0&0&0&0\\\frac{GJM_x(z)}{2EI_x}&-\frac{GJH_x(z)}{2EI_x}&0&0&0&0\\\frac{I_\omega V_y}{2I_x}&0&-\frac{I_\omega H_x(z)}{2I_x}&0&0&0\end{bmatrix} \tag{6.49}$$

Substituting the first variation of the displacement functions into the generalized strain vector yields

$$\{\delta\varepsilon\} = \begin{bmatrix} [N,z] & 0 \\ [N,zz] & 0 \\ [N,zzz] & 0 \\ 0 & [N] \\ 0 & [N,z] \\ 0 & [N,zz] \end{bmatrix} \begin{Bmatrix} \{\delta u\} \\ \{\delta\phi\} \end{Bmatrix} \tag{6.50}$$

which is substituted into Eq. (6.47) as follows.

$$\frac{1}{2}\lambda \int_L \begin{Bmatrix} \{\delta u\} \\ \{\delta\phi\} \end{Bmatrix}^T \begin{bmatrix} [N,z] & 0 \\ [N,zz] & 0 \\ [N,zzz] & 0 \\ 0 & [N] \\ 0 & [N,z] \\ 0 & [N,zz] \end{bmatrix}^T [D] \begin{bmatrix} [N,z] & 0 \\ [N,zz] & 0 \\ [N,zzz] & 0 \\ 0 & [N] \\ 0 & [N,z] \\ 0 & [N,zz] \end{bmatrix} \begin{Bmatrix} \{\delta u\} \\ \{\delta\phi\} \end{Bmatrix} dz \tag{6.51}$$

The geometric stiffness matrix can then be expressed as

$$[g_e]_P = \int_L \begin{bmatrix} [N,z] & 0 \\ [N,zz] & 0 \\ [N,zzz] & 0 \\ 0 & [N] \\ 0 & [N,z] \\ 0 & [N,zz] \end{bmatrix}^T [D] \begin{bmatrix} [N,z] & 0 \\ [N,zz] & 0 \\ [N,zzz] & 0 \\ 0 & [N] \\ 0 & [N,z] \\ 0 & [N,zz] \end{bmatrix} dz \tag{6.52}$$

The geometric stiffness matrix considering prebuckling deflections, $[g_e]_P$, is again an 8 by 8 matrix. The terms of $[g_e]_P$ are then rearranged to their appropriate locations as shown in Eq. (6.15) and listed in Appendix A.

7.0 SUMMARY

Lateral-torsional buckling occurs when a beam has a relatively small lateral and torsional stiffness compared to its stiffness in the plane of loading, causing the beam to deflect laterally and twist out of plane when it reaches a critical load. This load is known as the lateral-torsional buckling load, or LTB load. A review of existing literature was presented to demonstrated previous methods used to derive the LTB load, including the differential equilibrium method of stability and energy methods. The derivations of the LTB load for structures with doubly-symmetric cross-sections have been long discussed and readily available. Lateral-torsional buckling of a structure with a monosymmetric cross-section is an underdeveloped topic, with derivations complicated by the fact that the centroid and the shear center do not coincide in these cross sections. The purpose of this study was to derive equations for lateral-torsional buckling of structures with monosymmetric cross-sections, examine the validity of these equations using approximate shape functions and comparing these results to other analysis, and use the finite element method to obtain element elastic stiffness and geometric stiffness matrices that may be used in future research, in conjunction with computer software, to predict the LTB load for complex systems.

The energy equation for lateral-torsional buckling of a beam-column element is based on the theorem of minimum total potential energy. The total potential energy of the system is the sum of the strain energy and the potential energy of the external loads. This theorem indicates

that the critical condition for buckling occurs when the second variation of the total potential energy is equal to zero, representing the transition from a stable to an unstable state.

The energy equations in this paper are derived for cases both ignoring and considering prebuckling displacements. Prebuckling, or in-plane, displacements are considered so small for thin-walled structures that their effect on the lateral-torsional buckling load is negligible. This assumption is only valid when the ratios of minor axis flexural stiffness and torsional stiffness to the major axis flexural stiffness are very small. When these ratios are not small, the effects of prebuckling deformations will significantly alter the LTB load and cannot be ignored. A non-dimensional buckling equation is also presented for cases without prebuckling displacements. The advantage of this form is that the solution can be transferred to other structural systems with the same loading conditions.

The validity of these energy equations for the lateral-torsional buckling of beam-column elements with monosymmetric cross-sections is examined in the applications section of the paper. Suitable trigonometric shape functions for beams that are simply supported and cantilever are used to compare the buckling results obtained from the present research to results obtained in previous literature using the method of finite differences. The derived energy equations prove to be accurate in predicting critical loads for different boundary and loading conditions, with the degree of precision based on the ability of the shape function to predict the buckled shape of the beam.

The finite element method is used to project the energy equations for lateral-torsional buckling of a beam-column element onto a structure with complicated loads, boundary conditions, and geometry. The expression for the second variation of total potential energy is

used to derive element elastic stiffness and geometric stiffness matrices for the structure. These matrices can then be transformed to a global coordinate system for each element and assembled so boundary conditions can be used to transform the structure from unrestrained to restrained. The result is a generalized eigenvalue problem that will produce lateral-torsional buckling loads for the structure. The objective is that future research can utilize these stiffness matrices, along with computer software, to develop models of complex systems with monosymmetric beam-columns and predict the lateral-torsional buckling loads of that system.

APPENDIX A

A.1 ELEMENT ELASTIC STIFFNESS MATRIX

$$k_{11} = \frac{12E\,I_y}{L^3}$$

$$k_{12} = \frac{6E\,I_y}{L^2}$$

$$k_{15} = \frac{-12E\,I_y}{L^3}$$

$$k_{16} = \frac{6E\,I_y}{L^2}$$

$$k_{22} = \frac{4E\,I_y}{L}$$

$$k_{25} = \frac{-6E\,I_y}{L^2}$$

$$k_{26} = \frac{2E\,I_y}{L}$$

$$k_{33} = \frac{12E\,I_\omega}{L^3} + \frac{6G\,J}{5\,L}$$

$$k_{34} = \frac{6E\,I_\omega}{L^2} + \frac{G\,J}{10}$$

$$k_{37} = \frac{-12E\,I_\omega}{L^3} - \frac{6\,G\,J}{5}$$

$$k_{38} = \frac{6E\,I_\omega}{L^2} + \frac{G\,J}{10}$$

$$k_{44} = \frac{4E\,I_\omega}{L^2} + \frac{2G\,J\,L}{15}$$

$$k_{47} = \frac{-6E\,I_{\omega}}{L^2} - \frac{G\,J}{10}$$

$$k_{48} = \frac{2E\,I_{\omega}}{L} - \frac{G\,J\,L}{30}$$

$$k_{55} = \frac{12E\,I_{y}}{L^3}$$

$$k_{56} = \frac{-6E\,I_{y}}{L^2}$$

$$k_{66} = \frac{4E\,I_{y}}{L}$$

$$k_{77} = \frac{12E\,I_{\omega}}{L^3} + \frac{6\,G\,J}{5\,L}$$

$$k_{78} = \frac{-6E\,I_{\omega}}{L^2} - \frac{G\,J}{10}$$

$$k_{88} = \frac{4E\,I_{\omega}}{L} + \frac{2\,G\,J\,L}{15}$$

A.2 ELEMENT GEOMETRIC STIFFNESS MATRIX

$$g_{11} = \frac{6\,F}{5\,L}$$

$$g_{12} = \frac{F}{10}$$

$$g_{13} = \frac{1}{70\,L}\left[(-q)\,L^2 - 7\,L\,V_1 + 7\,L\,P - 84\,M_1 - 84\,P\,z_p + 84\,y_o\,F\right]$$

$$g_{14} = \frac{-1}{140}\,q\,L^2 - \frac{1}{10}\,M_1 - \frac{1}{10}\,P\,z_p + \frac{1}{10}\,y_o\,F$$

$$g_{15} = \frac{-6F}{5\,L}$$

$$g_{16} = \frac{F}{10}$$

$$g_{17} = \frac{-1}{70\,L}\left(34\,q\,L^2 - 77\,L\,V_1 + 77\,L\,P - 84\,M_1 - 84\,P\,z_p + 84\,y_o\,F\right)$$

$$g_{18} = \frac{3}{70}\,q\,L^2 - \frac{1}{10}\,L\,V_1 + \frac{1}{10}\,L\,P - \frac{1}{10}\,M_1 - \frac{1}{10}\,P\,z_p + \frac{1}{10}\,y_o\,F$$

$$g_{22} = \frac{2F\,L}{15}$$

$$g_{23} = \frac{11}{420}\,q\,L^2 - \frac{1}{5}\,L\,V_1 + \frac{1}{5}\,L\,P - \frac{11}{10}\,M_1 - \frac{11}{10}\,P\,z_p + \frac{1}{10}\,y_o\,F$$

$$g_{24} = \frac{1}{210}\,q\,L^3 - \frac{1}{30}\,L^2\,V_1 + \frac{1}{30}\,L^2\,P - \frac{2}{15}\,L\,M_1 - \frac{2}{15}\,L\,P\,z_p + \frac{2}{15}\,L\,y_o\,F$$

$$g_{25} = \frac{-\mathrm{F}}{10}$$

$$g_{26} = \frac{-F\,L}{30}$$

$$g_{27} = \frac{-23}{210}\,q\,L^2 + \frac{1}{5}\,L\,V_1 - \frac{1}{5}\,L\,P + \frac{1}{10}\,M_1 + \frac{1}{10}\,P\,z_p - \frac{1}{10}\,y_o\,F$$

$$g_{28} = \frac{1}{210}\,q\,L^3 + \frac{1}{30}\,L\,M_1 + \frac{1}{30}\,L\,P\,z_p - \frac{1}{30}\,L\,y_o\,F$$

$$g_{33} = \frac{1}{35\,L}\Big[13\,L^2\,q\,a - 13\,L^2\,q\,y_o - 6\,L^2\,q\,\beta_x + 21\,L\,\beta_x\,V_1 - 21\,L\,\beta_x\,P + 42\,F\,(r_o)^2$$

$$+ 42\,F\,(y_o)^2 + 42\,\beta_x\,M_1 + 42\,\beta_x\,P\,z_p\Big] + \frac{1}{L^6}\Big[2\,(z_p)^3 - 3\,(z_p)^2\,L + L^3\Big]^2\,P\,(e - y_o)$$

$$g_{34} = \frac{11}{210}L^2\,q\,a - \frac{11}{210}L^2\,q\,y_o - \frac{1}{28}L^2\,q\,\beta_x + \frac{1}{10}L\,\beta_x\,V_1 - \frac{1}{10}L\,\beta_x\,P + \frac{1}{10}F(r_o)^2 + \frac{1}{10}F(y_o)^2$$

$$+ \frac{1}{10}\beta_x M_1 + \frac{1}{10}\beta_x P z_p + \frac{1}{L^6}\Big[2(z_p)^3 - 3(z_p)^2 L + L^3\Big]P(e - y_o)\Big[(z_p)^3 L - 2(z_p)^2 L^2 + z_p L^3\Big]$$

$$g_{35} = \frac{1}{70\,L}\left(q\,L^2 + 7\,L\,V_1 - 7\,L\,P + 84\,M_1 + 84\,P\,z_p - 84\,y_o\,F\right)$$

$$g_{36} = \frac{-17}{420}\,q\,L^2 + \frac{1}{10}\,L\,V_1 - \frac{1}{10}\,L\,P - \frac{1}{10}\,M_1 - \frac{1}{10}\,P\,z_p + \frac{1}{10}\,y_o\,F$$

$$g_{37} = \frac{-3}{70L}\Big[(-3)\,L^2\,q\,a + 3\,L^2\,q\,y_o - 4\,L^2\,q\,\beta_x + 14L\,\beta_x\,V_1 - 14L\,\beta_x\,P + 28F(r_o)^2 + 28F(y_o)^2$$

$$+ 28\beta_x M_1 + 28\beta_x P z_p\Big] + \frac{1}{L^6}\Big[2\,(z_p)^3 - 3\,(z_p)^2\,L + L^3\Big]P(e - y_o)\Big[(-2)\,(z_p)^3 + 3\,(z_p)^2\,L\Big]$$

$$g_{38} = \frac{-13}{420} L^2 q\, a + \frac{13}{420} L^2 q\, y_o + \frac{1}{70} L^2 q\, \beta_x + \frac{1}{10} F\left(r_o\right)^2 + \frac{1}{10} F\left(y_o\right)^2 + \frac{1}{10} \beta_x M_1$$

$$+ \frac{1}{10} \beta_x P\, z_p + \frac{1}{L^6}\left[2\left(z_p\right)^3 - 3\left(z_p\right)^2 L + L^3\right] P\left(e - y_o\right)\left[\left(z_p\right)^3 L - \left(z_p\right)^2 L^2\right]$$

$$g_{44} = \frac{1}{105} L^3 q\, a - \frac{1}{105} L^3 q\, y_o - \frac{1}{105} q\, \beta_x L^3 + \frac{1}{30} L^2 \beta_x V_1 - \frac{1}{30} L^2 \beta_x P + \frac{2}{15} L F\left(r_o\right)^2$$

$$+ \frac{2}{15} L F\left(y_o\right)^2 + \frac{2}{15} L \beta_x M_1 + \frac{2}{15} L \beta_x P\, z_p + \frac{1}{L^6}\left[\left(z_p\right)^3 L - 2\left(z_p\right)^2 L^2 + z_p\, L^3\right]^2 P\left(e - y_o\right)$$

$$g_{45} = \frac{1}{140} q\, L^2 + \frac{1}{10} M_1 + \frac{1}{10} P\, z_p - \frac{1}{10} y_o\, F$$

$$g_{46} = \frac{-1}{84} q\, L^3 + \frac{1}{30} L^2 V_1 - \frac{1}{30} L^2 P + \frac{1}{30} L M_1 + \frac{1}{30} L P\, z_p - \frac{1}{30} L\, y_o F$$

$$g_{47} = \frac{13}{420} L^2 q\, a - \frac{13}{420} L^2 q\, y_o + \frac{1}{28} L^2 q\, \beta_x - \frac{1}{10} L \beta_x V_1 + \frac{1}{10} L \beta_x P - \frac{1}{10} F\left(r_o\right)^2 - \frac{1}{10} F\left(y_o\right)^2 - \frac{1}{10} \beta_x M_1$$

$$- \frac{1}{10} \beta_x P z_p + \frac{1}{L^6}\left[\left(z_p\right)^3 L - 2\left(z_p\right)^2 L^2 + z_p\, L^3\right] P\left(e - y_o\right)\left[(-2)\left(z_p\right)^3 + 3\left(z_p\right)^2 L\right]$$

$$g_{48}=\frac{-1}{140}L^3 q a+\frac{1}{140}L^3 q y_o+\frac{1}{140}q\beta_x L^3-\frac{1}{60}L^2\beta_x V_1+\frac{1}{60}L^2\beta_x P-\frac{1}{30}LF(r_o)^2-\frac{1}{30}LF(y_o)^2-\frac{1}{30}L\beta_x M_1$$

$$-\frac{1}{30}L\beta_x P z_p+\frac{1}{L^6}\left[(z_p)^3 L-2(z_p)^2 L^2+z_p L^3\right]P(e-y_o)\left[(z_p)^3 L-(z_p)^2 L^2\right]$$

$$g_{55}=\frac{6F}{5\,L}$$

$$g_{56}=\frac{-F}{10}$$

$$g_{57}=\frac{-1}{70\,L}\left[(-34)\,q\,L^2+77\,L\,V_1-77\,L\,P+84\,M_1+84\,P\,z_p-84\,y_o\,F\right]$$

$$g_{58}=\frac{-3}{70}\,q\,L^2+\frac{1}{10}\,L\,V_1-\frac{1}{10}\,L\,P+\frac{1}{10}\,M_1+\frac{1}{10}\,P\,z_p-\frac{1}{10}\,y_o\,F$$

$$g_{66}=\frac{2F\,L}{15}$$

$$g_{67}=\frac{-79}{210}\,q\,L^2+\frac{9}{10}\,L\,V_1-\frac{9}{10}\,L\,P+\frac{11}{10}\,M_1+\frac{11}{10}\,P\,z_p-\frac{1}{10}\,y_o\,F$$

$$g_{68}=\frac{4}{105}\,q\,L^3-\frac{1}{10}\,L^2\,V_1+\frac{1}{10}\,L^2\,P-\frac{2}{15}\,L\,M_1-\frac{2}{15}\,L\,P\,z_p+\frac{2}{15}\,L\,y_o\,F$$

$$g_{77} = \frac{1}{35\,L}\Big[13\,L^2\,q\,a - 13\,L^2\,q\,y_o - 6\,L^2\,q\,\beta_x + 21\,L\,\beta_x\,V_1 - 21\,L\,\beta_x\,P + 42\,F\left(r_o\right)^2 + 42\,F\left(y_o\right)^2$$

$$+ 42\,\beta_x\,M_1 + 42\,\beta_x\,P\,z_p\Big] + \frac{1}{L^6}\Big[(-2)\left(z_p\right)^3 + 3\left(z_p\right)^2 L\Big]^2\,P\left(e - y_o\right)$$

$$g_{78} = \frac{-11}{210}\,L^2\,q\,a + \frac{11}{210}\,L^2\,q\,y_o - \frac{1}{70}\,L^2\,q\,\beta_x - \frac{1}{10}\,F\left(r_o\right)^2 - \frac{1}{10}\,F\left(y_o\right)^2 - \frac{1}{10}\,\beta_x\,M_1 - \frac{1}{10}\,\beta_x\,P\,z_p$$

$$+ \frac{1}{L^6}\Big[(-2)\left(z_p\right)^3 + 3\left(z_p\right)^2 L\Big]\,P\left(e - y_o\right)\Big[\left(z_p\right)^3 L - \left(z_p\right)^2 L^2\Big]$$

$$g_{88} = \frac{1}{105}\,L^3\,q\,a - \frac{1}{105}\,L^3\,q\,y_o - \frac{3}{70}\,q\,\beta_x\,L^3 + \frac{1}{10}\,L^2\,\beta_x\,V_1 - \frac{1}{10}\,L^2\,\beta_x\,P + \frac{2}{15}\,L\,F\left(r_o\right)^2$$

$$+ \frac{2}{15}\,L\,F\left(y_o\right)^2 + \frac{2}{15}\,L\,\beta_x\,M_1 + \frac{2}{15}\,L\,\beta_x\,P\,z_p + \frac{1}{L^6}\Big[\left(z_p\right)^3 L - \left(z_p\right)^2 L^2\Big]^2\,P\left(e - y_o\right)$$

A.3 ELEMENT NON-DIMENSIONAL STIFFNESS MATRIX

$$k_{11} = 12$$

$$k_{12} = 6$$

$$k_{15} = -12$$

$$k_{16} = 6$$

$$k_{22} = 4$$

$$k_{25} = -6$$

$$k_{26} = 2$$

$$k_{33} = \frac{6}{5} + \frac{12\,K^2}{\pi^2}$$

$$k_{34} = \frac{1}{10} + \frac{6\,K^2}{\pi^2}$$

$$k_{37} = \frac{-6}{5} - \frac{12\,K^2}{\pi^2}$$

$$k_{38} = \frac{1}{10} + \frac{6\,K^2}{\pi^2}$$

$$k_{44} = \frac{2}{15} + \frac{4\,K^2}{\pi^2}$$

$$k_{47} = \frac{-1}{10} - \frac{6\,K^2}{\pi^2}$$

$$k_{48} = \frac{-1}{30} + \frac{2\,K^2}{\pi^2}$$

$$k_{55} = 12$$

$$k_{56} = -6$$

$$k_{66} = 4$$

$$k_{77} = \frac{6}{5} + \frac{12\,K^2}{\pi^2}$$

$$k_{78} = \frac{-1}{10} + \frac{6\,K^2}{\pi^2}$$

$$k_{88} = \frac{2}{15} + \frac{4\,K^2}{\pi^2}$$

A.4 ELEMENT NON-DIMENSIONAL GEOMETRIC STIFFNESS MATRIX

$$g_{11} = \frac{6\,\overline{F}}{5}$$

$$g_{12} = \frac{-2\,\overline{F}}{5}$$

$$g_{13} = \frac{\overline{P}}{10} - \frac{6\,\overline{M}_1}{5} - \frac{\overline{V}_1}{10} - \frac{\overline{P}}{70} + \frac{6\,\overline{F}\,\overline{y}_o}{5} - \frac{6\,\overline{P}\,\overline{z}_p}{5}$$

$$g_{14} = \frac{-\overline{P}}{140} - \frac{\overline{M}_1}{10} - \frac{\overline{P}\,\overline{z}_p}{10} - \frac{2\,\overline{F}\,\overline{y}_o}{5}$$

$$g_{15} = \frac{-6\,\overline{F}}{5}$$

$$g_{16} = \frac{\overline{F}}{10}$$

$$g_{17} = \frac{-17\,\overline{P}}{35} + \frac{11\,\overline{V}_1}{10} - \frac{11\,\overline{P}}{10} + \frac{6\,\overline{M}_1}{5} + \frac{6\,\overline{P}\,\overline{z}_p}{5} - \frac{6\,\overline{F}\,\overline{y}_o}{5}$$

$$g_{18} = \frac{3\,\overline{P}}{70} - \frac{\overline{V}_1}{10} + \frac{\overline{P}}{10} - \frac{\overline{M}_1}{10} - \frac{\overline{P}\,\overline{z}_p}{10} + \frac{\overline{F}\,\overline{y}_o}{10}$$

$$g_{22} = \frac{7\,\overline{F}}{15}$$

$$g_{23} = \frac{\overline{P}}{14} - \frac{4\,\overline{V}_1}{15} + \frac{4\,\overline{P}}{15} - \frac{3\,\overline{M}_1}{5} - \frac{3\,\overline{P}\,\overline{z}_p}{5} - \frac{2\,\overline{F}\,\overline{y}_o}{5}$$

$$g_{24} = \frac{2\,\overline{P}}{105} - \frac{\overline{V}_1}{15} + \frac{\overline{P}}{15} - \frac{2\,\overline{M}_1}{15} - \frac{2\,\overline{P}\,\overline{z}_p}{15} + \frac{7\,\overline{F}\,\overline{y}_o}{15}$$

$$g_{25} = \frac{2\,\overline{F}}{5}$$

$$g_{26} = \frac{-\overline{F}}{5}$$

$$g_{27} = \frac{3\,\overline{P}}{7} - \frac{16\,\overline{V}_1}{15} + \frac{16\,\overline{P}}{15} - \frac{7\,\overline{M}_1}{5} - \frac{7\,\overline{P}\,\overline{z}_p}{5} + \frac{2\,\overline{F}\,\overline{y}_o}{5}$$

$$g_{28} = \frac{-\overline{P}}{21} + \frac{2\,\overline{V}_1}{15} - \frac{2\,\overline{P}}{15} + \frac{\overline{M}_1}{5} + \frac{\overline{P}\,\overline{z}_p}{5} - \frac{\overline{F}\,\overline{y}_o}{5}$$

$$g_{33} = \frac{1}{70\pi}\left[13\overline{P}K\overline{a} - 13\overline{P}K\overline{y}_o - 6\overline{P}\overline{\beta}_x\pi + 21\overline{\beta}_x\pi\,\overline{V}_1 - 21\overline{\beta}_x\pi\,\overline{P} + 84\left(\overline{r}_o\right)^2\pi + 84\left(\overline{y}_o\right)^2\pi \right.$$
$$\left. + 42\overline{\beta}_x\pi\,\overline{M}_1 + 42\overline{\beta}_x\pi\,\overline{P}\overline{z}_p\right] + \frac{1}{2}\left[2\left(\overline{z}_p\right)^3 - 3\left(\overline{z}_p\right)^2 + 1\right]^2\overline{P}\left(\overline{e} - \overline{y}_o\right)\frac{\overline{K}}{\pi}$$

$$g_{34} = \frac{-1}{840\pi}\left[(-22)\,\overline{P}K\overline{a} + 22\overline{P}K\overline{y}_o - 3\overline{P}\overline{\beta}_x\pi + 42\overline{\beta}_x\pi\,\overline{V}_1 - 42\overline{\beta}_x\pi\,\overline{P} + 336\left(\overline{r}_o\right)^2\pi \right.$$
$$\left. + 336\left(\overline{y}_o\right)^2\pi + 168\overline{\beta}_x\pi\,\overline{M}_1 + 168\overline{\beta}_x\pi\,\overline{P}\overline{z}_p\right]$$
$$+ \frac{1}{2}\left[2\left(\overline{z}_p\right)^3 - 3\left(\overline{z}_p\right)^2 + 1\right]\left[\left(\overline{z}_p\right)^3 - 2\left(\overline{z}_p\right)^2 + \overline{z}_p\right]\overline{P}\left(\overline{e} - \overline{y}_o\right)\frac{K}{\pi}$$

$$g_{35} = \frac{-\overline{P}}{10} + \frac{6\overline{M}_1}{5} + \frac{\overline{V}_1}{10} + \frac{\overline{P}}{70} - \frac{6\overline{F}\overline{y}_o}{5} + \frac{6\overline{P}\overline{z}_p}{5}$$

$$g_{36} = \frac{-\overline{P}}{10} - \frac{\overline{\mathrm{M}}_1}{10} + \frac{\overline{V}_1}{10} - \frac{17\overline{P}}{420} + \frac{\overline{F}\overline{y}_o}{10} - \frac{\overline{P}\overline{z}_p}{10}$$

$$g_{37} = \frac{-3}{140\pi}\left[(-3)\,\overline{P}K\overline{a} + 3\overline{P}K\overline{y}_o - 4\overline{P}\overline{\beta}_x\pi + 14\overline{\beta}_x\pi\,\overline{V}_1 - 14\overline{\beta}_x\pi\,\overline{P} + 56\left(\overline{r}_o\right)^2\pi + 56\left(\overline{y}_o\right)^2\pi \right.$$
$$\left. + 28\overline{\beta}_x\pi\,\overline{M}_1 + 28\overline{\beta}_x\pi\,\overline{P}\overline{z}_p\right] + \frac{1}{2}\left[2\left(\overline{z}_p\right)^3 - 3\left(\overline{z}_p\right)^2 + 1\right]\left[(-2)\left(\overline{z}_p\right)^3 + 3\left(\overline{z}_p\right)^2\right]\overline{P}\left(\overline{e} - \overline{y}_o\right)\frac{K}{\pi}$$

$$g_{38} = \frac{1}{840\pi}\left[(-13)\,\bar{P}K\,\bar{a} + 13\bar{P}K\,\bar{y}_o + 6\,\bar{P}\,\bar{\beta}_x\,\pi + 84\left(\bar{r}_o\right)^2\pi + 84\left(\bar{y}_o\right)^2\pi + 42\bar{\beta}_x\,\pi\,\bar{M}_1 \right.$$
$$\left. + 42\bar{\beta}_x\,\pi\,\bar{P}\bar{z}_p\right] + \frac{1}{2}\left[2\left(\bar{z}_p\right)^3 - 3\left(\bar{z}_p\right)^2 + 1\right]\left[\left(\bar{z}_p\right)^3 - \left(\bar{z}_p\right)^2\right] P\left(\bar{e} - \bar{y}_o\right)\frac{K}{\pi}$$

$$g_{44} = \frac{1}{420\pi}\left[2\,\bar{P}K\,\bar{a} - 2\,\bar{P}K\,\bar{y}_o + 196\left(\bar{r}_o\right)^2\pi - 11\bar{P}\,\bar{\beta}_x\,\pi + 196\left(\bar{y}_o\right)^2\pi + 35\bar{\beta}_x\,\pi\,\bar{V}_1 - 35\bar{\beta}_x\,\pi\,\bar{P}\right.$$
$$\left. + 98\bar{\beta}_x\,\pi\,\bar{M}_1 + 98\bar{\beta}_x\,\pi\,\bar{P}\bar{z}_p\right] + \frac{1}{2}\left[\left(\bar{z}_p\right)^3 - 2\left(\bar{z}_p\right)^2 + \bar{z}_p\right]^2 \bar{P}\left(\bar{e} - \bar{y}_o\right)\frac{K}{\pi}$$

$$g_{45} = \frac{\bar{P}}{140} + \frac{\bar{M}_1}{10} + \frac{\bar{P}\bar{z}_p}{10} + \frac{2\,\bar{F}\,\bar{y}_o}{5}$$

$$g_{46} = \frac{-\bar{P}}{84} + \frac{\bar{V}_1}{30} - \frac{\bar{P}}{30} + \frac{\bar{M}_1}{30} + \frac{\bar{P}\bar{z}_p}{30} - \frac{\bar{F}\,\bar{y}_o}{5}$$

$$g_{47} = \frac{1}{840\pi}\left[13\bar{P}K\,\bar{a} - 13\bar{P}K\,\bar{y}_o - 3\,\bar{P}\,\bar{\beta}_x\,\pi + 42\bar{\beta}_x\,\pi\,\bar{V}_1 - 42\bar{\beta}_x\,\pi\,\bar{P} + 336\left(\bar{r}_o\right)^2\pi + 336\left(\bar{y}_o\right)^2\pi\right.$$
$$\left. + 168\bar{\beta}_x\,\pi\,\bar{M}_1 + 168\bar{\beta}_x\,\pi\,\bar{P}\bar{z}_p\right] + \frac{1}{2}\left[\left(\bar{z}_p\right)^3 - 2\left(\bar{z}_p\right)^2 + \bar{z}_p\right]\left[(-2)\left(\bar{z}_p\right)^3 + 3\left(\bar{z}_p\right)^2\right]\bar{P}\left(\bar{e} - \bar{y}_o\right)\frac{K}{\pi}$$

$$g_{48} = \frac{-1}{840\pi}\left[3\,\bar{P}K\,\bar{a} - 3\,\bar{P}K\,\bar{y}_o - 19\bar{P}\,\bar{\beta}_x\,\pi + 49\bar{\beta}_x\,\pi\,\bar{V}_1 - 49\bar{\beta}_x\,\pi\,\bar{P} + 168\left(\bar{r}_o\right)^2\pi + 168\left(\bar{y}_o\right)^2\pi\right.$$
$$\left. + 84\bar{\beta}_x\,\pi\,\bar{M}_1 + 84\bar{\beta}_x\,\pi\,\bar{P}\bar{z}_p\right] + \frac{1}{2}\left[\left(\bar{z}_p\right)^3 - 2\left(\bar{z}_p\right)^2 + \bar{z}_p\right]\left[\left(\bar{z}_p\right)^3 - \left(\bar{z}_p\right)^2\right]\bar{P}\left(\bar{e} - \bar{y}_o\right)\frac{K}{\pi}$$

$$g_{55} = \frac{6\,\overline{F}}{5}$$

$$g_{56} = \frac{-\overline{F}}{10}$$

$$g_{57} = \frac{17\overline{P}}{35} - \frac{11\,\overline{V}_1}{10} + \frac{11\overline{P}}{10} - \frac{6\,\overline{M}_1}{5} - \frac{6\,\overline{P}\,\overline{z}_p}{5} + \frac{6\,\overline{F}\,\overline{y}_o}{5}$$

$$g_{58} = \frac{-3\,\overline{P}}{70} + \frac{\overline{V}_1}{10} - \frac{\overline{P}}{10} + \frac{\overline{M}_1}{10} + \frac{\overline{P}\,\overline{z}_p}{10} - \frac{\overline{F}\,\overline{y}_o}{10}$$

$$g_{66} = \frac{2\,\overline{F}}{15}$$

$$g_{67} = \frac{-79\overline{P}}{210} + \frac{9\,\overline{V}_1}{10} - \frac{9\,\overline{P}}{10} + \frac{11\,\overline{M}_1}{10} + \frac{11\,\overline{P}\,\overline{z}_p}{10} - \frac{\overline{F}\,\overline{y}_o}{10}$$

$$g_{68} = \frac{4\,\overline{P}}{105} - \frac{\overline{V}_1}{10} + \frac{\overline{P}}{10} - \frac{2\,\overline{M}_1}{15} - \frac{2\,\overline{P}\,\overline{z}_p}{15} + \frac{2\,\overline{F}\,\overline{y}_o}{15}$$

$$g_{77} = \frac{1}{70\pi}\left[13\overline{P}\,K\,\overline{a} - 13\overline{P}\,K\,\overline{y}_o - 6\,\overline{P}\,\overline{\beta}_x\,\pi + 21\overline{\beta}_x\,\pi\;\overline{V}_1 - 21\overline{\beta}_x\,\pi\;\overline{P} + 84\left(\overline{r}_o\right)^2\pi + 84\left(\overline{y}_o\right)^2\pi\right.$$

$$+ 42\overline{\beta}_x \pi \overline{M}_1 + 42\overline{\beta}_x \pi \overline{P}\overline{z}_p\Big] + \frac{1}{2}\left[(-2)\left(\overline{z}_p\right)^3 + 3\left(\overline{z}_p\right)^2\right]^2 \overline{P}\left(\overline{e} - \overline{y}_o\right)\frac{K}{\pi}$$

$$g_{78} = \frac{-1}{420\pi}\left[11\overline{P}K\overline{a} - 11\overline{P}K\overline{y}_o + 3\overline{P}\overline{\beta}_x\pi + 42\left(\overline{r}_o\right)^2\pi + 42\left(\overline{y}_o\right)^2\pi + 21\overline{\beta}_x\pi\overline{M}_1 + 21\overline{\beta}_x\pi\overline{P}\overline{z}_p\right]$$
$$+ \frac{1}{2}\left[(-2)\left(\overline{z}_p\right)^3 + 3\left(\overline{z}_p\right)^2\right]\left[\left(\overline{z}_p\right)^3 - \left(\overline{z}_p\right)^2\right]\overline{P}\left(\overline{e} - \overline{y}_o\right)\frac{K}{\pi}$$

$$g_{88} = \frac{1}{420\pi}\left[2\overline{P}K\overline{a} - 2\overline{P}K\overline{y}_o - 9\overline{P}\overline{\beta}_x\pi + 21\overline{\beta}_x\pi\,\overline{V}_1 - 21\overline{\beta}_x\pi\,\overline{P} + 56\left(\overline{r}_o\right)^2\pi + 56\left(\overline{y}_o\right)^2\pi + 28\overline{\beta}_x\pi\,\overline{M}_1\right.$$
$$\left. + 28\overline{\beta}_x\pi\,\overline{P}\overline{z}_p\right] + \frac{1}{2}\left[\left(\overline{z}_p\right)^3 - \left(\overline{z}_p\right)^2\right]^2\overline{P}\left(\overline{e} - \overline{y}_o\right)\frac{K}{\pi}$$

A.5 ELEMENT PREBUCKLING STIFFNESS MATRIX

$$k_{p11} = \frac{-6C\,E\,I_{\omega}}{L^3} - \frac{C\,G\,J}{2\,L}$$

$$k_{p18} = \frac{6C\,E\,I_{\omega}}{L^3} + \frac{C\,G\,J}{2\,L}$$

$$k_{p23} = \frac{C\,G\,J}{2L}$$

$$k_{p24} = \frac{-3C\,E\,I_{\omega}}{L^2} - \frac{C\,G\,J}{4}$$

$$k_{p27} = \frac{-C\,G\,J}{2L}$$

$$k_{p28} = \frac{3C\,E\,I_{\omega}}{L^2} + \frac{C\,G\,J}{4}$$

$$k_{p36} = \frac{-C\,G\,J}{2L}$$

$$k_{p45} = \frac{6C\,E\,I_{\omega}}{L^3} + \frac{C\,G\,J}{2\,L}$$

$$k_{p46} = \frac{-3C\,E\,I_{\omega}}{L^2} - \frac{C\,G\,J}{4}$$

$$k_{p58} = \frac{-6C\,E\,I_{\omega}}{L^3} - \frac{C\,G\,J}{2\,L}$$

$$k_{p67} = \frac{C\,G\,J}{2\,L}$$

$$k_{p68} = \frac{3C\,E\,I_{\omega}}{L^3} + \frac{C\,G\,J}{4}$$

A.6 ELEMENT PREBUCKLING GEOMETRIC STIFFNESS MATRIX

$$g_{13} = \frac{1}{10L^4\left(EI_x\right)}\Big(5L^4 GJP - 15GJL^3 V_1 + 15GJL^3 P - 180LI_w V_1 E - 3L^4 I_y EP$$

$$+ 6L^3 I_y EV_1 - 6L^3 I_y EP - 30L^2 GJM_1 - 30L^2 GJPz_p - 360I_w EM_1 + 30I_w EPL^2$$

$$+ 120I_w ELP - 360I_w EPz_p\Big)$$

$$g_{14} = \frac{-1}{30L^3\left(EI_x\right)}\Big(180LI_w V_1 E - 39L^4 I_y EP + 84L^3 I_y EV_1 - 84L^3 I_y EP + 90L^2 GJM_1$$

$$- 30I_w EPL^2 - 120I_w ELP + 360I_w EPz_p - 14L^4 GJP - 45GJL^3 P + 360I_w EM_1$$

$$+ 60I_w EPL^3 + 28L^5 GJP + 90GJL^4 P - 180L^3 GJPz_p + 90L^2 GJPz_p + 45GJL^3 V_1$$

$$+ 240I_w EL^2 P - 90L^4 GJV_1 - 180L^3 GJM_1 - 360L^2 I_w V_1 E + 60L^2 I_y EM_1 + 48L^5 I_y EP -$$

$$- 120L^3 I_y EM_1 - 120L^3 I_y EPz_p - 108L^4 V_1 I_y E + 108L^4 PI_y E + 60L^2 I_y EPz_p - 720I_w ELPz_p$$

$$- 720I_w ELM_1\Big)$$

$$g_{17} = \frac{-1}{10L^4\left(E I_x\right)}\left(5L^4 GJP - 15GJL^3 V_1 + 15GJL^3 P - 180L I_w V_1 E - 3L^4 I_y EP\right.$$

$$+ 6L^3 I_y E V_1 - 6L^3 I_y EP - 30L^2 GJ M_1 - 30L^2 GJ P z_p - 360 I_w E M_1 + 30 I_w EP L^2$$

$$\left. + 120 I_w E L P - 360 I_w E P z_p\right)$$

$$g_{18} = \frac{1}{20L^3\left(E I_x\right)}\left(8L^4 GJP - 25GJL^3 V_1 + 25GJL^3 P - 50L^2 GJ M_1 - 50L^2 GJ P z_p\right.$$

$$- 180L I_w V_1 E + 6L^4 I_y EP - 14L^3 I_y E V_1 + 14L^3 I_y EP - 20L^2 I_y E M_1 - 20L^2 I_y E P z_p$$

$$\left. - 360 I_w E M_1 + 30 I_w EP L^2 + 120 I_w E L P - 360 I_w E P z_p\right)$$

$$g_{23} = \frac{1}{60L^3\left(E I_x\right)}\left(360L I_w V_1 E - 24L^4 I_y EP + 72L^3 I_y E V_1 - 72L^3 I_y EP - 60L^2 GJ M_1\right.$$

$$+ 60 I_w EP L^2 + 240 I_w E L P - 720 I_w E P z_p - 23L^4 GJP - 30GJL^3 P - 720 I_w E M_1$$

$$- 120 I_w EP L^3 + 16L^5 GJP + 120L^3 GJ P z_p - 60L^2 GJ P z_p + 30GJL^3 V_1 - 480 I_w E L^2 P -$$

$$+ 120L^3 GJ M_1 + 120L^2 I_y E M_1 + 48L^5 I_y EP - 240L^3 I_y E M_1 - 240L^3 I_y EP z_p - 144L^4 V_1 I_y E$$

$$\left. + 144L^4 P I_y E + 120L^2 I_y EP z_p + 1440 I_w E L P z_p + 1440 I_w E L M_1\right)$$

$$g_{24} = \frac{-1}{180L^2\left(EI_x\right)}\Big[(-360)\,L\,I_w\,V_1\,E - 210L^4\,I_y\,E\,P + 528L^3\,I_y\,E\,V_1 - 528L^3\,I_y\,E\,P - 60I_w\,E\,P\,L^2$$

$$- 240I_w\,E\,L\,P + 720I_w\,E\,P\,z_p + 65L^4\,GJ\,P + 120GJ\,L^3\,P + 720I_w\,E\,M_1 + 240I_w\,E\,P\,L^3$$

$$- 170L^5\,GJ\,P - 240GJ\,L^4\,P - 360L^3\,GJ\,P\,z_p - 120GJ\,L^3\,V_1 + 960I_w\,E\,L^2\,P + 240L^4\,GJ\,V_1$$

$$- 360L^3\,GJ\,M_1 + 720L^2\,I_w\,V_1\,E + 720L^2\,I_y\,E\,M_1 + 660L^5\,I_y\,E\,P - 2160L^3\,I_y\,E\,M_1 - 2160L^3\,I_y\,E\,P\,z_p$$

$$- 1632L^4\,V_1\,I_y\,E + 1632L^4\,P\,I_y\,E + 720L^2\,I_y\,E\,P\,z_p - 2880I_w\,E\,L\,P\,z_p - 2880I_w\,E\,L\,M_1 - 480L^6\,I_y\,E\,P$$

$$+ 1440L^4\,I_y\,E\,M_1 + 1440L^4\,I_y\,E\,P\,z_p + 1152L^5\,V_1\,I_y\,E - 1152L^5\,P\,I_y\,E + 2880I_w\,E\,L^2\,P\,z_p$$

$$+ 2880I_w\,E\,L^2\,M_1 - 240I_w\,E\,P\,L^4 + 80L^6\,GJ\,P + 720L^4\,GJ\,P\,z_p - 960I_w\,E\,L^3\,P + 720L^4\,GJ\,M_1\Big]$$

$$g_{27} = \frac{1}{60L^3\left(EI_x\right)}\Big[(-360)\,L\,I_w\,V_1\,E + 24L^4\,I_y\,E\,P - 72L^3\,I_y\,E\,V_1 + 72L^3\,I_y\,E\,P + 60L^2\,GJ\,M_1$$

$$- 60I_w\,E\,P\,L^2 - 240I_w\,E\,L\,P + 720I_w\,E\,P\,z_p + 23L^4\,GJ\,P + 30GJ\,L^3\,P + 720I_w\,E\,M_1$$

$$+ 120I_w\,E\,P\,L^3 - 16L^5\,GJ\,P - 120L^3\,GJ\,P\,z_p + 60L^2\,GJ\,P\,z_p - 30GJ\,L^3\,V_1 + 480I_w\,E\,L^2\,P$$

$$- 120L^3\,GJ\,M_1 - 120L^2\,I_y\,E\,M_1 - 48L^5\,I_y\,E\,P + 240L^3\,I_y\,E\,M_1 + 240L^3\,I_y\,E\,P\,z_p + 144L^4\,V_1\,I_y\,E$$

$$- 144L^4\,P\,I_y\,E - 120L^2\,I_y\,E\,P\,z_p - 1440I_w\,E\,L\,P\,z_p - 1440I_w\,E\,L\,M_1\Big]$$

$$g_{28} = \frac{1}{120L^2\left(EI_x\right)}\Big(360LI_wV_1E + 24L^4I_yEP - 48L^3I_yEV_1 + 48L^3I_yEP - 40L^2GJM_1$$

$$+ 60I_wEPL^2 + 240I_wELP - 720I_wEPz_p - 37L^4GJP - 60GJL^3P - 720I_wEM_1$$

$$- 120I_wEPL^3 + 24L^5GJP + 200L^3GJPz_p - 40L^2GJPz_p + 60GJL^3V_1 - 480I_wEL^2P$$

$$+ 200L^3GJM_1 - 40L^2I_yEM_1 - 48L^5I_yEP + 80L^3I_yEM_1 + 80L^3I_yEPz_p + 96L^4V_1I_yE$$

$$- 96L^4PI_yE - 40L^2I_yEPz_p + 1440I_wELPz_p + 1440I_wELM_1\Big)$$

$$g_{35} = \frac{1}{10L^4\left(EI_x\right)}\Big[(-5)L^4GJP + 15GJL^3V_1 - 15GJL^3P + 180LI_wV_1E + 3L^4I_yEP$$

$$- 6L^3I_yEV_1 + 6L^3I_yEP + 30L^2GJM_1 + 30L^2GJPz_p + 360I_wEM_1 - 30I_wEPL^2$$

$$- 120I_wELP + 360I_wEPz_p\Big]$$

$$g_{36} = \frac{-1}{10L^3\left(EI_x\right)}\Big[\left(-L^4\right)GJP + 5GJL^3V_1 - 5GJL^3P + 15L^2GJM_1 + 15L^2GJPz_p$$

$$+ 3L^4I_yEP - 8L^3I_yEV_1 + 8L^3I_yEP - 10L^2I_yEM_1 - 10L^2I_yEPz_p + 180I_wEM_1$$

$$+ 60LI_wV_1E - 15I_wEPL^2 - 60I_wELP + 180I_wEPz_p\Big]$$

$$g_{45}=\frac{1}{30L^3\left(EI_x\right)}\Big(180LI_wV_1E-39L^4I_yEP+84L^3I_yEV_1-84L^3I_yEP+90L^2GJM_1$$

$$-30I_wEPL^2-120I_wELP+360I_wEPz_p-14L^4GJP-45GJL^3P+360I_wEM_1$$

$$+60I_wEPL^3+28L^5GJP+90GJL^4P-180L^3GJPz_p+90L^2GJPz_p+45GJL^3V_1$$

$$+240I_wEL^2P-90L^4GJV_1-180L^3GJM_1-360L^2I_wV_1E+60L^2I_yEM_1+48L^5I_yEP$$

$$-120L^3I_yEM_1-120L^3I_yEPz_p-108L^4V_1I_yE+108L^4PI_yE+60L^2I_yEPz_p-720I_wELPz_p$$

$$-720I_wELM_1\Big)$$

$$g_{46}=\frac{1}{60L^2\left(EI_x\right)}\Big[(-120)LI_wV_1E+61L^4I_yEP-144L^3I_yEV_1+144L^3I_yEP-90L^2GJM_1$$

$$+30I_wEPL^2+120I_wELP-360I_wEPz_p+6L^4GJP+30GJL^3P-360I_wEM_1$$

$$-60I_wEPL^3-12L^5GJP-60GJL^4P+180L^3GJPz_p-90L^2GJPz_p-30GJL^3V_1$$

$$-240I_wEL^2P+60L^4GJV_1+180L^3GJM_1+240L^2I_wV_1E-160L^2I_yEM_1-72L^5I_yEP$$

$$+200L^3I_yEM_1+200L^3I_yEPz_p+168L^4V_1I_yE-168L^4PI_yE-160L^2I_yEPz_p+720I_wELPz_p$$

$$+720I_wELM_1\Big]$$

$$g_{57} = \frac{-1}{10L^4\left(EI_x\right)}\Big[(-5)\,L^4\,GJ\,P + 15GJ\,L^3\,V_1 - 15GJ\,L^3\,P + 180L\,I_w\,V_1\,E + 3L^4\,I_y\,E\,P$$

$$- 6L^3\,I_y\,E\,V_1 + 6L^3\,I_y\,E\,P + 30L^2\,GJ\,M_1 + 30L^2\,GJ\,P\,z_p + 360I_w\,E\,M_1 - 30I_w\,E\,P\,L^2$$

$$- 120I_w\,E\,L\,P + 360I_w\,E\,P\,z_p\Big]$$

$$g_{58} = \frac{1}{20L^3\left(EI_x\right)}\Big[(-8)\,L^4\,GJ\,P + 25GJ\,L^3\,V_1 - 25GJ\,L^3\,P + 50L^2\,GJ\,M_1 + 50L^2\,GJ\,P\,z_p$$

$$+ 180L\,I_w\,V_1\,E - 6L^4\,I_y\,E\,P + 14L^3\,I_y\,E\,V_1 - 14L^3\,I_y\,E\,P + 20L^2\,I_y\,E\,M_1 + 20L^2\,I_y\,E\,P\,z_p$$

$$+ 360I_w\,E\,M_1 - 30I_w\,E\,P\,L^2 - 120I_w\,E\,L\,P + 360I_w\,E\,P\,z_p\Big]$$

$$g_{67} = \frac{-1}{10L^3\left(EI_x\right)}\Big(L^4\,GJ\,P - 5\,GJ\,L^3\,V_1 + 5\,GJ\,L^3\,P - 15L^2\,GJ\,M_1 - 15L^2\,GJ\,P\,z_p$$

$$- 3L^4\,I_y\,E\,P + 8L^3\,I_y\,E\,V_1 - 8L^3\,I_y\,E\,P + 10L^2\,I_y\,E\,M_1 + 10L^2\,I_y\,E\,P\,z_p - 180I_w\,E\,M_1$$

$$- 60L\,I_w\,V_1\,E + 15I_w\,E\,P\,L^2 + 60I_w\,E\,L\,P - 180I_w\,E\,P\,z_p\Big)$$

$$g_{68} = \frac{-1}{60L^2\left(EI_x\right)}\Big[(-5)\,L^4\,GJ\,P + 25GJ\,L^3\,V_1 - 25GJ\,L^3\,P + 75L^2\,GJ\,M_1 + 75L^2\,GJ\,Pz_p$$

$$- 12L^4\,I_y\,EP + 26L^3\,I_y\,EV_1 - 26L^3\,I_y\,EP + 30L^2\,I_y\,EM_1 + 30L^2\,I_y\,EPz_p + 540I_w\,EM_1$$

$$+ 180L\,I_w\,V_1\,E - 45I_w\,EP\,L^2 - 180I_w\,ELP + 540I_w\,EPz_p\Big]$$

APPENDIX B

B.1 MATRIX [*A*] FROM SECTION 5.4

$$A_{11} = \frac{\pi^2}{32} \qquad A_{82} = \frac{K^2}{32} + \frac{1}{8}$$

$$A_{23} = \frac{81\,\pi^2}{32} \qquad A_{94} = \frac{81\,K^2}{32} + \frac{9}{8}$$

$$A_{35} = \frac{625\,\pi^2}{32} \qquad A_{10.6} = \frac{625\,K^2}{32} + \frac{25}{8}$$

$$A_{47} = \frac{2401\,\pi^2}{32} \qquad A_{11.8} = \frac{2401\,K^2}{32} + \frac{49}{8}$$

$$A_{59} = \frac{6561\,\pi^2}{32} \qquad A_{12.10} = \frac{6561\,K^2}{32} + \frac{81}{8}$$

$$A_{6.11} = \frac{14641\,\pi^2}{32} \qquad A_{13.12} = \frac{14641\,K^2}{32} + \frac{121}{8}$$

$$A_{7.13} = \frac{28561\,\pi^2}{32} \qquad A_{14.14} = \frac{28561\,K^2}{32} + \frac{169}{8}$$

*Only non-zero terms from Matrix [*A*] are listed.

B.1 MATRIX [*B*] FROM SECTION 5.4

$$B_{12} = \frac{1}{16} - \frac{3}{4\,\pi^{2}} \qquad B_{22} = \frac{5}{4\,\pi^{2}}$$

$$B_{14} = \frac{-3}{4\,\pi^{2}} \qquad B_{24} = \frac{9}{16} - \frac{3}{4\,\pi^{2}}$$

$$B_{16} = \frac{-35}{36\,\pi^{2}} \qquad B_{26} = \frac{5}{4\,\pi^{2}}$$

$$B_{18} = \frac{-35}{36\,\pi^{2}} \qquad B_{28} = \frac{-91}{100\,\pi^{2}}$$

$$B_{1.10} = \frac{-99}{100\,\pi^{2}} \qquad B_{2.10} = \frac{-3}{4\,\pi^{2}}$$

$$B_{1.12} = \frac{-99}{100\,\pi^{2}} \qquad B_{2.12} = \frac{-187}{196\,\pi^{2}}$$

$$B_{1.14} = \frac{-195}{196\,\pi^{2}} \qquad B_{2.14} = \frac{-91}{100\,\pi^{2}}$$

$$B_{32} = \frac{-11}{36\,\pi^2}$$

$$B_{34} = \frac{21}{4\,\pi^2}$$

$$B_{36} = \frac{25}{16} - \frac{3}{4\,\pi^2}$$

$$B_{38} = \frac{21}{4\,\pi^2}$$

$$B_{3.10} = \frac{-171}{196\,\pi^2}$$

$$B_{3.12} = \frac{-11}{36\,\pi^2}$$

$$B_{3.14} = \frac{-299}{324\,\pi^2}$$

$$B_{42} = \frac{13}{36\,\pi^2}$$

$$B_{44} = \frac{-51}{100\,\pi^2}$$

$$B_{46} = \frac{45}{4\,\pi^2}$$

$$B_{48} = \frac{49}{16} - \frac{3}{4\,\pi^2}$$

$$B_{4.10} = \frac{45}{4\,\pi^2}$$

$$B_{4.12} = \frac{-275}{324\,\pi^2}$$

$$B_{4.14} = \frac{13}{36\,\pi^2}$$

$$B_{52} = \frac{-19}{100\,\pi^2}$$

$$B_{54} = \frac{5}{4\,\pi^2}$$

$$B_{56} = \frac{-115}{196\,\pi^2}$$

$$B_{58} = \frac{77}{4\,\pi^2}$$

$$B_{5.10} = \frac{81}{16} - \frac{3}{4\,\pi^2}$$

$$B_{5.12} = \frac{77}{4\,\pi^2}$$

$$B_{5.14} = \frac{-403}{484\,\pi^2}$$

$$B_{62} = \frac{21}{100\,\pi^2}$$

$$B_{64} = \frac{-75}{196\,\pi^2}$$

$$B_{66} = \frac{85}{36\,\pi^2}$$

$$B_{68} = \frac{-203}{324\,\pi^2}$$

$$B_{6.10} = \frac{117}{4\,\pi^2}$$

$$B_{6.12} = \frac{121}{16} - \frac{3}{4\,\pi^2}$$

$$B_{6.14} = \frac{117}{4\,\pi^2}$$

$$B_{72} = \frac{-27}{196\,\pi^{2}}$$

$$B_{74} = \frac{69}{100\,\pi^{2}}$$

$$B_{76} = \frac{-155}{324\,\pi^{2}}$$

$$B_{78} = \frac{133}{36\,\pi^{2}}$$

$$B_{7.10} = \frac{-315}{484\,\pi^{2}}$$

$$B_{7.12} = \frac{165}{4\,\pi^{2}}$$

$$B_{7.14} = \frac{169}{16} - \frac{3}{4\,\pi^{2}}$$

$$B_{81} = \frac{1}{16} - \frac{3}{4\pi^2}$$

$$B_{82} = \frac{-\beta x}{16} + \frac{\beta x}{4\pi^2}$$

$$B_{83} = \frac{-27}{4\pi^2}$$

$$B_{84} = \frac{-3\beta x}{4\pi^2}$$

$$B_{85} = \frac{-875}{36\pi^2}$$

$$B_{86} = \frac{5\beta x}{36\pi^2}$$

$$B_{87} = \frac{-1715}{36\pi^2}$$

$$B_{88} = \frac{-7\beta x}{36\pi^2}$$

$$B_{89} = \frac{-8019}{100\pi^2}$$

$$B_{8.10} = \frac{9\beta x}{100\pi^2}$$

$$B_{8.11} = \frac{-11979}{100\pi^2}$$

$$B_{8.12} = \frac{-11\beta x}{100\pi^2}$$

$$B_{8.13} = \frac{-32955}{196\pi^2}$$

$$B_{8.14} = \frac{13\beta x}{196\pi^2}$$

$$B_{91} = \frac{5}{36\pi^2}$$

$$B_{92} = \frac{-3\,\beta\,x}{4\,\pi^2}$$

$$B_{93} = \frac{9}{16} - \frac{3}{4\pi^2}$$

$$B_{94} = \frac{-9\beta\,x}{16} + \frac{\beta\,x}{4\,\pi^2}$$

$$B_{95} = \frac{125}{36\pi^2}$$

$$B_{96} = \frac{-15\,\beta\,x}{4\,\pi^2}$$

$$B_{97} = \frac{-4459}{900\pi^2}$$

$$B_{98} = \frac{21\,\beta\,x}{100\,\pi^2}$$

$$B_{99} = \frac{-27}{4\pi^2}$$

$$B_{9.10} = \frac{-3\,\beta\,x}{4\,\pi^2}$$

$$B_{9.11} = \frac{-22627}{1764\pi^2}$$

$$B_{9.12} = \frac{33\,\beta\,x}{196\,\pi^2}$$

$$B_{9.13} = \frac{-15379}{900\pi^2}$$

$$B_{9.14} = \frac{-39\,\beta\,x}{100\,\pi^2}$$

$$B_{10.1} = \frac{-11}{900\pi^2}$$

$$B_{10.2} = \frac{5\beta x}{36\pi^2}$$

$$B_{10.3} = \frac{189}{100\pi^2}$$

$$B_{10.4} = \frac{-15\beta x}{4\pi^2}$$

$$B_{10.5} = \frac{25}{16} - \frac{3}{4\pi^2}$$

$$B_{10.6} = \frac{-25\beta x}{16} + \frac{\beta x}{4\pi^2}$$

$$B_{10.7} = \frac{1029}{100\pi^2}$$

$$B_{10.8} = \frac{-35\beta x}{4\pi^2}$$

$$B_{10.9} = \frac{-13851}{4900\pi^2}$$

$$B_{10.10} = \frac{45\beta x}{196\pi^2}$$

$$B_{10.11} = \frac{-1331}{900\pi^2}$$

$$B_{10.12} = \frac{-55\beta x}{36\pi^2}$$

$$B_{10.13} = \frac{-50531}{8100\pi^2}$$

$$B_{10.14} = \frac{65\beta x}{324\pi^2}$$

$$B_{11.1} = \frac{13}{1764\pi^2}$$

$$B_{11.2} = \frac{-7\,\beta_x}{36\,\pi^2}$$

$$B_{11.3} = \frac{-459}{4900\pi^2}$$

$$B_{11.4} = \frac{21\,\beta_x}{100\,\pi^2}$$

$$B_{11.5} = \frac{1125}{196\pi^2}$$

$$B_{11.6} = \frac{-35\,\beta_x}{4\,\pi^2}$$

$$B_{11.7} = \frac{49}{16} - \frac{3}{4\pi^2}$$

$$B_{11.8} = \frac{-49\,\beta_x}{16} + \frac{\beta_x}{4\,\pi^2}$$

$$B_{11.9} = \frac{3645}{196\pi^2}$$

$$B_{11.10} = \frac{-63\,\beta_x}{4\,\pi^2}$$

$$B_{11.11} = \frac{-33275}{15876\pi^2}$$

$$B_{11.12} = \frac{77\,\beta_x}{324\,\pi^2}$$

$$B_{11.13} = \frac{2197}{1764\pi^2}$$

$$B_{11.14} = \frac{-91\,\beta_x}{36\,\pi^2}$$

$$B_{12.1} = \frac{-19}{8100\pi^2}$$

$$B_{12.2} = \frac{9\,\beta_x}{100\,\pi^2}$$

$$B_{12.3} = \frac{5}{36\pi^2}$$

$$B_{12.4} = \frac{-3\,\beta_x}{4\,\pi^2}$$

$$B_{12.5} = \frac{-2875}{15876\pi^2}$$

$$B_{12.6} = \frac{45\,\beta_x}{196\,\pi^2}$$

$$B_{12.7} = \frac{3773}{324\pi^2}$$

$$B_{12.8} = \frac{-63\,\beta_x}{4\,\pi^2}$$

$$B_{12.9} = \frac{81}{16} - \frac{3}{4\pi^2}$$

$$B_{12.10} = \frac{-81\beta_x}{16} + \frac{\beta_x}{4\,\pi^2}$$

$$B_{12.11} = \frac{9317}{324\pi^2}$$

$$B_{12.12} = \frac{-99\,\beta_x}{4\,\pi^2}$$

$$B_{12.13} = \frac{-68107}{39204\pi^2}$$

$$B_{12.14} = \frac{117\,\beta_x}{484\,\pi^2}$$

$$B_{13.1} = \frac{21}{12100\pi^2}$$

$$B_{13.2} = \frac{-11\,\beta_x}{100\,\pi^2}$$

$$B_{13.3} = \frac{-675}{23716\pi^2}$$

$$B_{13.4} = \frac{33\,\beta_x}{196\,\pi^2}$$

$$B_{13.5} = \frac{2125}{4356\pi^2}$$

$$B_{13.6} = \frac{-55\,\beta_x}{36\,\pi^2}$$

$$B_{13.7} = \frac{-9947}{39204\pi^2}$$

$$B_{13.8} = \frac{77\,\beta_x}{324\,\pi^2}$$

$$B_{13.9} = \frac{9477}{484\pi^2}$$

$$B_{13.10} = \frac{-99\,\beta_x}{4\,\pi^2}$$

$$B_{13.11} = \frac{121}{16} - \frac{3}{4\pi^2}$$

$$B_{13.12} = \frac{-121\beta_x}{16} + \frac{\beta_x}{4\,\pi^2}$$

$$B_{13.13} = \frac{19773}{484\pi^2}$$

$$B_{13.14} = \frac{-143\,\beta_x}{4\,\pi^2}$$

$$B_{14.1} = \frac{-27}{33124\pi^2}$$

$$B_{14.2} = \frac{13\,\beta\,x}{196\,\pi^2}$$

$$B_{14.3} = \frac{621}{16900\pi^2}$$

$$B_{14.4} = \frac{-39\,\beta\,x}{100\,\pi^2}$$

$$B_{14.5} = \frac{-3875}{54756\pi^2}$$

$$B_{14.6} = \frac{65\,\beta\,x}{324\,\pi^2}$$

$$B_{14.7} = \frac{6517}{6084\pi^2}$$

$$B_{14.8} = \frac{-91\,\beta\,x}{36\,\pi^2}$$

$$B_{14.9} = \frac{-25515}{81796\pi^2}$$

$$B_{14.10} = \frac{117\,\beta\,x}{484\,\pi^2}$$

$$B_{14.11} = \frac{19965}{676\pi^2}$$

$$B_{14.12} = \frac{-143\,\beta\,x}{4\,\pi^2}$$

$$B_{14.13} = \frac{169}{16} - \frac{3}{4\pi^2}$$

$$B_{14.14} = \frac{-169\beta\,x}{16} + \frac{\beta\,x}{4\,\pi^2}$$

BIBLIOGRAPHY

WORKS CITED

1. Anderson, J. M. and Trahair, N.S. (1972). Stability of Monosymmetric Beams and Cantilevers. *Journal of the Structural Division*, ASCE, 98(1), 269-285.

2. Arfken, G. and Weber, H. (2005). *Mathematical Methods for Physicists,* 6th ed. Burlington, MA: Elsevier Academic Press..

3. Chajes, A. (1993). *Principles of Structural Stability Theory.* Englewood Cliffs, New Jersey: Prentice-Hall.

4. Chen, W. F. and Lui, E. M. (1987). *Structural Stability Theory and Implementation*. Upper Saddle River, New Jersey: Prentice-Hall.

5. Kitipornchai, S. and Trahair, N. S. (1980). Buckling Properties of Monosymmetric I-Beams. *Journal of the Structural Division*. ASCE, 106(5), 941-957.

6. Kitipornchai, S. and Wang, C. M. (1989). New Set of Buckling Parameters for Monosymmetric Beam-Column/Tie-Beams. *Journal of Structural Engineering*. ASCE, 115(6), 1497-1513.

7. Lee, L. H. N. (1959). On the Lateral Buckling of a Tapered Narrow Rectangular Beam. *Journal of Applied Mechanics*. 26, 457-458.

8. Love, A. E. H. (1944). *A Treatise on the Mathematical Theory of Elasticity*. 4th ed., Dover, New York, N. Y.

9. Mohri, F., Brouki, A., and Roth, J. C. (2003). Theoretical and Numerical Stability Analyses of Unrestrained, Monosymmetric Thin-Walled Beams. *Journal of Constructional Steel Research.* Elsevier, 59, 63-90.

10. Pi, Y. L. and Trahair, N. S. (1992a). Prebuckling Deflections and Lateral Buckling. I: Theory. *Journal of Structural Engineering*, ASCE, 118(11), 2949-2966.

11. Pi, Y. L. and Trahair, N. S. (1992b). Prebuckling Deflections and Lateral Buckling. II: Theory. *Journal of Structural Engineering*, ASCE, 118(11), 2967-2986.

12. Pilkey, W.D. and Wunderlich, W. (1994). *Mechanics of Structures Variational and Computational Methods*. Boca Patom, Florida: CRC Press Inc.

13. Roberts, E. R. (2004). Elastic Flexural-Torsional Buckling Analysis Using Finite Element Method and Object-Oriented Technology with C/C++. *M.S. Thesis*. School of Engineering, Univ. of Pittsburgh.

14. Torkamani, M. A. M. (1998). Transformation Matrices for Finite and Small Rotations. *Journal of Engineering Mechanics*, ASCE, 124(3), 359-362.

15. Trahair, N. S. and Nethercot, D. A. (1984) *Bracing Requirements in Thin-Walled Structures*.

16. Vlasov, V. Z. (1961). *Thin-walled Elastic Beams* (2nd ed.). Jerusalem, Israel: Israel Program for Scientific Translation.

17. Wang, C.M., and Kitipornchai, S. (1986). On Stability of Monosymmetric Cantilevers. *Engineering Structures*, ASCE, 8, 169-180.

18. Wang, C.M., Wang, C.Y., and Reddy, J.N. (2005). *Exact Solutions for Buckling of Structural Members.* Boca Raton, Florida: CRC Press LLC.

WORKS CONSULTED

1. Andrade, A. and Camotim, D. (2005). Lateral-Torsional Buckling of Singly Symmetric Tapered Beams: Theory and Applications. *Journal of Engineering Mechanics*, ASCE, 586-597.

2. Bradford, M. A. (1988). Elastic Buckling of Tapered Monosymmetric I-Beams. *Journal of Structural Engineering*, ASCE, 114(5), 977-992.

3. Boyce, W. E. and DiPrima, R. C. (2001). *Elementary Differential Equations and Boundary Value Problems*. New York, New York: John Wiley & Sons, Inc.

4. Clark, J. W. and Hill, H. N. (1960). Lateral Buckling of Beams. *Journal of the Structural Division*, ASCE, 86(7), 175-196.

5. Clark, J. W. and Hill, H. N. (1962). Lateral Buckling of Beams and Girders. *Civil Engineering Transactions*, ASCE, 127(7), 180-201.

6. Dontree, P. (1994). Elastic Flexural-Torsional Buckling Analysis Using Object-Oriented Technology and C/C++. *M.S. Thesis*. School of Engineering, Univ. of Pittsburgh

7. Kitipornchai, S. and Trahair, N. S. (1975). Elastic Behavior of Tapered Monosymmetric I-Beams Under Moment Gradient. *Journal of the Structural Division*, ASCE, 101(8), 1661-1678.

8. Kitipornchai, S. and Trahair, N. S. (1972). Elastic Stability of Tapered I-Beams. *Journal of the Structural Division*. ASCE, 98(3), 713-728.

9. Kitipornchai, S., Wang, C. M. and Trahair, N. S. (1986). Buckling of Monosymmetric I-Beams Under Moment Gradient. *Journal of Structural Engineering*. ASCE, 112(4), 781-787.

10. Mohri, F., Brouki, A., and Roth, J. C. (2003). Theoretical and Numerical Stability Analyses of Unrestrained, Monosymmetric Thin-Walled Beams. *Journal of Constructional Steel Research.* Elsevier, 59, 63-90.

11. Pi, Y. L., Trahair, N. S. and Rajasekaran, S. (1991). Energy Equation for Beam Lateral Buckling. *Research Report No. R635*, School of Civ. And Mining Engrg., Univ. of Sydney, Australia.

12. Powell, G. and Klingner, R. (1970). Elastic Lateral Buckling of Steel Beams. *Journal of the Structural Division*, ASCE, 96(6), 1919-1932.

13. Roberts, T. M. and Burt, C. A. (1984). Instability of Monosymmetric I-Beams and Cantilevers. , ASCE, , 313-324.

14. Tedesco, J. W., McDougal, W. G., and Ross, C. A. (1999). *Structural Dynamics: Theory and Applications*. Boston, MA: Addison-Wesley.

15. Tehe, Lip H. (2005). Spatial Rotation Kinematics and Flexural-Torsional Buckling. *Journal of Engineering Mechanics*, ASCE, 131(6), 598-605.

16. Trahair, N. S. (1993). *Flexural-Torsional Buckling of Structures*. Boca Raton, Florida: CRC Press.

17. Vacharajittiphan, P., and Trahair, N.S. (1974). Effect of In-plane Deformation on Lateral Buckling. *Journal of Structural Mechanics*, ASCE, 3(1), 29-60.

18. Wang, C.M., and Kitipornchai, S. (1986). On Stability of Monosymmetric Cantilevers. *Engineering Structures*, ASCE, 8, 169-180.

19. Weaver, W. Jr., and Gere, J.M. *Matrix Analysis of Framed Structures*. 3rd edition. New York: Van Nostrand Reinhold.

20. Zhang, L. and Tong, G.E. (2008). Elastic Flexural-Torsional Buckling of Thin-Walled Cantilevers. *Thin-Walled Structures*, Elsevier, 46, 27-37.